UNIVERSITY OF CALIFORNIA
LOS ALAMOS SCIENTIFIC LABORATORY
LOS ALAMOS, N. M.

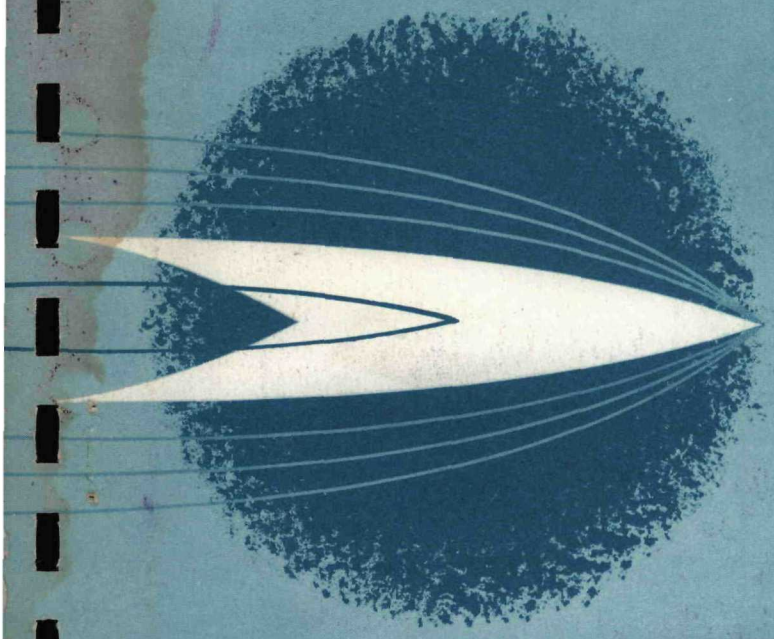

23 December 1958
Report No. 1537
(Final)
Copy No. 87

MECHANICAL PROPERTY MEASUREMENTS ON PURE AND URANIUM-LOADED GRAPHITES AT ELEVATED TEMPERATURES

Contract CTU 86039-1

Corporate Research Operation

Aerojet-General CORPORATION

AZUSA, CALIFORNIA — SACRAMENTO, CALIFORNIA

A SUBSIDIARY OF THE GENERAL TIRE & RUBBER COMPANY

DISCLAIMER

AGC-1537

23 December 1958

Report No. 1537
(Final)

MEASUREMENTS OF MECHANICAL PROPERTIES OF PURE AND URANIUM-LOADED GRAPHITES AT ELEVATED TEMPERATURES

Contract CTU 86039-1

Written by:

Leon Green, Jr.
Melvin L. Stehsel
Cecil E. Waller

No. of Pages: 145

Period Covered:

27 June 1957 through 15 December 1958

Approved by:

L. Green

for Y. C. Lee, Director
Corporate Research Operation

The data presented in this report was compiled by the Aerojet-General Corporation in contract with the Los Alamos Scientific Laboratory, University of California, Los Alamos, New Mexico, CTU 86039-1. The financial support and other supporting features such as choice and supply of the graphites to be investigated, fabrication of the samples, and supply of the inert gases were undertaken by LASL as their contribution to this work.

AEROJET-GENERAL CORPORATION

Azusa, California

CONTENTS

CONTENTS (cont.)

CONTENTS (cont.)

CONTENTS (cont.)

CONTENTS (cont.)

CONTENTS (cont.)

CONTRACT FULFILLMENT STATEMENT

This final report completes fulfillment of the contract.

ABSTRACT

Various mechanical-property measurements on several grades of manufactured (polycrystalline) graphite stock include tensile-strength determinations at temperatures from 20 to 2400°C (plus a few at 2500°C), tensile stress-strain and creep tests in the range 2000-2400°C, torsional strength and stress-strain measurements from 20 to 2600°C, torsional creep and stress-relaxation tests in the range from 2000 to 2800°C, dynamic Young's-modulus determinations from 20 to 2450°C, and evaluation of average coefficients of linear thermal expansion for the ranges 20-1050°C and 1300-2400°C.

The materials studied include a commercial grade of graphite (Great Lakes Carbon Co. Grade H4LM) molded in 36-in.-dia pieces, both as the standard stock with a nominal density of 1.74 g/cc and as stock re-impregnated to a nominal density of 1.80-1.85 g/cc, and four grades of graphite manufactured by the Los Alamos Scientific Laboratory containing normal uranium (added as UO_2 during the manufacture) in varying concentrations. The tensile-strength and creep data obtained are compared with the results of Los Alamos measurements upon similar materials.

Continued research on the elastic-anelastic properties and the creep and relaxation characteristics of polycrystalline graphites is recommended.

I. INTRODUCTION

General interest in the field of high temperature properties of material plus the specific interest in this domain of Project Rover (1) at the Los Alamos Scientific Laboratory were motivating forces in initiating a program of high temperature property measurement. In this case interest centered on measurements of some of the high temperature mechanical properties of some selected graphites over a temperature interval. This report is a summary of the results which were obtained in the pursuit of this goal.

II. REVIEW OF PREVIOUS INVESTIGATIONS

The first published investigation of the thermal-mechanical properties of graphite at high temperatures appears to be the measurements of thermal-expansion coefficients reported by Hidnert (2). Similar measurements using X-ray diffraction methods were later reported by Nelson and Riley (3,4) and Duwez (5), and more recently the thermal-expansion characteristics of graphitic materials has been the subject of intensive study (6 to 15).

Investigation of structure and of other physical properties (including electrical, magnetic, thermal, chemical, etc.) constitute a literature too extensive to be referenced here, but general reviews have been provided by Udy and Boulger (16), Howe (17), Slyh (18), and Currie, Hamister, and MacPherson (19). The last survey includes many otherwise unpublished data accumulated by investigators at the National Carbon Company. Also, a valuable

*Numbers in parenthesis refer to references listed at end of text.

collection of information on graphite is provided by the Biennial Conferences on Carbon organized by Professor S. Mrozowski, of the University of Buffalo, and his associates.

Until very recently, the purely mechanical properties of graphite have received somewhat less attention. Not counting the routine measurements performed (but not widely disseminated) by the various manufacturers, tensile-strength data for several grades of material at room temperature were first reported by Duwez (5). Measurement of tensile strength and creep properties at high temperature were initiated in 1947 by Malmstrom and his associates at North American Aviation, Inc. (20) and independently by Adams and Nelson at the Battelle Memorial Institute (21). These investigations revealed that the breaking strength of graphite increased with temperature up to about 2500°C, beyond which maximum point it decreased as a result of rapidly increasing thermal softening or creep effects. A similar temperature dependence for the elastic moduli, fatigue-endurance limit, and compressive breaking strength was also demonstrated (20,22,23,24).

Following these disclosures, the attractiveness of graphite as a high-temperature structural material was widely recognized, and tensile strength and creep data for various grades of material have recently been reported by Keen (25), Loch (26,27), Martens, Jaffe, and Jepson (28,29), Simbeck, Wiener, and Harvey (30), Wagner, Driesner, Kmetko, and MacMillan (15,31), Martens, Jaffee, and Button (32) and Stieber and Stroup (33). Compressive strength and creep data were presented by Wagner, et al. (15, 31). Selected preliminary results of the present investigation have been reported by the present authors (34,35). In addition to the extensive use of graphite as a material for rocket-nozzle inserts and jet vanes, its use in a wide variety of fluid-flow and heat-transfer systems has been either demonstrated or suggested (25,36 to 5

Various theoretical explanations for the increase in strength of graphite with increasing temperature have been advanced, but the most satisfactory is that of Mrozowski (10), who attributes this behavior to the relief of

"frozen-in" microscopic stress fields which arise from the anisotropy of therma contraction of the individual single crystallites constituting the formed polycrystalline mass. Such stresses are relaxed by diffusional (creep) effects during cooling from graphitization temperature to about 2000-2200°C, but below this temperature the rate of relaxation becomes so slow that essentially no relief mechanism exists.

An idealized theoretical model of a polycrystalline graphite structure ha also been examined by Mrozowski (52) as a basis for estimating the dependence of various physical and mechanical constants (including elastic moduli) upon mix composition, but, as noted by Faris et al. (22), no satisfactory theoretical explanation of the observed thermal dependence of the elastic moduli has been found. However, as will be noted in the following discussion, an heuristi argument may be advanced to the effect that the observed dependence is analogous to polymer behavior, and thus that the concepts of polymer-elasticity theory may be pertinent to the graphite-elasticity problem.

III. DESIGN OF EXPERIMENT

A. TYPES OF MATERIAL

1. Commercial Grades

The type of commercial graphite to which most attention was given in the present program of measurements was Grade H4LM graphite* in molded cylindrical stock of 36-in. O.D. Both the standard stock with a nominal density of 1.74 g/cc and a stock reimpregnated to a density of 1.80-1.85 g/cc were studied. Specimens were machined from various positions in the block according to the pattern described by Wagner et al. (31), with their long axes either parallel or perpendicular to the grain (i.e., either perpendicular or parallel to the molding pressure vector).

*Great Lakes Carbon Company.

In addition, a few tensile-strength determinations were made on Grade 3499 commercial graphite.* All specimens were fabricated at Los Alamos, and no individual specimen-density measurements were made for correlation with observed strength values, although such a correlation presumably does exist for a given grade or block of material (20). No detailed data on the manufacture or characteristic properties of the H4LM stock was available, but it was stated by GLC personnel (53) that the manufacturing process outlined by Hader, Gamson, and Bailey (54) and the typical property values reported by Hodge (55) could be considered representative.

2. Los Alamos Grades

The graphites were manufactured at the Los Alamos Scientific Laboratory by the conventional procedure which has been described by Currie et al. (19) and Hader et al. (54). Normal UO_2 was added to yield grades of finished material with uranium concentrations identified as follows:

Grade Identification	Volume Concentration of Uranium (mg/cc)
CK	0
LDH	125
LDC	250
LDP	350

The test specimens were machined with their long axes parallel to the grain (perpendicular to the molding-pressure vector).

The uranium presumably was converted to the dicarbide during the graphitization process, since UC_2 (m.p. 2350-2400°C) is the stable phase at high temperature. However, according to the studies of Eatherly, et al. (56), the transformation

*Speer Carbon Company.

$$UC_2 \rightleftharpoons UC + C \qquad (1)$$

appears to be reversible, with the transformation temperature estimated to be in the range 1800-2000°C. Therefore, the possible transformation to the lower-melting UC (m.p. 2250°C) during cooling following graphitization, or during subsequent heating of specimens to intermediate temperature levels, might be expected to influence the mechanical-properties measurements to some degree. However, the magnitude of any such effect was not considered to be significant enough to warrant an increase in the scope of the test program, and the effect of heat treatment was not investigated.

B. TYPES OF MEASUREMENT

The program was carried out in the high-temperature-materials research laboratory shown schematically in Figure 1.

1. Tensile Properties

a. Stress-Strain Characteristics

Although measurements of the tensile strength of graphites at elevated temperature had been made previously, no tensile stress-vs-strain characteristics had been reported. Such data are of obvious importance in the design of structural members, and the elevated temperatures involved in the present application also suggested that time or strain-rate effects should be significant. In a temperature regime where time effects are important, the strain rate (or loading rate) influences both the shape of the stress-strain curve (and hence the value of the time-dependent tangent modulus) and the variation of the ultimate breaking strength with temperature. Accordingly, the tensile stress-strain measurements were performed using the Instron* machine shown in Figure 2 at two head rates, 0.02 and 0.002 in./min.

*Instron Engineering Corp. (Quincy, Mass.), Model TT-B-L.

The furnace used in the tensile strength measurements is diagramed in Figure 3. It had been found in the earlier experiments (20,24) that the use of self-resistance heating of the specimen created large, radial, temperature gradients therein, which complicated interpretation of the data obtained. Therefore, the present furnace design employed specimens which were heated indirectly by radiation from a surrounding self-resistance-heated, cylindrical element specially slotted to provide a high-resistance path.

In the interest of short heating and cooling times to permit rapid testing operations, thermal insulation within the furnace was held to a minimum, and consisted primarily of radiation shields fabricated from graphite and/or ungraphitized carbon or molybdenum sheet, contained in a water-cooled brass shell. An inert atmosphere was preserved by a slow flow of helium through the furnace. The gas entered at the top through the plastic-bag seal and at each sight window to prevent the migration of carbon vapor to the window surface (where condensation would produce a deposit which would introduce an error in the optical temperature measurement), and left through the bottom loading-member port. These members, or "pull-rods," were fabricated from ungraphitized carbon to minimize heat-conduction losses and consequent axial temperature gradients in the specimen.

Power was supplied by one of two 35-kw ac-dc motor-generator sets shown in Figure 4. It was found that this amount of power was sufficient to effect specimen temperatures of about 2600°C, but test temperatures were generally limited to 2400°C (a few were conducted at 2500°C) owing to overheating of the upper cover plate. The specimen temperature was measured by a Leeds and Northrup disappearing-filament optical pyrometer calibrated by viewing an NBS standard lamp through the quartz sight window actually employed; provision was made for automatic control of this temperature by a Brown "Radiamatic" total-radiation pyrometer, and a Brown recording potentiometer which could control the field current in the d-c generator supplying power to the heater element.

Block and schematic diagrams of this control circuit are shown in Figures 5 and 6, and the control consoles for the two separate power supplies are shown in Figure 7. In practice, however, the power supplies proved so stable that no automatic control was required, and only an initial manual setting was required to establish a specimen-temperature level which, within the precision of the optical pyrometer reading (about $\pm 5^{\circ}C$), remained constant throughout the test.

The tensile specimens employed in the present program were fabricated according to a design previously employed in Los Alamos studies by Wagner, et al. (15,31), which is shown in Figure 8. Strain was measured by projecting the image of the specimen gage length (using an anastigmat lens mounted in one of the furnace windows) upon a ground-glass screen. This screen was mounted on a projection panel which also contained an electric timer and a Leeds and Northrop "Speedomax" potentiometer to indicate the load on the specimen, as measured by the strain-gage load cell on the Instron testing machine. Using a technique similar to that previously employed (24), this panel was viewed by a Traid Corporation, double-frame, 35-mm "Automax" Model R recording camera (shown in Figure 9) capable either of slow-speed cine operation or pulse operation at variable intervals predetermined by the setting of a Gordent Type 15A electric intervalometer.

The first series of tests revealed that the ultimate strains at failure (of the low-density, Grade H4LM specimens) were so small that considerable optical magnification was required to resolve them with adequate precision. This magnification was achieved by employing two front-surfaced mirrors to split the beam projected from the furnace and reflect the images of the two machined fiducial marks upon the ground-glass screen, as diagramed in Figure 10. By this means, a 50-dia magnification could be reconciled with a usably small separation of the two fiducial marks.

Figure 11 presents a typical frame from a photographic record, from which it may be seen that the machined fiducial marks appeared as rounded humps under high magnification, and it was necessary to provide

finer marks in the form of razor nicks in the region of increased cross section. Strain measurements were then reduced by reading the film record with a 35-mm Vanguard Model M-35 motion analyzer (also shown in Figure 9) with micrometer cross-hair movements calibrated to resolve a displacement of 0.001 in. on a 5-dia projected image of the photographic negative, and it was found that the apex of the razor cut could be reproducibly located within ±0.001 inch.

Since the "unfolded" gage length of the specimen image on the viewer was approximately 16 in., a total error of 0.002 in. in the location of the apex thus corresponded to a nominal precision of strain measurement of approximately 1.2×10^{-4}, although with practice this precision could be improved. This measurement was corrected for emulsion shrinkage by employing the image of a 6-in. scale cemented to the ground glass (as shown in Figure 11) as a standard reference length.

b. Creep Characteristics

The measurements of creep (or specimen strain vs time under constant load) employed the same type of test furnace and strain-vs-time measuring technique used in the stress-strain experiments. A standard Arcweld constant-load creep machine was modified to accommodate the furnace, as shown in Figures 12 and 13. In this machine, the load is applied by dead weights acting through a pivoted-beam system. The weights are released by the motion of a motor-driven table, thus permitting the rate of load application to be controlled. Such control (which was lacking in the earlier creep measurements) is required, since transient-creep curves may sometimes be noticeably influenced by variations in the rate of initial load application. For the small total strains involved, the constant-load creep data could be corrected and correlated by methods assuming constant stress.

c. Stress-Relaxation Behavior

A phenomenon analogous to creep, which must be considered in the design of high-temperature structures, is the relaxation of

stress in a member constrained to remain in a constant state of strain. For this reason, knowledge of the stress-relaxation behavior of the material at high temperatures was desirable. However, the design of the Los Alamos tensile specimen (Figure 8) accepted for the present investigation was such that relaxation would be effected by diffusional processes operating without as well as within the gage length. For this reason, the present program did not include measurement of tensile-stress relaxation.

d. Note on Tensile-Strain Measurements

Owing to the high degree of gage-length magnification involved in the image projection, small lateral displacements of the specimen in the test furnace would throw the images of the razor cuts slightly out of focus, and precise displacement measurements could be made only when the specimen was accurately positioned by the application of a slight tensile load to the specimen load train. This fact did not affect the stress-strain measurements made under slowly and monotonically increasing load, since the specimen was quickly positioned at very low load levels, and a short, linear, backward extrapolation of the initial displacement data served to establish the stress-strain origin with good precision.

In the case of the creep measurements, however, the load was applied rapidly, and the fast primary strain-vs-time transient following load application is highly nonlinear. The backward extrapolation to establish the strain-time origin was thus nonlinear, and enough uncertainty was involved to produce a scatter of points in the very short time region which is noticeable in the tensile-creep data presented later.

2. Torsional Properties

a. Torque-Twist Characteristics

In order to obtain measurements of shear properties in torsion, the test furnace diagramed in Figure 14 was designed. In this arrangement, the test specimen shown in Figure 15 was heated by radiation from a surrounding cylindrical graphite element locally cut in helical pattern

to provide a high-resistance path. Temperature control was maintained by the same means described above. The radiation shields, supports, and specimen-gripping rods were fabricated from ungraphitized carbon in order to minimize conduction losses. Since specimen temperatures ranging up to 2800°C were employed in the testing, however, some local graphitization of those parts adjacent to the hot zone may have taken place.

Torque was applied to the specimen by a wire, which is pulled by the moving platen of a wide-frame Instron machine, runs over a pulley connected to the load cell (thus registering load on the machine's Speedomax strip-chart recorder), and thus drives a 5-in.-radius wheel mounted on the specimen torque shaft. This arrangement of furnace mounting and torque application is shown in Figures 16 and 17. All components of the torque train were made sufficiently rigid that any twist detectable could safely be attributed to deformation within the specimen gage length. Total platen head rates of 2 and 10 in./min were used to effect rates of specimen twist per unit length of 0.1 and 0.5 rad/in.-min. Knowledge of the chart speed on the Speedomax recording the load thus defined the torque vs unit-twist curves discussed later. Measurement of the initial slopes of these curves then permitted calculation of an average shear modulus from the simplified strength-of-materials relation (57).

$$G = \frac{M}{\theta I_p} \qquad (2)$$

where

G = shear modulus (psi)

M = torque (in.-lb)

θ = angle of twist per unit length (rad/in.)

I_p = polar moment of inertia of specimen section

$$= \frac{\pi d^4}{32} = \frac{\pi (0.25)^4}{32} = 3.83 \times 10^{-4} \text{ in.}^4$$

d = specimen dia (in.)

The maximum shear stress at the outer fiber was similarly calculated as

$$S_{max} = \frac{Md}{2 I_p} \qquad (3)$$

$$= 3.26 \times 10^2 \text{ll(psi)}$$

b. Torsional-Creep Measurements

The torsional creep (twist-vs-time) measurements were performed under constant torque by applying a weight to the loading wire shown in Figure 11. The degree of twist, recorded as a function of time on the Speedomax strip chart, was indicated by a rotary potentiometer attached to the specimen torque shaft, as diagramed in Figure 18.

c. Torsional-Stress Relaxation

Relaxation of shear stresses in the specimen at constant strain was measured by rapidly twisting the specimen to a given initial torque level as in the torque-twist tests, but then stopping the moving platen and recording the load-vs-time decay curve on the Speedomax strip chart.

3. Dynamic Young's Modulus

When the tensile-test program was initiated with the low-density H4LM material, it soon became evident that the tensile strains achieved prior to failure were so small (generally less than 1%) that the initial portion of the stress-strain curve could not be defined with sufficient precision to permit confident calculation of Young's modulus from the slope of this curve at the origin. This problem was also complicated by the occasional occurrence of S-shaped curves with low initial slopes, thus producing an order of magnitude variation in calculated modulus values.

In view of this situation, a dynamic measurement was desired. For this purpose it was necessary to adapt a machine originally designed for the fatigue-testing of graphite specimens in reversed bending. To permit this adaptation, graphite specimens were fabricated by the Los Alamos Scientific Laboratory, and later were modified to the configuration shown in Figure 19.* In use, the specimen was clamped at one end (as shown in Figure 20), was heated by radiation from a surrounding graphite d-c helix, and was subjected to forced vibration as a cantilever beam by an electromagnetic driver attached to the "free" end by a linkage consisting of a flat molybdenum wire. The driving mechanism was a commercial fatigue-testing shaker system.** The oscillator, amplifier, power supply, and signal monitor for the electromagnetic shaker are shown in Figure 21.

In order to determine the elastic modulus of the beam material by measuring the resonant frequency of the mechanical system, it was necessary to idealize the system as having one degree of freedom. That is, the reduced section of the beam (which is really a many-degrees-of-freedom system) is considered as a simple elastic member with an effective (lumped) spring constant k and lumped mass m_1, to which is attached another mass m_e. Mass m_e represents the mass of the other moving parts of the system, including the mass and rotary inertia of the large, relatively rigid, "free" end of the beam to which the driving linkage is attached.

Damping in the system is provided by internal friction in the beam and linkage materials and by unavoidable support and radiation losses. The displacement of the linkage under a periodic force of amplitude P_o and angular frequency ω is thus related to the elastic and damping restraints by the expression

$$m\ddot{x} + c\dot{x} + kx = P_o \sin\omega t \qquad (4)$$

---

*In the original design, the section of reduced thickness was only 1.5 in. long; it was later lengthened to 2.0 in.

**Calidyne Company (Winchester, Mass.) Shaker System 6/77.

where $m = 0.23\, m_l + m_e$, and c = equivalent viscous-damping coefficient. Assuming that this displacement can be represented as $x = x_o \sin(\omega t - \phi)$, the amplitude and phase angle of the oscillation are given as

$$\frac{x_o}{P_o/k} = \frac{1}{\sqrt{\left(1 - \frac{\omega^2}{\omega_n^2}\right)^2 + \left(2\,\frac{c}{c_c}\,\frac{\omega}{\omega_n}\right)^2}} \tag{5}$$

and

$$\tan \phi = \frac{2\,\frac{c}{c_c}\,\frac{\omega}{\omega_n}}{1 - \left(\frac{\omega}{\omega_n}\right)^2} \tag{6}$$

where $P_o/k = x_{stat}$ is the static deflection under constant load P_o as $\omega \longrightarrow o$, c_c is the critical damping required for the most effective suppression of the oscillation, and ω_n is the natural frequency of the system with no damping.

Curves of the amplitude ration x_o/x_{stat} vs the frequency ratio ω/ω_n for various values of damping, reproduced from Den Hartog (58) are presented in Figure 22. The feature of the figure important in the present discussion is that the maxima of the various curves for finite damping do not occur at $\omega/\omega_n = 1$, but at a lower frequency. As noted by Den Hartog, three different frequencies must be distinguished, all of which coincide for c = o. These are:

(1) The undamped natural frequency

$$\omega_n = \sqrt{\frac{k}{m}} \tag{7}$$

(2) The damped natural frequency (of free vibration)

$$q = \sqrt{\frac{k}{m} - \left(\frac{c}{2m}\right)^2} \tag{8}$$

(3) The resonant frequency ω_r, or frequency of maximum forced amplitud

For systems with small damping, $\omega_n \cong q$. This approximation provides the basis of the conventional experiments for the determination of elastic moduli and the internal damping capacity (logarithmic decrement) of metals. In the present experiment, however, the natural (undamped) frequency cannot be determined by a direct measurement. The quantity that is measured directly is the resonant frequency ω_r. It is determined by recording the amplitude x_o of the forced vibration (indicated by the signal monitor in the control console) vs frequency. Typical resonance curves for graphite specimen that were obtained in the present investigation are presented in Figure 23. A comparison of Figures 17 and 18 indicates that the degree of damping is finite ($c/c_c = 0.3 - 0.4$) and that the approximation $\omega_r \cong \omega_n$ is not valid.

Fortunately, however, the approximation that $\omega_r \cong q$ is still admissible for finite damping. By equating the work (per cycle) done by the external force at resonance conditions to the work dissipated in damping at resonance, an expression for the resonance amplification R may be derived:

$$R \equiv \frac{(x_o)_r}{P_o/k} = \frac{k}{c\omega_r} \tag{9}$$

By eliminating the damping coefficient c between Equations 9 and 10,

$$\frac{k}{m} - q^2 = \left(\frac{k}{2mR\omega_r}\right)^2 \tag{10}$$

and making the approximation that $q \cong \omega_r$, the resulting quadratic expression for the spring constant k is solved as follows:

$$k = 2mR\omega_r^2 \left[R \pm \sqrt{R^2 - 1}\right] \tag{11}$$

Examination shows that the negative root is the physically reasonable one. It is also seen that the spring constant is related to the

resonant frequency in a manner similar to that of Equation 7, except for a damping correction factor which is a function of the resonance amplification ratio R:

$$k = m\omega_r^2 \left[f(R)\right] \tag{12}$$

A graph of $f(R) \equiv 2R\left[R - \sqrt{R^2 - 1}\right] = (\omega_n/\omega_r)^2$ vs R is presented in Figure 24. This graph indicates that as R becomes large (i.e., c becomes small) $f(R) \longrightarrow 1$ and $\omega_r \longrightarrow \omega_n$.

Equation 12 and Figure 19 thus provide a basis for the calculation of the spring constant (and, hence, Young's modulus) of the reduced beam section from measurements of the resonant frequency and resonance-amplification factor, such as are shown in Figure 17. This calculation takes consideration of the fact that the flexibility of the thickened end sections is not completely negligible, as indicated in Figure 25. It is shown there that, for the present specimen, the spring constant k_1 of the reduced-section "gage length" which provides the desired Young's-modulus measurement is 10% greater than the effective spring constant k for the entire beam as calculated by Equation 12.

The magnitudes of the various component masses which constitute the equivalent concentrated mass m_e may be identified as follows:

Specimen end block m_2 (typ.)	0.248 lbm
First-order correction for rotational inertia of m_2	0.037
Armature of electromagnetic shaker	0.564
0.23 x mass of shaker flex plates	0.037
Flexible connector, nuts, shields, etc.	0.023
Total m_e	0.909 lbm

Once the effective spring constant k (lbf/in.) is determined from the experimental measurements, the Young's modulus value for the gage

length region is calculated as shown in Figure 20; i.e., $k_1 = 1.10\ k$ and $E_1 = 400\ k_1$. This calculation neglects the variation in modulus arising from the temperature gradient along the specimen, but such a correction is negligible in view of the relatively mild temperature dependence involved and the minor contribution of the specimen and sections to the total compliance.

4. Thermal Expansion Properties

In the temperature range from 20 to about 1100°C, the linear thermal expansion properties of the various materials were measured under a vacuum in a standard Leitz dilatometer. In the range from about 1250 to 2400°C, the tensile creep-test furnace with the optical elongation measurement method described above was employed.

5. X-Ray Diffraction

As part of an earlier investigation (23), a brief effort was made to detect evidence for or against the existence of possible "cold working" of graphite. Filings of AUF graphite were pulverized with a mortar and pestle, and a sample of the finest fraction of this powder (from Tyler screen analysis) was vacuum-annealed at 1500°C. The annealed sample and another unannealed sample were subjected to X-ray diffraction analysis, and no evidence of line broadening due to working was detected.

The current investigation presented an opportunity to pursue this question further, and X-ray samples were cut from the central region of torsion-test specimens of each type of material under consideration, both from virgin specimens and specimens subjected to creep at 2600°C. These samples were transmitted to Professor B. Henke of Pomona College for X-ray diffraction analysis, using the standard North American Philips equipment.

IV. EXPERIMENTAL RESULTS

A. STRESS-STRAIN CHARACTERISTICS

1. Tensile Measurements

a. Commercial Grades

The tensile testing of commercial grades of material was initiated, using the standard (low-density) H4LM molded stock. Stress-strain curves for specimens cut with long axes both parallel and perpendicular to the grain, obtained at 2200, 2310, 2400, and 2500°C and at a total head or platen rate of 0.02 in./min, are presented in Figure 26. Similar data obtained at the two intermediate temperatures and at a platen rate of 0.002 in./min are presented in Figure 27, and it may be seen by comparison that the effect of strain rate appears to become noticeable at temperatures of about 2400°C. The large variation in observed properties among specimens in a given group manifests the typical non-uniformity of structure within a given block of manufactured graphite, a lack of uniformity recognized by all users of common commercial grades.

The most interesting feature of Figures 26 and 27 is the occurrence of several instances of S-shaped, stress-strain curves with inflection points between regions of positive and negative curvature. In other cases, only the region of negative (concave downward) curvature is defined This behavior, which is discussed later at greater length, was the factor which indicated the need for dynamic measurements of Young's modulus. In addition, it was desired to see whether the phenomenon might indicate possible hysteresis effects in repeated-loading tests. For this purpose, two specimens of each grain orientation at 2400°C were loaded to a point short of failure, unloaded to a low stress level, and reloaded to failure, all processes being conducted at a platen rate of 0.02 in./min. The results are presented in Figure 28, which again shows wide variations in specimen behavior. Examples of both large "plastic hysteresis" and of essentially elastic (although nonlinear)

recovery are evidenced. Figure 28 also suggests that the specimens stressed perpendicularly to their grain might show reduced hysteresis effects, but such a conclusion would have to be substantiated by further tests.

Whereas the testing described above sometimes compared as many as four specimens under a given test condition, and tests were performed at temperature intervals of 100°C, it was quickly discovered that such a procedure was not compatible with the scope of the contract; in subsequent measurements only two specimens per test condition were employed, and test temperatures were standardized at 2000, 2200, and 2400°C for the tensile stress-strain measurements. The data obtained with the reimpregnated (high-density) grade H4LM stock at platen rates of 0.02 and 0.002 in./min are shown in Figures 29 and 30, respectively.

In addition to the stress-strain measurements, ultimate tensile-strength determinations were conducted at temperatures ranging from the ambient level, and the results are shown in Figure 31. It should be noted that although the reimpregnated H4LM stock appears appreciably stronger than its standard counterpart, both materials must be regarded as relatively weak in comparison with the grades studied in other investigations (20, 21, 25, 28, 29, 30). Data corresponding to failure at the razor cut were discarded.

Although the present program concentrated on the H4LM commercial grades, a few tensile stress-strain determinations on Speer Carbon Company Grade 3499 at a platen rate of 0.02 in./min were included, and the results are shown in Figure 32. It may be noted that, in this small sample, at least, the 3499 stock exhibited marked superiority to the H4LM grades in ultimate breaking strength, ultimate elongation at failure, and reproducibility of behavior.

b. Los Alamos Grades

Tensile stress-strain characteristics of the four grades of stock manufactured at the Los Alamos Scientific Laboratory were measured at 2000, 2200, and 2400°C. The curves obtained for CK stock at

platen rates of 0.02 and 0.002 in./min are shown in Figures 33 and 34, respectively; those for LDH stock in Figures 35 and 36; those for LDC stock in Figures 37 and 38; and those for LDP stock in Figures 39 and 40. The ultimate breaking strength values measured over the range from ambient temperature to 2400°C are shown in Figure 41. It may be seen that the strength of the uranium-loaded grades increases with temperature in this range, just as does that of the pure grades. Grade LDH (containing 125 mg uranium per cc graphite) exhibited the highest strength at elevated temperature, a result confirming the similar measurements of Wagner, et al. (15). Owing to the scatter of the data (resulting from the well known lack of structural uniformity in most manufactured graphites mentioned earlier) no clear ranking of the other three grades could be established.

The stress-strain curves indicated that the pure (CK) grade of material showed the least plasticity at 2000°C, failing at an ultimate elongation of about 0.1%, compared with values ranging from 0.2 to 0.4% for the three loaded grades. At 2400°C, the ultimate elongations obtained with the pure material varied from 0.45 to 2.0%, whereas those of the U-loaded grades were somewhat more consistent: 0.6 to 1.2% for the LDH stock; 1.7 to 2.2% for the LDC stock; and 0.9 to 2.2% for the LDP stock. In most cases, the curves were of the conventional shape with monotonically decreasing slope, but a few examples of S-shaped characteristics were encountered.

2. Torsion Tests

a. Commercial Grades

By the time the torsion-testing was initiated, interest in the commercial grade of graphite had centered on the reimpregnated (high-density) H4LM stock; hence, this material was the only grade investigated. Torque-vs-twist data for H4LM specimens were obtained at temperatures from 20 to 2600°C. Torque-twist curves for specimens with long axes cut parallel to the grain obtained at unit-twist rates of 0.5 and 0.1 rad/min-in. are shown in Figures 42 and 43, respectively; those for the other orientation in

Figures 44 and 45. The curves are seen to be of the conventional shape, and fairly similar to one another.

To facilitate an evaluation of the rate effect, high-temperature data for one grain orientation at the two unit-twist rates are compared in Figure 46. Values of the maximum shear stress (in the outer fiber) at failure are presented versus temperature in Figure 47, from which it may be seen that the effect of grain orientation is not great. However, the rate effect becomes significant at high temperature, with the lower rate yielding higher ultimate strength values.

b. Los Alamos Grades

No torsion specimens of the stock with the highest uranium loading (LDP) were furnished for testing, so the measurements were limited to the CK, LDH, and LDC grades. The torque-twist curves for these materials (made under the same conditions described above) are presented in Figures 48 to 53, and the values for the ultimate shear stress at failure are presented in Figure 54. It should be noted that the LDC grade appeared to show the greatest shear-strength values at high temperature (but with a large scatter), whereas the LDH stock had exhibited superior tensile strength.

B. CREEP CHARACTERISTICS

1. Tensile Measurements

a. Commercial Grades

Tensile-creep measurements for the low-density H4LM stock were carried out early in the program at 2300 and 2400°C, and at stresses estimated (from the tensile-strength measurements) to be a certain fraction of the breaking strength. Following completion of the tests (which were arbitrarily limited to a duration of 60 min) the specimens were loaded to failure in 80-psi increments. These data are presented in Figure 55. With the later shift in emphasis to the re-impregnated stock, the temperatures were standardized at 2000, 2200, and 2400°C and the stress levels at 1720 and 2040 psi. The data from these tests are shown in Figure 56.

As a supplement to the systematic program, two exploratory tests were made in which specimens of the high-density stock were unloaded to a low stress following initial creep, allowed to recover, and reloaded at the initial stress to study the subsequent transient. This single example, shown in Figure 57, indicates that the specimen cut with axis perpendicular to the grain showed similar transient creep characteristics on both loadings, whereas the parallel-cut specimen exhibited a noticeably sharper transient on the second loading.

b. Los Alamos Grades

The creep measurements on the Los Alamos specimens were made at three temperatures (2000, 2200, and 2400°C) and at three stress levels (1630, 2130, and 2540 psi). The creep-strain vs time data obtained for the pure CK specimens* are shown in Figures 58 to 60, those for the uranium loaded specimens (LDH, LDC, LDP) in Figures 61 to 69.

c. Discussion

With the exception of the creep-recovery creep curves for the re-impregnated H4LM stock shown in Figure 57, the curves are presented on logarithmic coordinates in order to permit resolution of the data for times less than 5 min. It may be noticed that the shape of the smoothed curves for the LASL grades (on logarthmic coordinates) differs from the shape usually associated with metals; there appears to be no extended region of linearity characterizable by the approximation $\epsilon = Ct^m$, and the average curvature is negative. There did not appear to be any significant evidence of accelerated tertiary, or third-stage, creep among the curves from LASL materials, but the parallel-cut specimens of re-impregnated H4LM stock tested at 2000, and 2200°C indicated two instances of possible tertiary creep, suggesting imminent failure

*Due to its relatively low breaking strength the grade CK material could not be tested at the highest stress.

The most striking feature to be observed, however, is the frequency of instances in which specimens of nominally identical materials under identical conditions yielded markedly different creep histories. This effect is a manifestation of the unfortunate fact that the structure of manufactured graphites varies appreciably, not only between grades but also between lots of a given grade, between pieces of a given lot, and between locations in a given piece. Reduction of these variations by means of stringent quality control of manufacturing processes is currently under investigation by at least one commercial supplier. Even with the custom-made Los Alamos grades, a variation in the appearance of different batches of the non-loaded CK grade was observed; as indicated in Figure 70, the CK-64 material exhibited a rougher, more porous structure than did other batches of the same grade. This structural difference, which is attributed to introduction of a new batch of filler flour in the manufacture, is reflected in the creep behavior.

The results of tensile-creep studies on similar materials by Wagner et al. (15) at Los Alamos were correlated by the expression

$$\dot{\epsilon} = \frac{d\epsilon}{dt} = f(U)\left(\frac{\sigma}{\sigma_b}\right)^n e^{-\frac{\Delta H}{RT}} \qquad (13)$$

where

ϵ = Creep strain

σ = Stress

σ_b = Breaking stress

U = Uranium content (g/cc)

n = Empirical constant

ΔH = Activation energy (cal/mole)

R = Gas constant (cal/mole ^{o}K)

T = Absolute temperature (^{o}K)

The several adjustable parameters were evaluated by employing the "steady" creep rate $\dot{\epsilon}$ in the pseudo-linear, strain-vs-time region at the high end of the time scale. This procedure indicated that f(U) was a double-valued function of the creep rate

$$f(U) = 4 + 80U - 125U^2 \tag{14}$$

since grades LDC of intermediate uranium content showed higher creep rates than did the other grades, and that n = 3.8 and ΔH = 69 kcal/mole.

This procedure was not employed in the present study for several reasons. First, the concept of "steady-state" creep, which is dubious at best, is definitely inapplicable to the present results which showed that the observed creep rates decreased with time throughout the duration of the tests. Although use of the breaking stress, σ_b, as a basis for obtaining the reduced stress group, σ/σ_b, corrects for the large property variation between specimens, this device is of only aesthetic value. By its very nature, σ_b is an empirical constant which cannot be evaluated <u>a priori</u> without destruction of the actual piece of material concerned, and hence a correlation based on σ_b is of no use to the structural designer. Finally, it is not physically reasonable that the uranium content should influence the pre-exponential factor alone. The creep rate is generally expressable (59) as

$$\dot{\epsilon} = f(\sigma, T, st) \exp\left[\frac{-\Delta H(\sigma, T, st)}{RT}\right] \tag{15}$$

where st designates structure, and the influence of uranium content upon structure should thus also be manifested in the activation energy. A similar observation can be made for the stress dependence.

The method of correlation of the present data, selected after reviewing the recent surveys of Schoeck (59) and Dorn (60, 61) is that

employed by Tietz and Dorn (62), which assumes that the structure developed during the course of creep depends upon a temperature-compensated time, $\theta = t \exp(-\Delta H/RT)$, and that $\epsilon = \epsilon(\theta)$. Thus identical values of θ are achieved during creep at the same stress at two temperatures at the same total strain

$$t_1 e^{-(\Delta H/RT_1)} = t_2 e^{-(\Delta H/RT_2)} \tag{16}$$

and with the assumption that the temperature dependence of ΔH is mild in the region from T_1 to T_2,

$$\Delta H = \frac{R \ln(t_1/t_2)}{\frac{1}{T_1} - \frac{1}{T_2}} \tag{17}$$

In keeping within the belief of Dorn (61) that the most direct approach for investigating the creep mechanism and its dependence upon structural and environmental variables rests in studying not the time nor stress laws, but rather the activation energies, the data were reduced by the above method and no attention was given to effects manifested in a pre-exponential or frequency factor.

The reference creep strain selected for evaluation of activation energies was 0.1%, and the t-values employed were the averages of the times for the two specimens tested under each condition of creep to this strain value. Owing to the variation in stress level employed at the outset of the work, the data for the standard (low-density) H4LM stock shown in Figure 55 could not be used to derive activation energies. However, values of ΔH for the re-impregnated H4LM stock are shown in Table 1, and those for the Los Alamos grades in Table 2. It was noted that the creep curves shown in Figures 56 through 69 reveal a large piece-to-piece variation in the time required to achieve this strain under nominally identical conditions of

material and environment, and this effect is manifested in the large variation in the calculated values of ΔH summarized in Tables 1 and 2. These data generally indicate that any temperature dependence of ΔH has been obscured by the material variation, but in general the gross average ΔH (averaged for a given stress level) appears to decrease with increasing stress.

This result is dissimilar to those reported by Dorn and his associates for metals, in which the activation energy was found to be independent of stress, but is in agreement with the findings of Sherby and Dorn (63), using high-polymeric materials. Whereas Dorn and associates also reported strain-insensitive activation energies, a few calculations were made using a reference creep strain of 0.2% for comparison with the data presented above, and in almost every case an increased value of ΔH was obtained. However, in view of the large material variation, a comprehensive study of this trend was deferred.

It was suggested by Dorn and co-workers that the activation energy for creep of metals at high temperatures (i.e., $T/T_m \geq 0.5$) is equal to that for self-diffusion. Although the values of ΔH collected in Tables 1 and 2 cover a wide range, they are generally lower than the value 163 $\pm$12 kcal/mole reported by Kanter (64) for carbon self-diffusion. The large variation observed should also be contrasted to the results reported for similar materials by Wagner et al. (15), who assumed that the effects of uranium content and stress were isolated in the frequency factor, and obtained an activation energy which was roughly constant for all materials under all conditions.

2. Torsional Measurements

a. Commercial Grades

As mentioned earlier, the re-impregnated H4LM stock was the only commercial grade subjected to torsional measurements. Duplicate torsional creep (twist vs time under constant torque) tests of this stock for both specimen orientations were conducted at 2000, 2200, 2400, 2600, and 2800°C

under torques of 3.6 and 2.5 in.-lb for a duration of 60 min, and the data obtained are shown in Figure 71. It may be noted that the shape of the curves (again on logarithmic coordinates) is generally similar to that exhibited by the tensile creep curves.

In order to investigate the effect of work history on the transient creep behavior, a single sample of each orientation was subjected to creep under a torque of 2.5 in.-lb at 2600°C for 30 min, unloaded, cooled to room temperature, and then subjected to a repeated test under the identical conditions. The results of these measurements, as shown in Figure 72, clearly indicate a marked difference between the primary creep behavior exhibited by the first test of the virgin specimen and the repeated test of the pre-crept specimen.

b. Los Alamos Grades

Torsional-creep tests of the type described above were performed on specimens CK, LDH, and CK stocks under constant torques of 1.37, 2.04, and 2.75 in.-lb and at temperatures of 2000, 2200, 2400, 2600, and 2800°C. The curves obtained from these tests, which are presented in Figures 73 through 77, again show the typical shape described earlier. In addition, duplicate tests of these materials (but only at the highest torque level) were performed at 1800°C, and the results are collected in Figure 78. Finally, as in the case of the commercial stock, repeated tests on a single specimen of each grade were performed at 2600°C and, as shown in Figure 79, the effect of specimen work history upon transient creep behavior is again evident.

c. Discussion

The torsional creep data obtained from tests of the H4LM and Los Alamos graphites were employed to derive apparent activation energies for creep by the method outlined above. Owing to the wider temperature range covered in the torsion tests, however, it was necessary to employ two reference levels of creep strain (creep twist per unit length), 0.4 and

1.0 deg/in. This procedure was required by the fact that, at the higher temperature levels, creep proceeded so rapidly that it was difficult to resolve the time to achieve a unit twist of 0.4 deg/in. with adequate precision, whereas, at the lower temperatures, unit strains of 1.0 deg/in. were not realized during the 60-min tests.

The apparent ΔH values for torsional creep of the H4LM stock are presented in Table 3, and it may be noted that, in some cases, the effect of material variation was great enough to effect negative values of the apparent activation energy; i.e., the average time t_2 required for the two specimens tested at the higher temperature T_2 to achieve the reference twist was greater than the average time t_1 required at the lower temperature. No significance is attached to these negative ΔH values (other than as a manifestation of large property variations), and the values were included in the gross averages presented in Table 3 for each torque level.

Similar activation energies for torsional creep of the Los Alamos graphites are collected in Table 4, which also reveals a wide spread of ΔH values (again, a few negative) manifesting large piece-to-piece or batch-to-batch variations in structural properties. Examination of the data of Tables 3 and 4 indicates that any effect of temperature upon the apparent activation was completely masked by material variations, but suggests that, on the average, ΔH decreases with increasing stress and decreasing strain.

The effect of strain or work history on creep behavior could not be investigated systematically during the present program, but it appears pronounced enough to raise questions concerning the interpretation of those creep data reported by Wagner et al. (15, 31) and Martens et al. (32) which were derived from measurements of the "steady-state" slopes of individual sections of strain-vs-time curves obtained from tests in which a single specimen was subjected to a series of different stresses or temperatures.

C. STRESS RELAXATION

As discussed earlier, the stress-relaxation measurements were performed only with specimens loaded in torsion.

1. Commercial Grades

Torsional stress relaxation measurements using specimens of the re-impregnated H4LM stock with axes parallel and perpendicular to the grain were performed at 2000, 2200, 2400, 2600, and 2800°C using initial torque levels of 6.83 and 4.38 in.-lb. The torque-decay curves obtained are shown in Figure 80.

2. Los Alamos Grades

Stress relaxation tests of the Los Alamos grades CK, LDH, and LDC were conducted at 2000, 2200, 2400, and 2600°C under varying initial torques. The torque-decay curves obtained with the three grades are presented in Figures 81-83.

3. Discussion

Activation-energy values for the relaxation process were derived by the method of Mason and Anderson (65) and Anderson and Andreatch (66), which leads to an expression for ΔH identical with Equation (18), except that the t-values refer to the time required for the stress (or, in the present case, torque) to decay to a given fraction of its original value. The reference torque ratio employed in the present study was $M/M_o = 0.8$ and the t-values represent the average time for the two specimens tested under each condition to relax to this degree.

Figures 80-83 exhibit the same type of variation among nominally identical specimens, which was revealed by the stress-strain and creep measurements, and again this variation is reflected in a wide scatter of apparent activation energies (including some negative values) assembled in Table 5 for the H4LM stock and Table 6 for the Los Alamos grades. The ΔH values for the latter grades represent average estimates for a given narrow range of initial torque levels, rather than for a constant level as maintained in the H4LM tests.

This approximation is considered justified by the fact that the material variation appears to mask the effect of both temperature and stress (or strain) level upon the activation energy. These results may be compared with those of Anderson and Andreatch (66) on gold wires obtained over a wide range of tensile stresses, which indicated a strong negative variation of ΔH with stress level which extrapolated to the value for self-diffusion at the zero-stress intercept.

D. ELASTIC MODULI

1. Young's Modulus

a. Commercial Grades

The values of dynamic Young's modulus for the standard and re-impregnated H4LM stock, obtained by the technique described earlier, are presented in Figure 84. It may be noted that the modulus ratios show the thermal dependence expected on the basis of earlier measurements (22), i.e., an increase with increasing temperature up to about 2000-2200°C, followed by a decrease due to thermal softening. It is noteworthy, however, that the absolute magnitude of the observed moduli at high temperature are of the order $2\text{-}3 \times 10^5$ psi, a value which is low by comparison to the average slopes of the tensile stress-strain curves presented in Figures 26 to 30.

This apparent discrepancy is attributed to the fact that the maximum fiber strain produced in the flexural vibration technique employed was small, of the order of 0.01%, and thus the dynamic-modulus values obtained corresponded to small oscillations along the "toe" of an S-shaped, stress-strain curve of the type illustrated in Figures 26 to 30. Measurement of the slope of the "toe" regions shown in these figures yielded static modulus values of the same magnitude as the dynamic values indicated in Figure 84. It was desired to confirm the above belief by experiments using vibration forced at higher amplitude, but it was found that the electromagnetic shaker was not capable of effecting an increased amplitude. Whereas greater deflections could have been realized by using a more slender specimen section, the natural

frequency would thus have been reduced to a value too low to permit use of the available oscillator.

b. Los Alamos Grades

In the case of the Los Alamos graphites, which were manufactured in the form of relatively thin plates, specimens of the size required for the dynamic measurements could not be fabricated, and the tensile stress-strain curves thus provided the only Young's modulus information on these materials. The values derived from measurement of the slope at the stress-strain origin for the two limiting temperature levels (2000 and 2400°C) are presented in Table 7. Although these values appear to be of the proper order of magnitude, and show the anticipated decrease in the range from 2000 to 2400°C, they must be regarded as strictly provisional pending confirmation by dynamic measurements.

2. Shear Moduli

Since only static measurements were made in torsion, mean values for the shear modulus were derived from the slopes of the torque-twist curves of Figures 42 to 53 according to Equation 3. The results for the re-impregnated H4LM stock and the Los Alamos Grades are presented in Figures 85 and 86, respectively. No pronounced rate effect is evident, but the scatter is considerable, and no attempt to fit a smoothed curve to the data, as was possible for earlier dynamic measurements (22), was made.

3. Discussion

It was noted in the introductory review that no satisfactory theoretical explanation for the observed thermal dependence of the elastic moduli of graphite had been advanced. Four separate results of the present investigation, however, suggest that the mechanical behavior may be considered analogous to that of high polymers. These results were, in order of mention in the preceding discussion, as follows:

a. Instances of S-shaped, tensile stress-strain curves with regions of positive curvature at low strain levels were observed. On some occasions, this inflected curvature could be questioned on the basis of

the precision of measurement of the small strains involved, but on other occasions the behavior was observed at easily measurable strains, and is not considered debatable.

b. Despite a wide scatter arising from material-properties variations among individual specimens, on the average a negative dependence of the apparent activation energy for creep upon stress level was discernible, a trend which is strongly evidenced by polymer creep bahavior (63).

c. Dynamic measurements at low strain level yielded values of Young's modulus of the same low order as the slopes of the "toes" of the S-shaped stress-strain curves.

d. The Young's and shear moduli increase with increasing temperature up to the range 2000-2200°C, at which point thermal softening (creep) produces a decrease.

In considering the proposed comparison between graphite and high-polymer behavior, the following observations concerning polymeric behavior should be recalled. Since ordinary polymers exhibit softening at low temperatures, their dynamic moduli initially decrease with increasing temperature until the transition from the regime of "glassy" behavior to that of "rubbery" behavior is achieved. When stressed in the rubbery state, these materials at high elongations (i.e., > 200%) exhibit stress-strain curves of positive curvature owing to the commencement of what, in the vocabulary of rheology (67), is called "strain-induced crystallinity." Under this condition the molecules line up from regions of crystalline order as diagramed schematically in Figure 87. Also included in Figure 87 are schematic representations of polycrystalline graphite structures, as envisaged by Castle (68) and Mrozowski (10); a certain degree of similarily between the representations is obvious.

The dynamic modulus of polymers in the rubbery state increases with temperature in a fashion which is expressable in the form of a modified "equation of state"

$$E \propto \frac{\rho}{M} RT \qquad (18)$$

where

E = Young's modulus

ρ = density of solid

M = molecular weight between crosslinks

and this type of expression is used to determine the molecular weight of polymers from experimental modulus measurements.

Since the individual layers of the graphite crystal are bound together by relatively weak van der Waals forces, it does not seem inadmissible to regard these layers as planar molecules loosely bonded to form structures analogous to the regions of strain-induced crystallinity in rubber-like polymers. The graphite structure is crystalline without any pre-strain, and thus stress-strain characteristics with positive curvature could be expected at low strain levels, with the inflection to negative curvature at higher strain levels being attributed to plastic deformation in the conventional sense. The increase in Young's modulus with temperature is directly analogous to polymer behavior, with the melting point of the material determining at which end of the temperature spectrum thermal softening leads to a decrease in modulus with temperature.

The analogy drawn above is by no means conclusively supported, but is advanced as an heuristic argument suggesting that the concepts of polymer physics may be useful in interpreting the results of mechanical-properties measurements on polycrystalline graphites.

E. THERMAL-EXPANSION COEFFICIENTS

The results of the measurements of coefficient of linear thermal expansion for the H4LM and Los Alamos graphites are presented in Table 8. Each value tabulated represent an average of two measurements. The coefficients for the pure grades are seen to be of the same order of magnitude as those previously reported for other types of stock, and also exhibit the same increase

with temperature. The addition of uranium, however, appears to counteract this temperature effect, by increasing the average coefficient for the low-temperature range (20-1050°C) to the point that it may exceed that for the high-temperature range (1300-2400°C).

F. X-RAY DIFFRACTION

The results of the x-ray diffraction scanning in search of possible line broadening attributable to "hot" working during torsional creep at 2600°C were negative. Comparison of traces from virgin and twisted samples of each type of stock revealed no evidence of any working.

V. CONCLUSIONS AND RECOMMENDATIONS

The foregoing discussion has described the results of various mechanical properties measurements on several grades of pure and uranium-loaded graphites at elevated temperatures. Tensile-strength determinations indicated that the breaking strength of the uranium-laden grades showed the same temperature dependence exhibited by the pure grades, a result confirming previous measurements at Los Alamos, and a similar result was obtained using specimens stressed in torsion. On some occasions, the tensile stress-strain curves showed an S-shape, with initial slopes corresponding to static Young's modulus values of the order of 10^5 psi. Low-amplitude dynamic measurements for the H4LM commercial stock yielded similar values, but it was not possible to study the effect of increased amplitude.

It is recommended that the elastic and anelastic properties of various graphites be made the subject of continuing investigation, and that such work should include study of the internal-friction and Poisson's-ratio variations with environmental and processing variables. If a correlation between elastic-anelastic properties and strength properties could be established, a much-needed means of nondestructive inspection of manufactured stock would be at hand

Measurements of tensile-creep properties were conducted under a relatively narrow range of stress and temperature. Creep and relaxation properties in torsion were studied over a wider temperature range, but still within only a narrow stress range. The data were used to calculate apparent activation energies for the thermally-activated diffusional processes involved.

The scatter of the results emphasizes the need for continuing efforts to produce graphites of increased homogeniety and reproducibility of properties from batch to batch. Extension of the present investigation to include a wider range of environmental conditions is recommended, in order to delineate the effects of stress and temperature upon the activation energy, to study the effect of strain history in a systematic fashion, and to investigate the effect of a fast-neutron field upon creep and relaxation behavior. This latter effect is of obvious importance for high-temperature reactor applications; calculations by Schock (69) indicate that, for pure graphite at temperature $T_m/2$, a flux of 10^{13} fast neutrons/cm^2-sec would double the creep rate otherwise obtaining without radiation. Tenfold increases in the flux above this value would produce corresponding order-of-magnitude increases in creep rate. The effect of fission-fragment bombardment on the creep of fuel-loaded graphites is not so easily estimated. In view of the above situation, it is recommended that in-pile creep and/or relaxation measurements on pure and fuel-laden graphites be undertaken.

REFERENCES

1. R. E. Schreiber, "Nuclear Rocket Propulsion Program at Los Alamos," Amer. Rocket Soc. Preprint 689-58, New York, November 1958.

2. P. Hidnert, "Thermal Expansion of Artificial Graphite and Carbon," J. Research, National Bureau of Standards, Vol. 13, pp. 37-51, 1934.

3. J. B. Nelson and D. P. Riley, "Thermal Expansion of Graphite from 15°C to 800°C," Proc. Phys. Soc. (London), Vol. 57, pp 477-495, 1945.

4. H. L. Riley, "Amorphous Carbon and Graphite," Quart. Revs. (London), Vol. 1, pp. 59-72, 1947.

5. P. Duwez, "A Comparison of Some Physical Properties of Five Grades of Graphite," Jet Propulsion Laboratory Progress Report No. 4-30, California Institute of Technology, 26 February 1947.

6. S. Mrozowski, "Anisotropy of Thermal Expansion and Internal Stresses in Graphite and Carbons," Bull. Amer. Phys. Soc., Vol. 27, p. 47, 1952.

7. P. L. Walker, H. A. McKinstry, and C. C. Wright, "X-Ray Diffraction Studies of a Graphitized Carbon; Changes in Interlayer Spacing and Binding Energy with Temperature," Ind. Eng. Chem., Vol 45, pp 1711-1715, 1953.

8. C. F. Lucks and H. W. Deem, "Thermal Conductivities, Heat Capacities, and Linear Thermal Expansion of Five Materials," WADC Technical Report 55-496, ASTIA Document AD 97185, August 1956.

9. N. S. Rasor and J. D. McClelland, "Thermal Properties of Materials. Part 1 - Properties of Graphite, Molybdenum, and Tantalum to Their Destruction Temperatures," WADC Technical Report 56-400, Part I, AI-1672, August 1956.

10. S. Mrozowski, "Mechanical Strength, Thermal Expansion and Structure of Cokes and Carbons," Proc. First and Second Conferences on Carbon, University of Buffalo, pp. 31-45, 1956.

11. F. M. Collins, "Dimensional Changes During Heat Treatment and Thermal Expansion of Polycrystalline Carbons and Graphite," Ibid., pp. 177-187.

12. P. Cornuault, H. Hering, and M. Seguin, "Correlation Between Raw Materials and Mechanical Treatment of the Green Paste, and Some Properties of the Resulting Graphite," presented at the Third Biennial Carbon Conference, University of Buffalo, 17 to 21, June 1957.

REFERENCES (cont.)

13. P. L. Walker, Jr., F. Rusinko, Jr., J. F. Rakszawski, and L. M. Liggett, "Effect of Different Cokes on Physical Properties of Graphitized Carbon Plates," Ibid.

14. F. M. Collins, "Thermal Expansion of Polycrystalline Carbons," Ibid.

15. P. Wagner, A. R. Driesner, and E. A. Kmetko, "Some Mechanical Properties of Graphite in the Temperature Range 20° to 3000°C," United Nations Paper No. 702, presented at the Second United Nations International Conference on Peaceful Uses of Atomic Energy, Geneva, Switzerland, 1 to 13 September 1958.

16. M. C. Udy and F. W. Boulger, "The Properties of Graphite," BMI-T-35, 20 June 1950.

17. J. P. Howe, "Properties of Graphite," J. Am. Ceram. Soc., Vol. 35, pp. 275-283, 1952.

18. J. A. Slyh, "Graphite," Chapter 1.9 of General Properties of Materials, Vol. 3, Section 1 of The Reactor Handbook, AECD-3647, March 1955.

19. L. M. Currie, V. C. Hamister, and H. G. MacPherson, "The Production and Properties of Graphite for Reactors," Proc. United Nations International Conference on the Peaceful Uses of Atomic Energy, (Geneva, Switzerland, 8 to 20 August 1955).

20. C. Malmstrom, R. Keen, and L. Green, Jr., "Some Mechanical Properties of Graphite at Elevated Temperatures," North American Aviation, Inc. Report No. NAA-SR-79, 28 September 1950; also, J. Applied Phys., Vol. 22, pp 593-600, 1951.

21. R. E. Adams and H. R. Nelson, "Tensile and Creep Properties of Graphite," BMI-N-45, 1 May 1950.

22. F. E. Faris, L. Green, Jr., and C. A. Smith, "The Thermal Dependence of the Elastic Moduli of Polycrystalline Graphite," J. Applied Phys., Vol. 23, pp. 89-95, 1952.

23. L. Green, Jr., "The Behavior of Graphite Under Alternating Stress," North American Aviation, Inc., Report No. NAA-SR-115, 4 May 1951. Also, J. Applied Mechanics, Trans. ASME, Vol. 73, p. 345, 1951.

24. L. Green, Jr., "High-Temperature Compression Testing of Graphite," North American Aviation, Inc., Report No. NAA-SR-165, 7 January 1952. Also, J. Applied Mechanics, Vol. 20, pp. 289-294, 1953.

REFERENCES (cont.)

25. R. D. Keen, "Experience with Graphite as a Fabrication Material in High-Temperature Heat-Transfer Systems," Nuclear Engineering, CEP Symposium Series, Vol. 50, No. 11, 1954, pp. 45-51.

26. L. D. Loch and J. A. Slyh, "The Technology and Fabrication of Graphite," Ibid., pp. 39-44.

27. L. D. Loch, "How Graphite Performs at High Temperatures," Materials and Methods, pp. 126-129, May 1956.

28. H. E. Martens, L. D. Jaffe, and J. O. Jepson, "Tensile Properties of Some Graphites at 4000°F to 5000°F," presented at the Third Biennial Carbon Conference, University of Buffalo, 17 to 21 June 1957.

29. H. E. Martens, L. D. Jaffe, and J. E. Jepson, "High-Temperature Tensile Properties of Graphites," Jet Propulsion Laboratory Progress Report No. 20-326, California Institute of Technology, 30 September 1957.

30. L. Simbeck, F. Wiener, and I. L. Harvey, "Graphite: Unique Properties Help Solve Missile Design Problems," Missile Design & Development, pp. 16-18, May 1958.

31. P. Wagner, A. R. Driesner, E. A. Kmetko, and D. P. MacMillan, "Some Physical Properties of a Commercial Graphite from Ambient Temperature to 2500°C," presented at the 114th Meeting of the Electrochemical Society, Ottawa, Canada, 29 September 1958.

32. H. E. Martens, L. D. Jaffe, and D. D. Button, "High-Temperature Short-Time Creep of Graphite," Ibid.

33. H. C. Stieber and R. C. Stroup, "Measurement of Creep in Graphite at 2500-3000°C," Ibid.

34. L. Green, Jr., M. L. Stehsel, and C. E. Waller, "High-Temperature Mechanical Property Measurements on Pure and Uranium-Loaded Graphites," (Unclassified) contained in Proceedings of the Refractory Materials Meeting, Los Angeles, California, 27, 28 May 1958, NAA-SR-2790, September 15, 1958 (Classified).

35. L. Green, Jr., M. L. Stehsel, and C. E. Waller, "High-Temperature Mechanical Properties of Two Commercial Graphites," presented at 114th Meeting of the Electrochemical Society, Ottawa, Canada, 29 September 1958.

REFERENCES (cont.)

36. L. Green, Jr., "The Erosion of Graphite by High Temperature Helium Jets," North American Aviation, Inc. Report No. NAA-SR-77, 24 May 1950.

37. L. Green, Jr., "Gas Cooling of a Porous Heat Source," North American Aviation, Inc. Report No. NAA-SR-163, 13 December 1951. Also, J. App. Mech., Vol. 19, pp 173-178, 1952.

38. W. D. Smiley, "Investigation of Carbon (Graphite) Base Materials Suitable for Rocket and Ram-Jet Applications," WADC Technical Report 54-491, Part 2, Stanford Research Institute, November 1955.

39. D. J. Masson and C. Gazley, Jr., "Surface-Protection and Cooling Systems for High-Speed Flight," The Rand Corp. Report No. P-829, 23 March 1956; Also, Aeronautical Engineering Review, Vol. 15, November 1956.

40. Daniels, F., "Small Gas-Cycle Reactor Offers Economic Promise," Nucleonics, Vol. 14, p. 34, 1956.

41. L. Green, Jr., "Graphite as a Material for High-Temperature Gas Flow Systems," American Rocket Society Preprint No. 382-56, New York, November 1956.

42. W. F. Courtis and C. Rodziewicz, "Investigations of Selected Graphites for High Temperature and Surface Erosion Conditions," presented at the Third Biennial Conference on Carbon, University of Buffalo, 17 to 21 June 1957.

43. F. P. Durham, R. C. Neal, and H. J. Newman, "High Temperature Heat Transfer to a Gas Flowing in Heat-Generating Tubes with High Heat Flux," Los Alamos Scientific Laboratory, Los Alamos, New Mexico.

44. H. Marcus, P. W. Dimiduk, and G. Sonnenschein, "Endothermic Cooling of High-Temperature Surfaces," presented at AFOSR-Rand Corp. Symposium on Mass-Transfer Cooling for Hypersonic Flight, Santa Monica, California, 24 to 26 June 1957.

45. E. R. G. Eckert and J. P. Hartnett, "The Effect of Combustion on Heat Transfer to the Skin of a Vehicle Re-Entering the Atmosphere," Ibid.

46. H. L. Wheeler and P. Duwez, "Materials for Sweat-Cooled Walls," Ibid.

47. M. R. Denison and D. A. Dooley, "Combustion in the Laminar Boundary Layer of Chemically Active Sublimators," Aeronutronic Systems, Inc. Publ. No. C-110, Glendale, California, 23 September 1957.

REFERENCES (cont.)

48. J. R. Stalder, "The Useful Heat Capacity of Several Materials for Ballistic Nose-Cone Construction," NACA TN 4141, November 1957.

49. M. H. Rosenblum, W. T. Rinehart, and T. L. Thompson, "Rocket Propulsion with Nuclear Energy," American Rocket Society Preprint No. 559-57, New York, December 1957.

50. L. Green, Jr., and K. L. Nall, "Heat Removal from a Resistance-Heated Porous Solid," Aerojet Report No. 1380, Azusa, California, 31 December 1957.

51. L. Green, Jr. and J. M. Carter, "Performance Calculations for Hybrid Nuclear-Chemical Rocket Propulsion Systems," American Rocket Society Preprint No. 595-58, Dallas, March 1958.

52. S. Mrozowski, "Physical Properties of Carbon and the Formulation of the Green Mix," Proc. First and Second Conferences on Carbon, University of Buffalo, pp. 195-215, 1956.

53. L. H. Juel, Private Communications, 8 and 29 September 1958.

54. R. N. Hader, B. W. Gamson, and B. L. Bailey, "Graphite Electrodes: A Staff-Industry Collaborative Report," Ind. Eng. Chem., Vol. 46, pp. 2-11, 1954.

55. N. C. Hodge, "Typical Distributions of Graphite Properties," presented at the 114th Meeting of the Electrochemical Society, Ottawa, Canada, 29 September 1958.

56. W. P. Eatherly, M. Janes, R. L. Mansfield, R. A. Bourdeau, and R. A. Meyer, "Physical Properties of Graphite Materials for Special Nuclear Applications," presented at the Second United Nations International Conference on Peaceful Applications of Atomic Energy, Geneva, Switzerland, 1 to 13 September 1958.

57. S. Timoshenko and G. H. MacCullough, Elements of Strength of Materials, (2nd Edition), D. Van Nostrand Company, Inc., New York, 1940.

58. J. P. Den Hartog, Mechanical Vibrations (2nd Edition), McGraw-Hill Book Company, Inc., New York, p. 64, 1940.

59. G. Schoeck, "Theory of Creep," Creep and Recovery, American Society for Metals, Cleveland, Ohio, pp. 199-226, 1957.

REFERENCES (cont.)

60. J. E. Dorn, "The Spectrum of Activation Energies for Creep," Ibid. pp. 225-283.

61. J. E. Dorn, "A Survey of Recent Results on Experimental Determinations of Activation Energies for Creep," Fourth Sagamore Ordnance Materials Research Conference, Raquette Lake, New York, 21 to 23 August 1957.

62. T. E. Tietz and J. E. Dorn, "Creep of Copper at Intermediate Temperatures," J. Metals (Trans. AIME), pp. 156-162, February 1956.

63. O. D. Sherby and J. E. Dorn, "Anelastic Creep of Polymethyl Methacrylate," J. Mech. Phys. Solids, Vol. 6, pp. 145-162, 1958.

64. M. A. Kanter, "Diffusion of Carbon Atoms in Natural Graphite Crystals," Ph.D. Thesis, Illinois Institute of Technology, June 1955.

65. W. P. Mason and O. L. Anderson, "Stress Systems in the Solderless Wrapped Connection and Their Performance," Bell Syst. Tech. Jour., Vol. 33, pp. 1093-1110, 1954.

66. O. L. Anderson and P. Andreatch, "Stress Relaxation in Gold Wire," J. App. Phys., Vol. 20, pp. 1518-1519, 1955.

67. P. J. Flory, Principles of Polymer Chemistry, Cornell University Press, Ithaca, N. Y., p. 432 ff., 1953.

68. J. G. Castle, Jr., "Heat Conduction in Carbon Materials," Proc. First and Second Conferences on Carbon, University of Buffalo, pp. 13-19, 1956.

69. G. Schoeck, "Influence of Irradiation on Creep," J. App. Phys., Vol. 29, pp. 112, 1958.

TABLE 1

APPARENT ACTIVATION ENERGIES FOR TENSILE CREEP
OF RE-IMPREGNATED H4LM STOCK

(Reference Creep Strain 0.1 Percent)

Av Temp. °C	Stress psi	ΔH kcal/mole	Av ΔH kcal/mole
	Specimen Axis Parallel to Grain		
2100	1720	69.3	67
2300	1720	65.3	
2100	2040	6.1	43
2300	2040	80.2	
	Specimen Axis Perpendicular to Grain		
2100	1720	114	112
2300	1720	109	
2100	2040	97.5	99
2300	2040	99.6	

TABLE 2

APPARENT ACTIVATION ENERGIES FOR TENSILE CREEP
OF LOS ALAMOS GRADES

(Reference Creep Strain 0.1 Percent)

Av Temp. °C	Stress psi	ΔH kcal/mole	Av ΔH kcal/mole
	Grade CK Stock		
2100	1630	93.9	74
2300	1630	54.8	
2100	2130	83.2	77
2300	2130	70.8	
	Grade LDH Stock		
2100	1630	203	126
2300	1630	49.0	
2100	2130	80.0	88
2300	2130	96.2	
2100	2540	18.4	25
2300	2540	31.2	
	Grade LDC Stock		
2100	1630	130	85
2300	1630	39.2	
2100	2130	0.8	73
2300	2130	146	
2100	2540	37.1	72
2300	2540	108	
	Grade LDP Stock		
2100	1630	111	58
2300	1630	5.1	
2100	2130	32.8	78
2300	2130	123	
2100	2540	81.0	91
2300	2540	101	

TABLE 3

APPARENT ACTIVATION ENERGIES FOR TORSIONAL CREEP OF RE-IMPREGNATED H4LM STOCK

Av. Temp. °C	Torque in.-lb		ΔH (kcal/mole) Ref. Unit Twist (deg/in.) 0.4	1.0
		Specimen Axis Parallel to Grain		
2100	2.5		86.5	-
2300	2.5		-3.3	-4.1
2500	2.5		128	208
2700	2.5		-	174
		Av	70	126
2100	3.6		121	-
2300	3.6		85.2	89.2
2500	3.6		147	134
2700	3.6		-	172
		Av	118	132
		Specimen Axis Perpendicular to Grain		
2100	2.5		85.2	-
2300	2.5		70.2	136
2500	2.5		96.7	127
2700	2.5		-	153
		Av	83	139
2100	3.6		61.5	-
2300	3.6		164	24.3
2500	3.6		8.5	46.1
2700	3.6		-	16.7
		Av	78	29

TABLE 4

APPARENT ACTIVATION ENERGIES FOR TORSIONAL CREEP OF LOS ALAMOS GRADES

Av ^{o}C Temp.	Torque in.-lb		ΔH (kcal/mole) Ref. Unit Twist (deg/in.) 0.4	1.0
		CK Stock		
2100	1.37		-	-
2300	1.37		185	-
2500	1.37		57.3	74.9
2700	1.37		238	254
		Av	160	164
2100	2.04		-73.8	-
2300	2.04		151	-
2500	2.04		53.2	150
2700	2.04		-	189
		Av	43	170
1900	2.75		28.1	-
2100	2.75		72.7	-
2300	2.75		56.9	-
2500	2.75		120	159
2700	2.75		-	-133
		Av	69	13
		LDH Stock		
2100	1.37		-	-
2300	1.37		249	-
2500	1.37		-13.9	-
2700	1.37		152	-
		Av	129	
2100	2.04		87.3	-
2300	2.04		182	-
2500	2.04		-	214
2700	2.04		-	45.5
		Av	135	130

TABLE 4 (cont.);

Av Temp. (°C)	Torque (in.-lb)		ΔE (kcal/mole) Ref. Unit Twist (deg/in.) 0.4	1.0
1900	2.75		54.7	-
2100	2.75		15.9	34.1
2300	2.75		75.4	147
2500	2.75		-39.1	162
2700	2.75		-	41.2
		Av	27	96
		LDC Stock		
2100	1.37		23.2	-
2300	1.37		8.0	-
2500	1.37		106	-
2700	1.37		159	366
		Av	74	366
2100	2.04		81.5	-
2300	2.04		29.2	180
2500	2.04		143	175
2700	2.04		-	117
		Av	85	157
1900	2.75		-31.3	-
2100	2.75		112	51.2
2300	2.75		56.0	125
2500	2.75		-	156
		Av	46	111

TABLE 5

APPARENT ACTIVATION ENERGIES FOR TORSIONAL-STRESS RELAXATION OF RE-IMPREGNATED H4LM STOCK

Av ^{o}C Temp	Initial Torque in.-lb		ΔH kcal/mole
	Specimen Axis Parallel to Grain		
2100	6.88		34.4
2300	6.88		46.3
2500	6.88		72.3
2700	6.88		161
		Av	79
2100	4.38		115
2300	4.38		-29.2
2500	4.38		60.2
2700	4.38		133
		Av	70
	Specimen Axis Perpendicular to Grain		
2100	6.88		35.6
2300	6.88		49.8
2500	6.88		39.6
2700	6.88		130
		Av	64
2100	4.38		112
2300	4.38		75.8
2500	4.38		-42.7
2700	4.38		151
		Av	74

TABLE 6

APPARENT ACTIVATION ENERGIES FOR TORSIONAL-STRESS RELAXATION OF LOS ALAMOS GRADES

Av ^{o}C Temp	Initial Torque in.-lb	ΔH kcal/mole
	Grade CK Stock	
2100	6.25 - 6.88	40.5
2300	6.88 - 7.75	80.8
2500	7.75 - 6.88	62.9
2100	3.75 - 4.38	70.1
2300	4.38 - 5.00	72.2
2500	5.00 - 5.00	26.8
	Grade LDH Stock	
2100	6.25 - 6.88	50.5
2300	6.88 - 7.75	13.3
2500	7.75 - 6.88	23.6
2100	3.75 - 4.38	46.6
2300	4.38 - 5.00	19.7
2500	5.00 - 5.00	0
	Grade LDC Stock	
2100	6.25 - 6.88	58.7
2300	6.88 - 7.75	0.98
2500	7.75 - 6.88	41.1
2100	3.75 - 4.38	5.1
2300	4.38 - 5.00	93.8
2500	5.00 - 5.00	9.8

TABLE 7

PROVISIONAL YOUNG'S MODULUS VALUES FOR LOS ALAMOS GRAPHITES DERIVED FROM SLOPE OF STATIC STRESS-STRAIN CURVES AT ORIGIN

Grade of Stock		Young's Modulus (10^6 psi) 2000°C	2400°C
CK		1.5	1.2
CK		1.5	0.6
CK		1.6	0.6
	Av	1.3	0.8
LDH		1.1	0.6
LDH		1.0	0.25
LDH		1.2	0.25
	Av	1.1	0.37
LDC		4.5	0.6
LDC		1.6	0.8
LDC		0.5	3.5
	Av	3.3	1.6
LDP		1.7	0.9
LDP		0.7	0.5
LDP		4.0	0.6
	Av	2.1	0.67

TABLE 8

AVERAGE COEFFICIENTS OF LINEAR THERMAL EXPANSION
FOR PURE AND URANIUM-LOADED GRAPHITES

Type of Stock	Temperature Range °C	Av Linear Expansion Coefficient (10^{-6}/°C)
Standard H4LM (Parallel to Grain)	20 - 1090	2.53
	1260 - 2400	4.32
Standard H4LM (Perpendicular to Grain)	20 - 1090	2.88
	1260 - 2400	4.58
Re-impregnated H4LM (Parallel to Grain)	20 - 1050	2.29
	1260 - 2400	4.08
Re-impregnated H4LM (Perpendicular to Grain)	20 - 1050	3.02
	1260 - 2400	4.53
CK	20 - 1050	2.37
	1300 - 2400	4.80
LDH	20 - 1050	2.90
	1300 - 2400	4.85
LDC	20 - 1050	3.95
	1300 - 2400	4.00
LDP	20 - 1050	4.50
	1300 - 2400	4.16

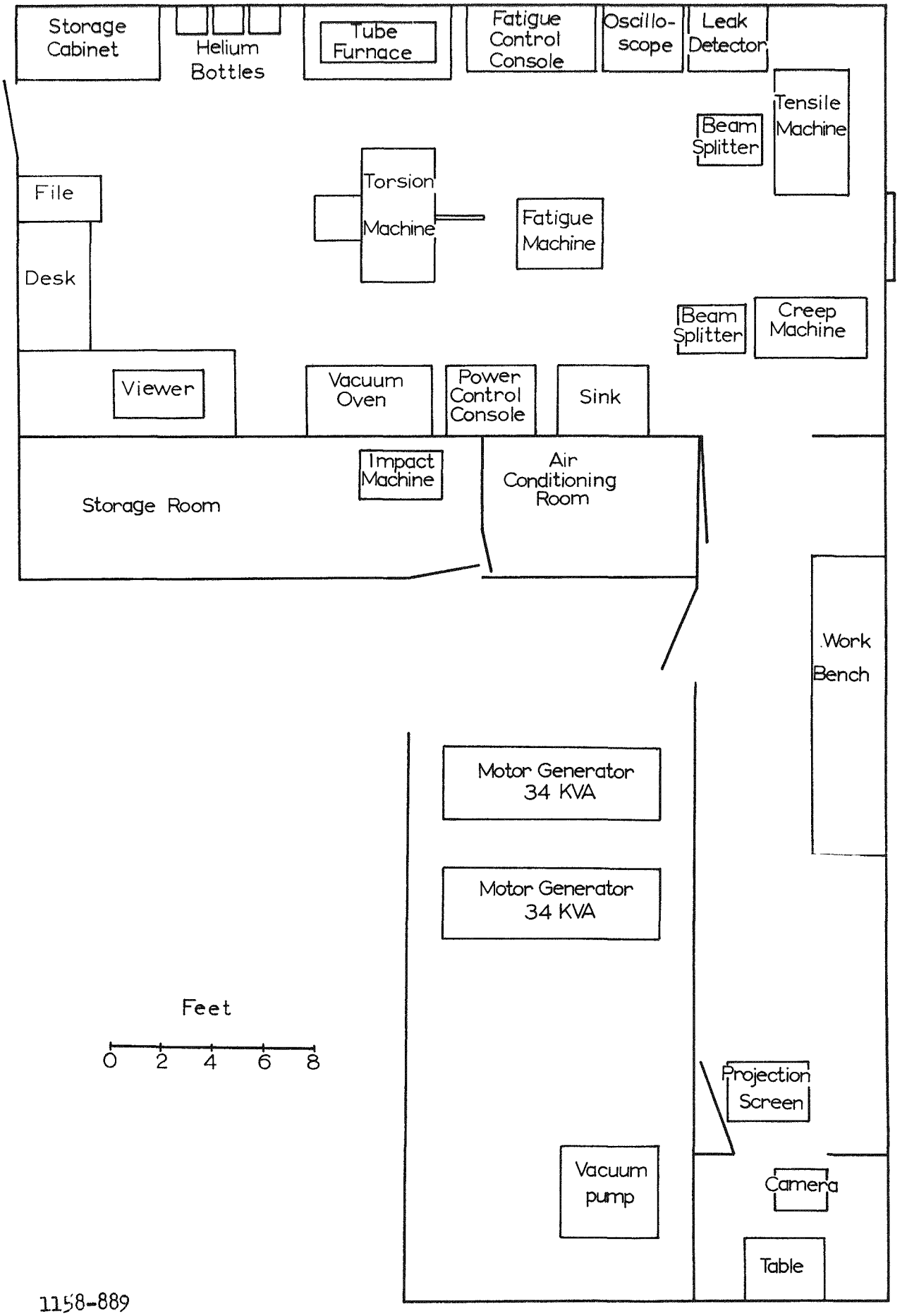

1158-889

Layout of High-Temperature Materials-Research Laboratory

Figure 1

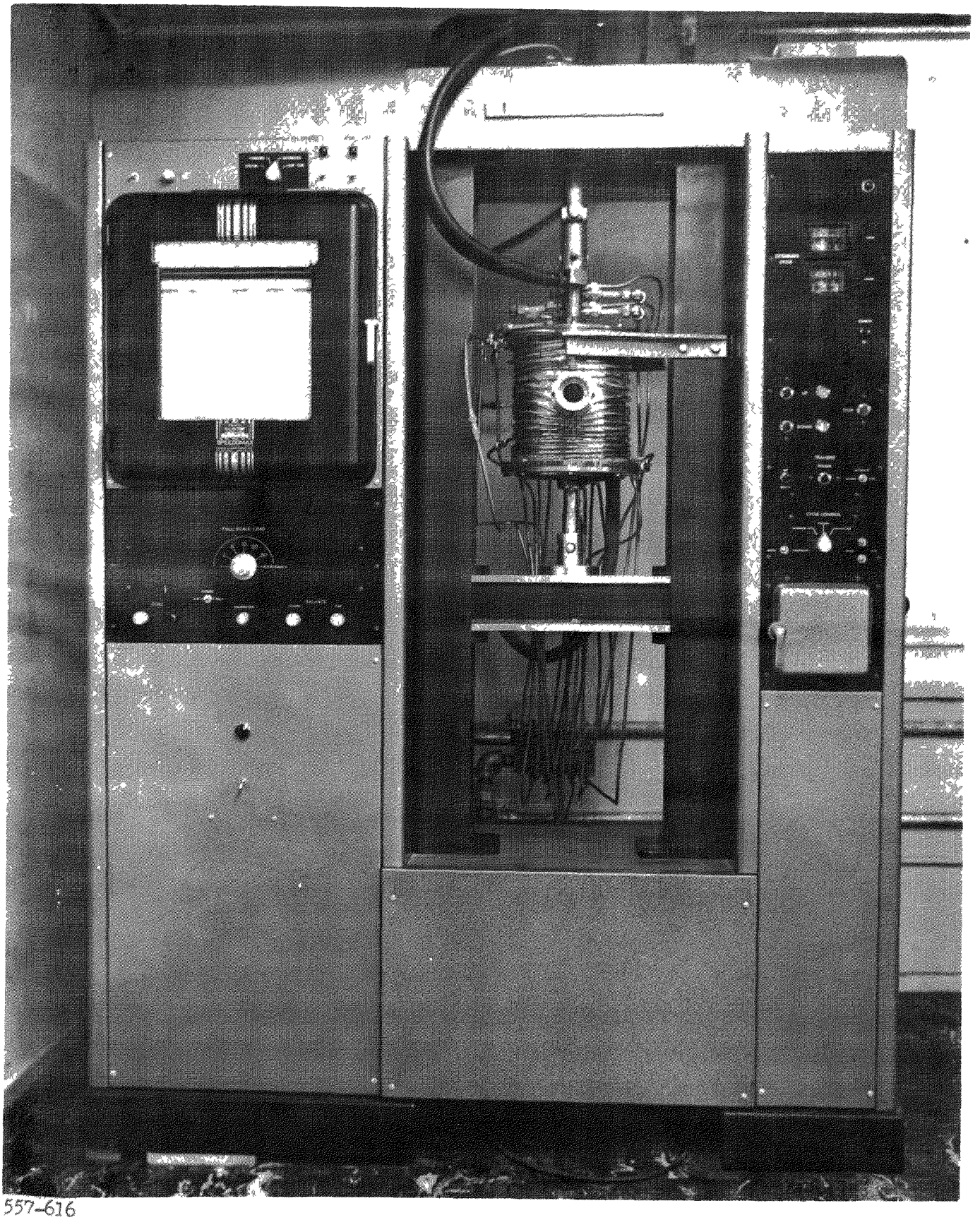

557-616

View of Tensile Furnace Mounted on Instrom Machine

Figure 2

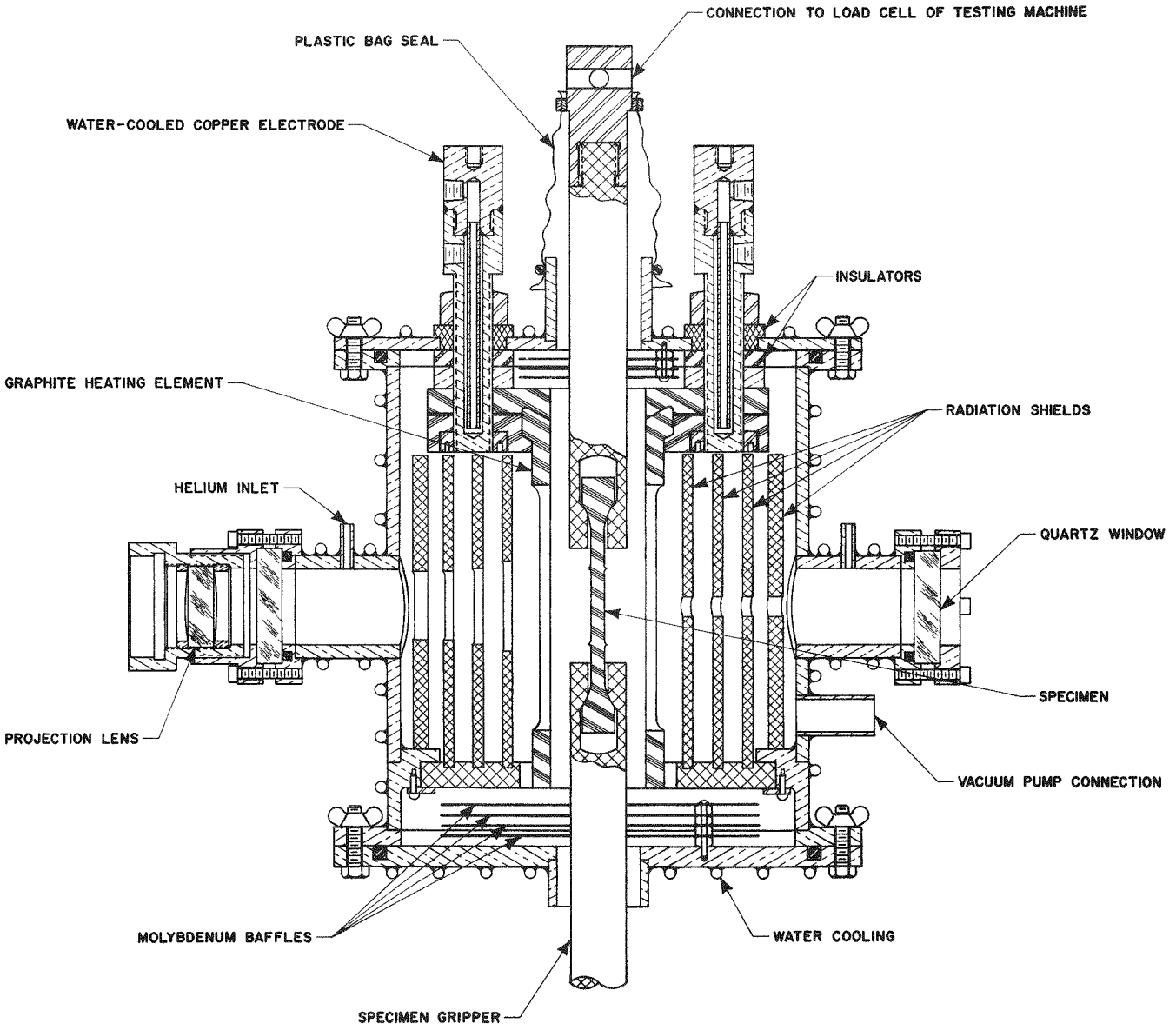

Schematic Diagram of Tensile Furnace

Figure 3

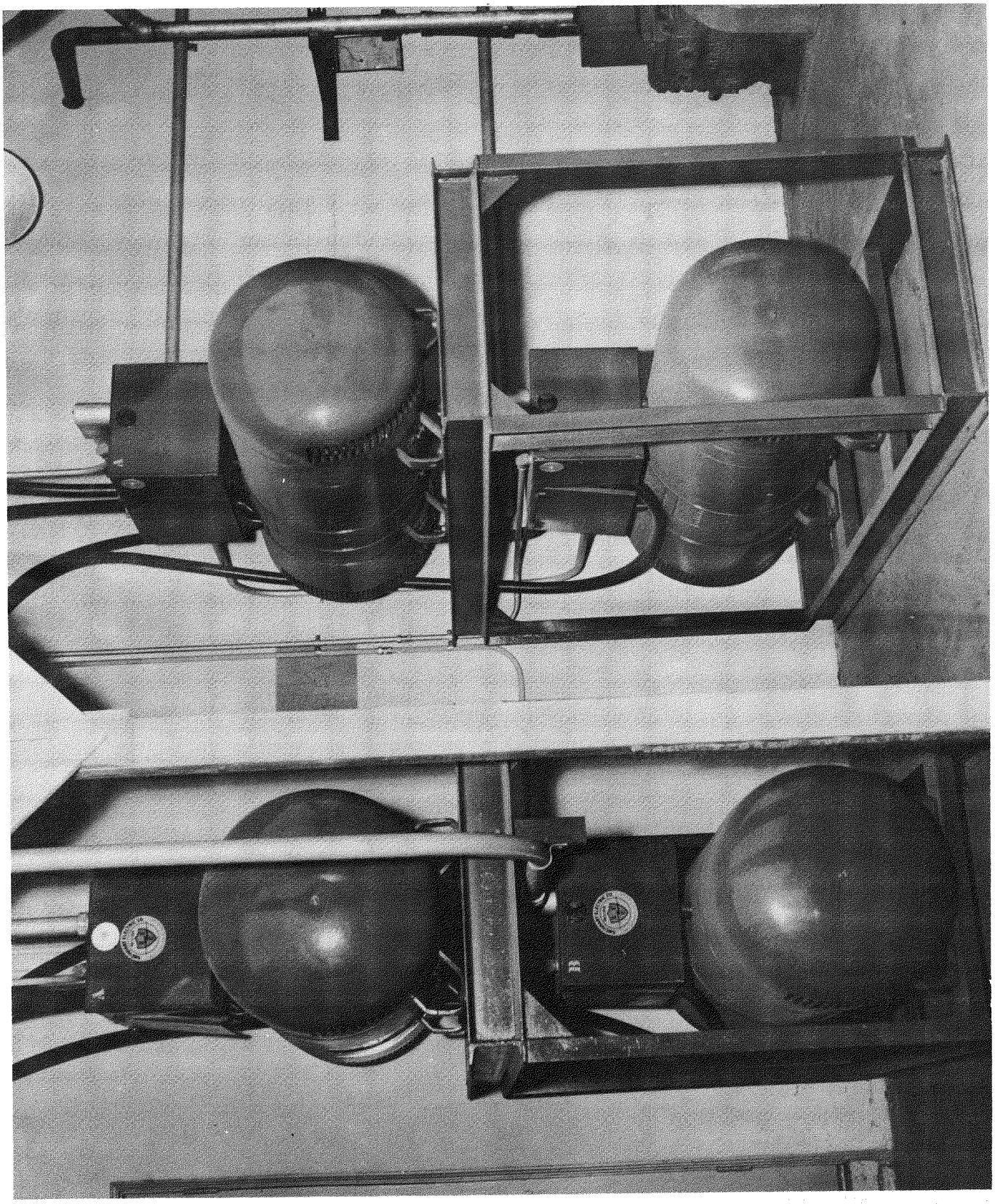

557-624

View of Motor-Generator Sets, 440 v, ac to 25-50 v, dc

Figure 4

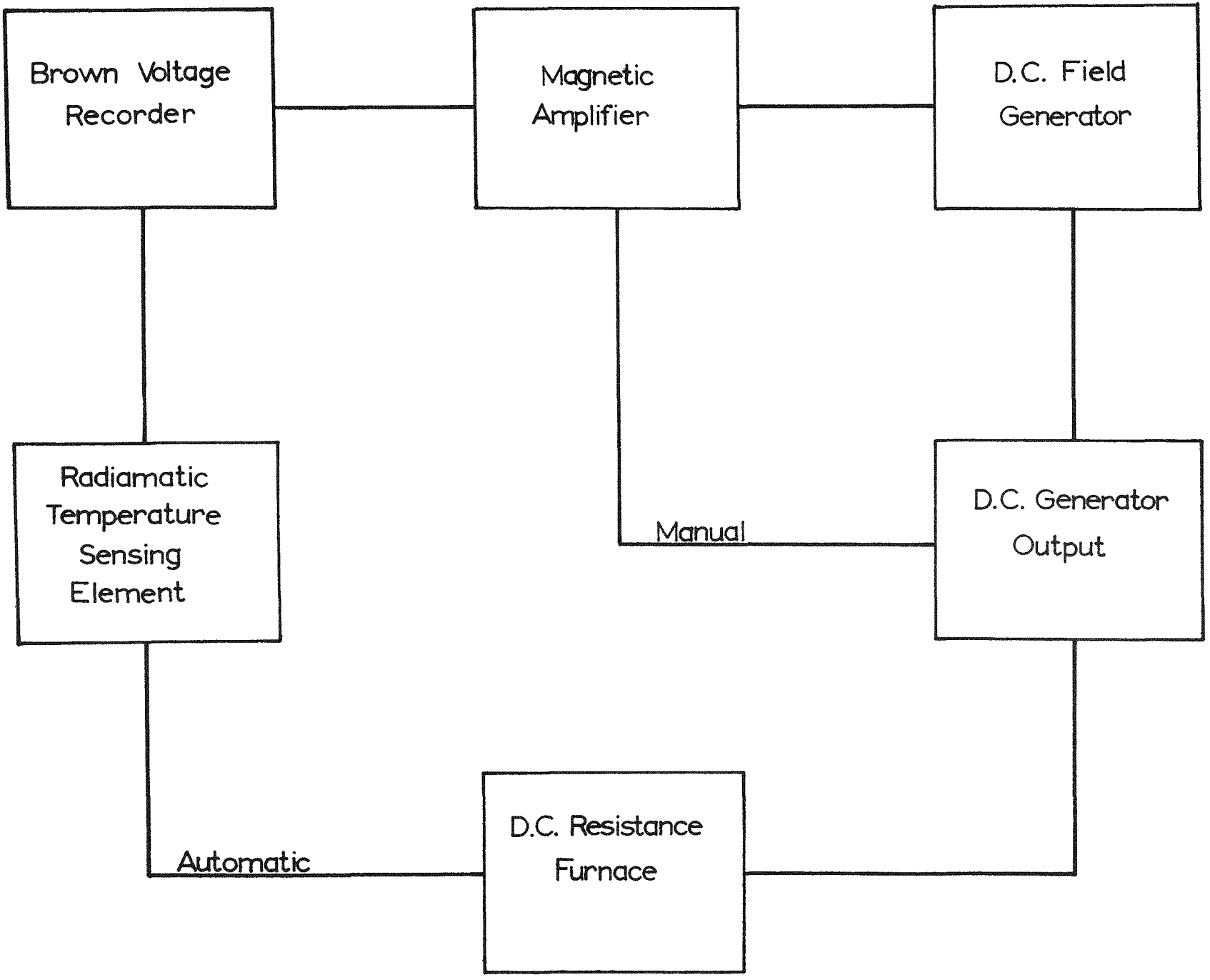

Figure 5

Block Diagram of Temperature-Control System

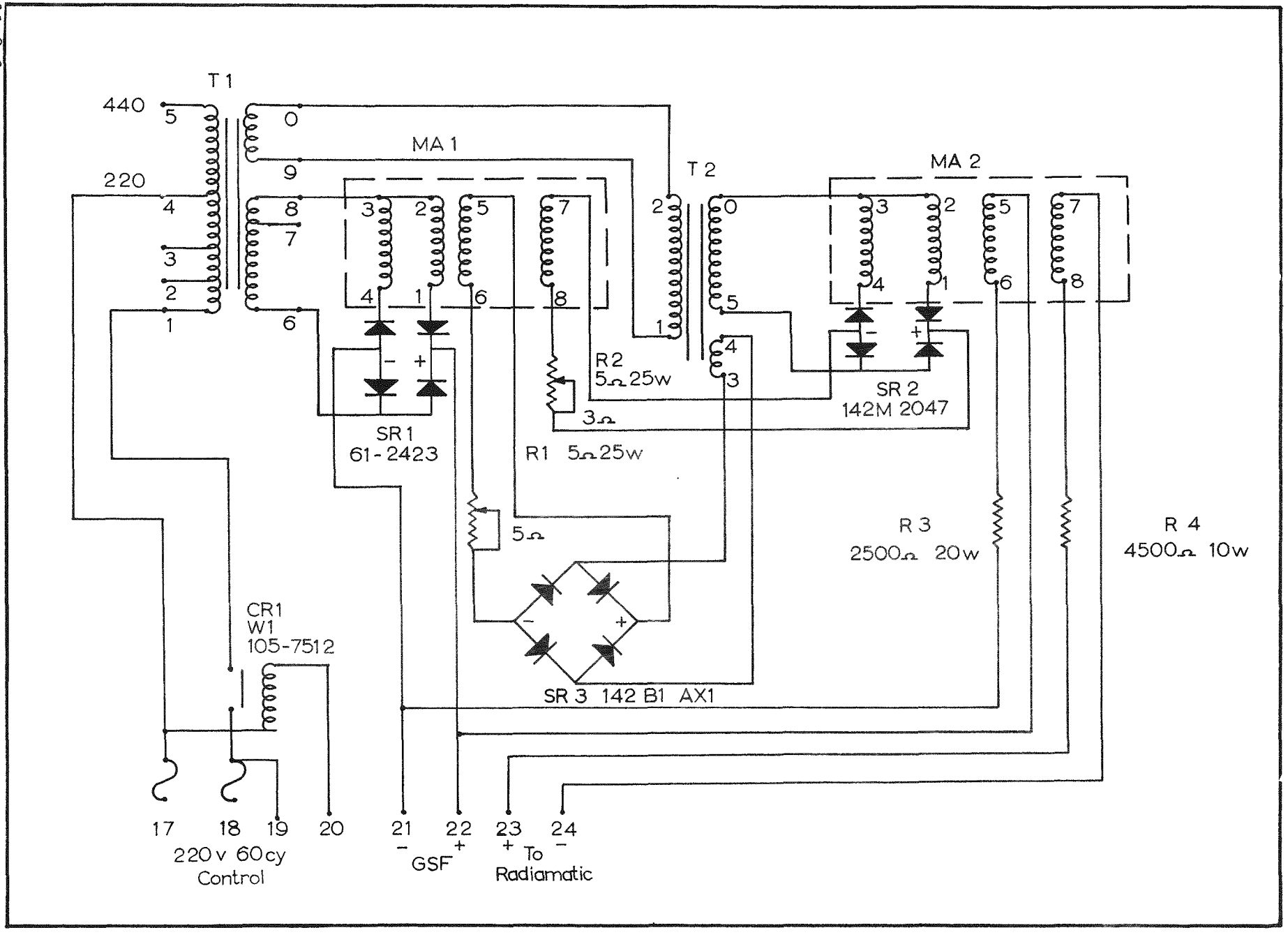

Figure 6

Schematic Diagram of Temperature-Control System

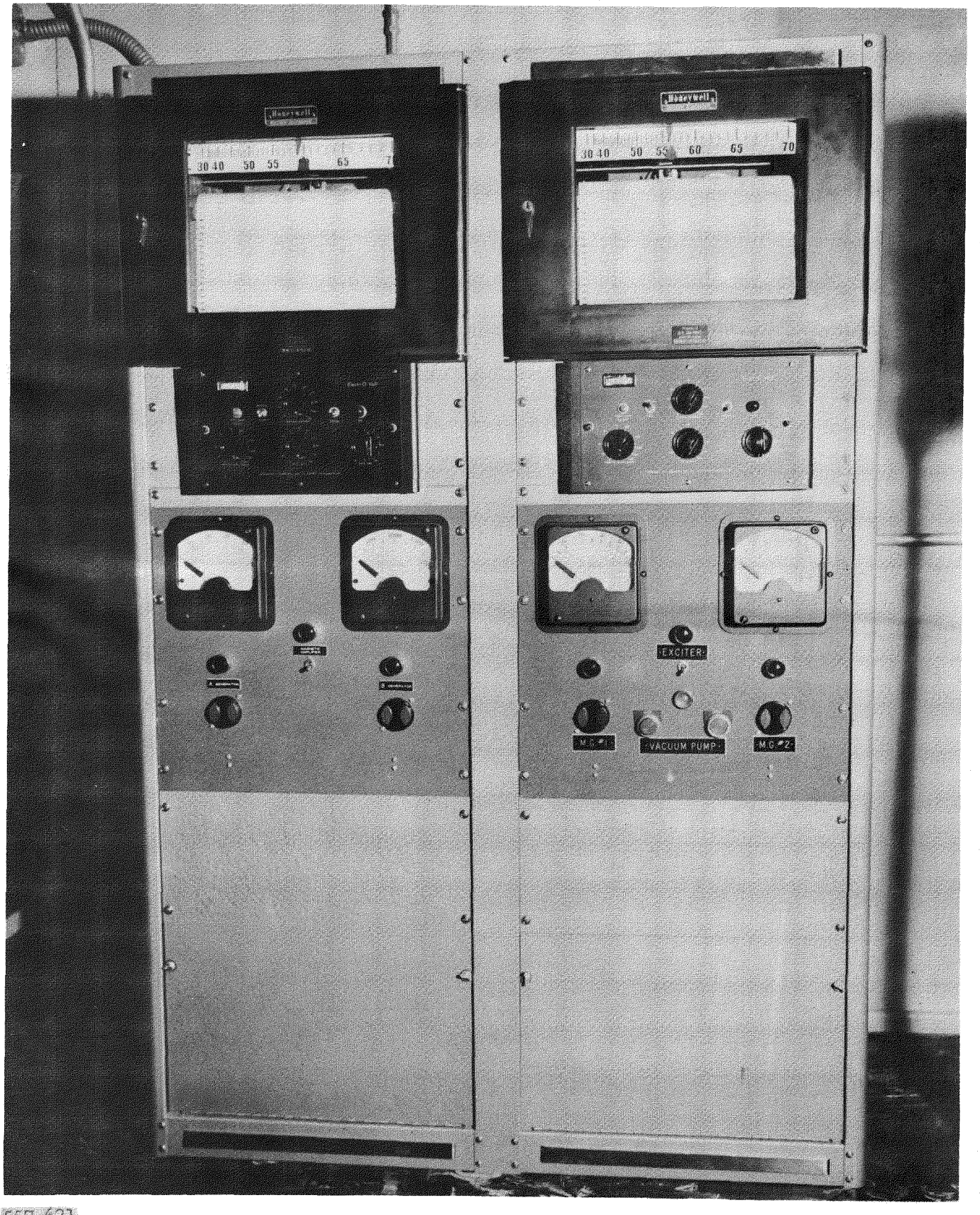

557-621

Recording and Control Consoles

Figure 7

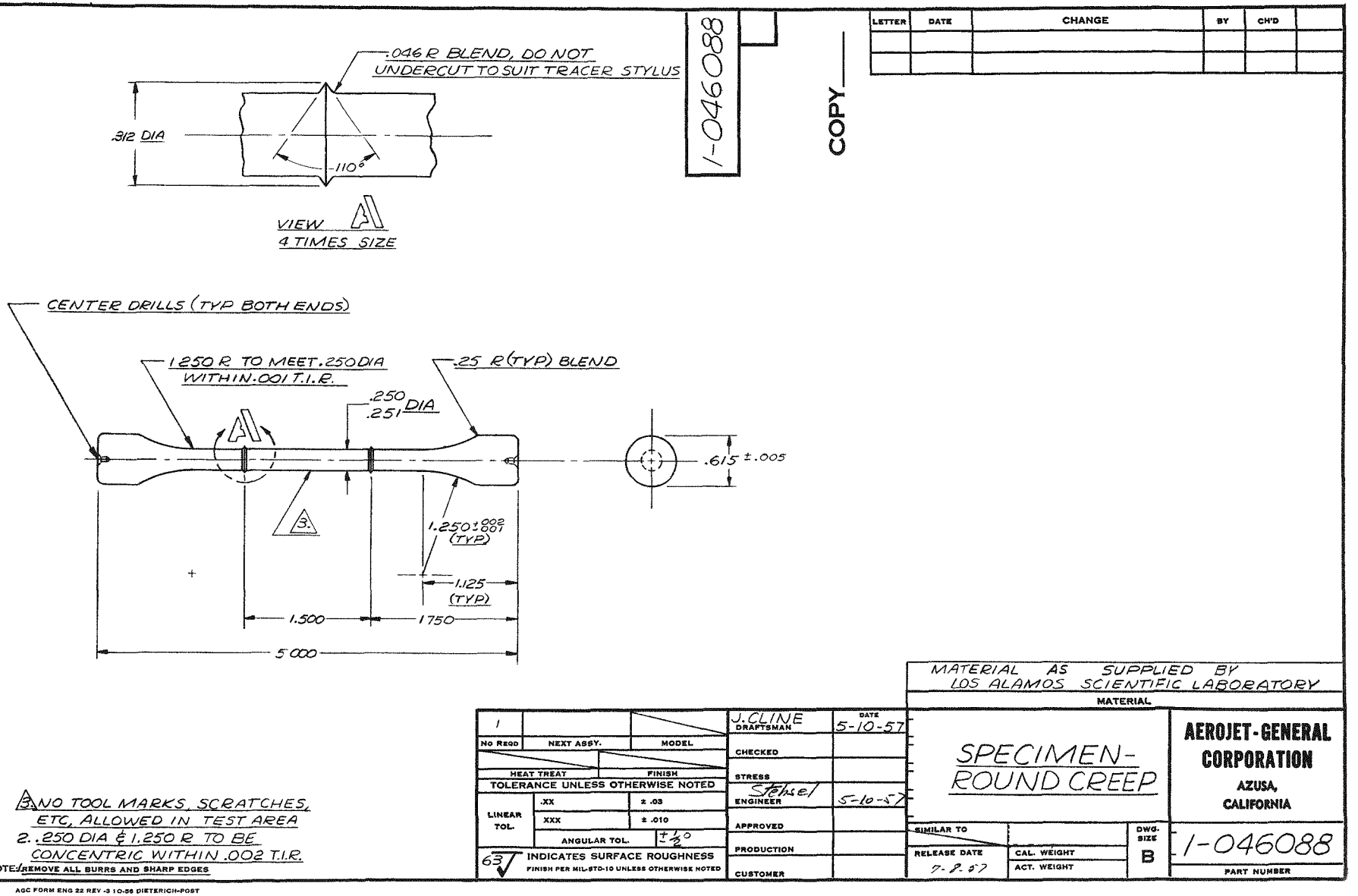
.046 R BLEND, DO NOT UNDERCUT TO SUIT TRACER STYLUS
.312 DIA
110°
VIEW A
4 TIMES SIZE
1-046088
COPY
LETTER | DATE | CHANGE | BY | CH'D
CENTER DRILLS (TYP BOTH ENDS)
1.250 R TO MEET .250 DIA WITHIN .001 T.I.R.
.250 .251 DIA
.25 R (TYP) BLEND
.615 ±.005
1.250 +.002 -.001 (TYP)
1.125 (TYP)
1.500
1.750
5.000
3.
NO TOOL MARKS, SCRATCHES, ETC, ALLOWED IN TEST AREA
2. .250 DIA & 1.250 R TO BE CONCENTRIC WITHIN .002 T.I.R.
NOTE: REMOVE ALL BURRS AND SHARP EDGES
MATERIAL AS SUPPLIED BY LOS ALAMOS SCIENTIFIC LABORATORY
MATERIAL
1
NO REQD | NEXT ASSY. | MODEL
HEAT TREAT | FINISH
TOLERANCE UNLESS OTHERWISE NOTED
LINEAR TOL. .XX ± .03 | XXX ± .010
ANGULAR TOL. ± 1/2°
63 INDICATES SURFACE ROUGHNESS
FINISH PER MIL-STD-10 UNLESS OTHERWISE NOTED
J. CLINE DRAFTSMAN 5-10-57
CHECKED
STRESS
Stehsel ENGINEER 5-10-57
APPROVED
PRODUCTION
CUSTOMER
SPECIMEN-ROUND CREEP
AEROJET-GENERAL CORPORATION
AZUSA, CALIFORNIA
SIMILAR TO
RELEASE DATE 7-8-57
CAL. WEIGHT
ACT. WEIGHT
DWG. SIZE B
1-046088
PART NUMBER
AGC FORM ENG 22 REV -3 10-56 DIETERICH-POST

Figure 8

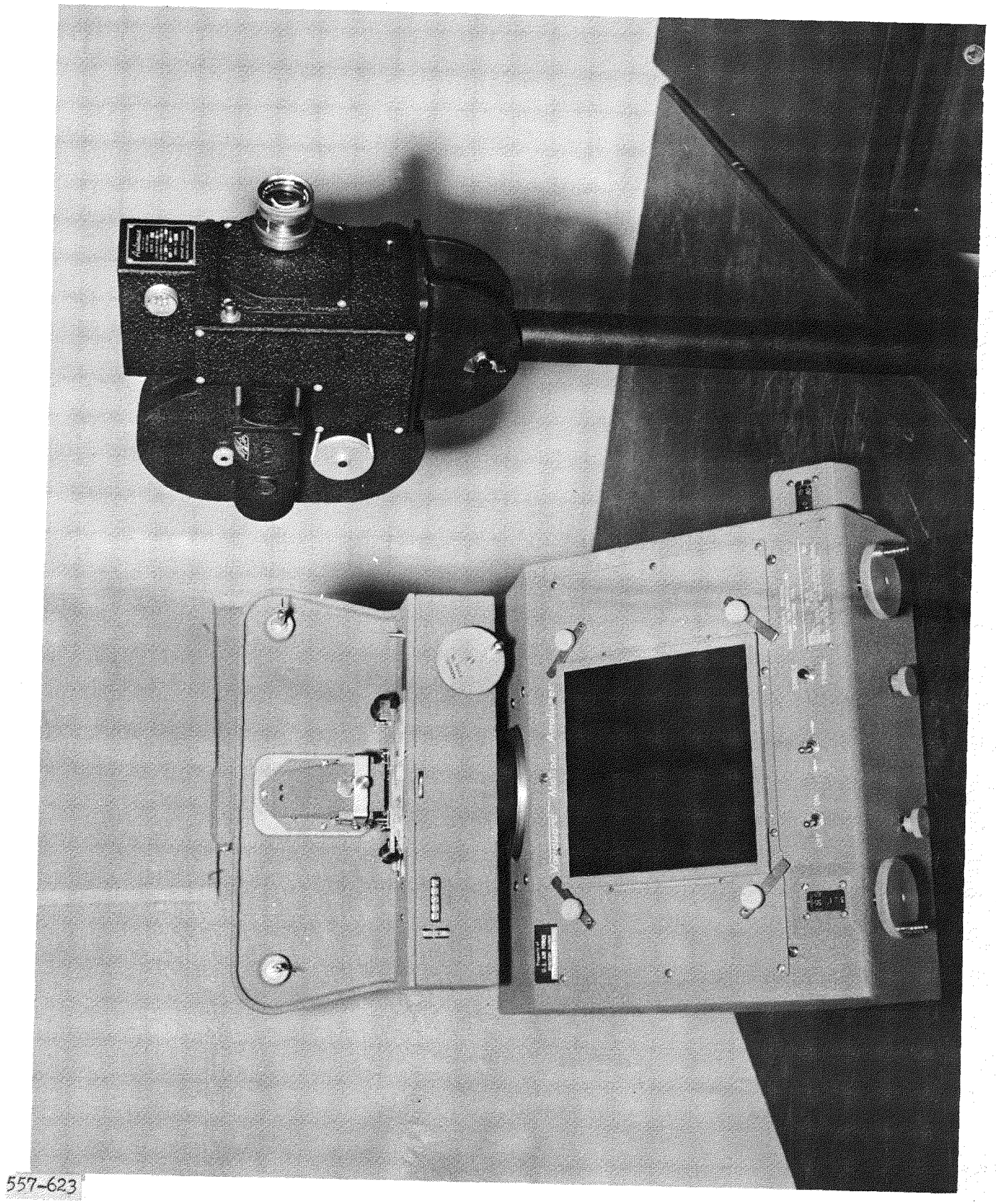

557-623

Camera and Motion Analyzer

Figure 9

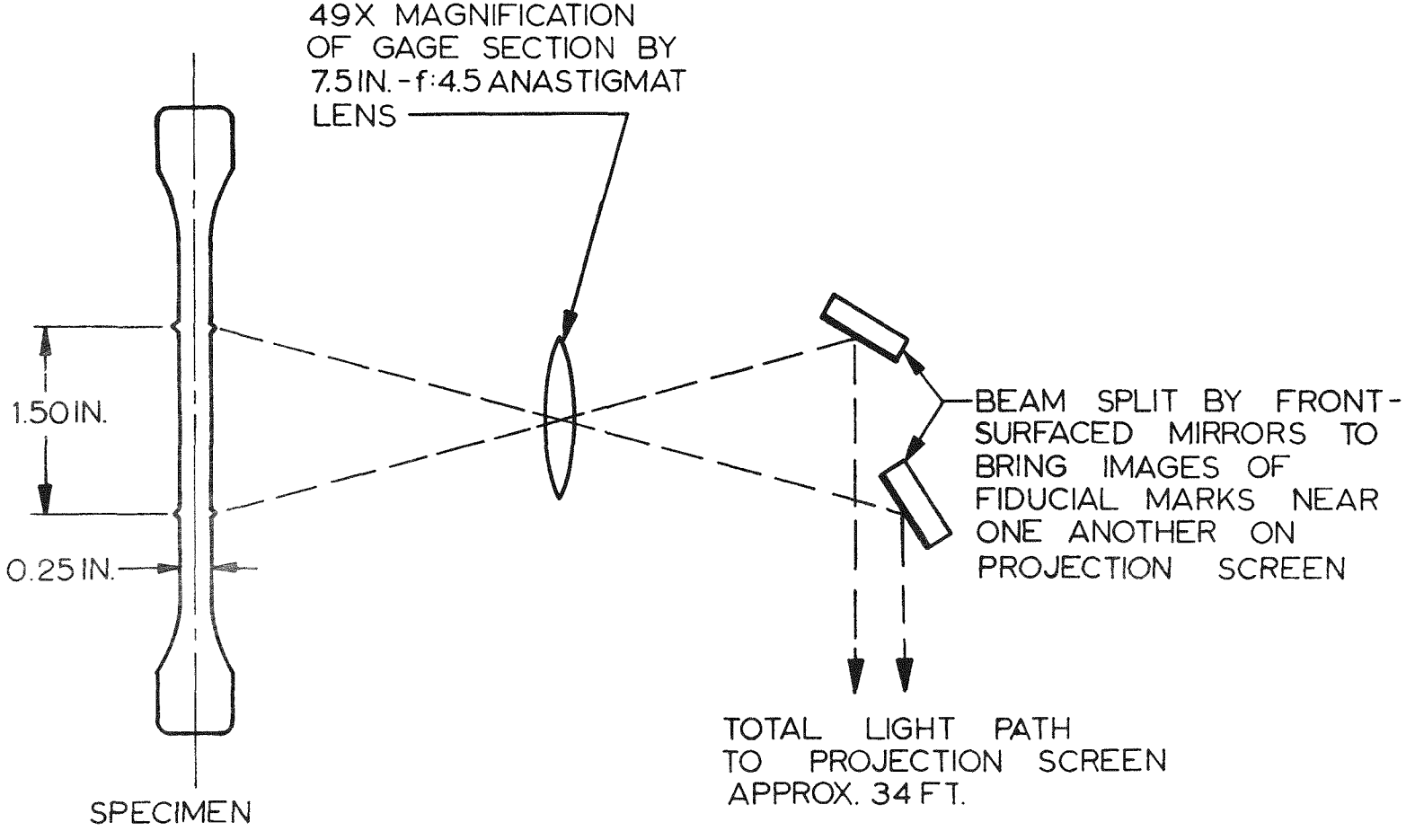

SCHEMATIC DIAGRAM OF OPTICAL SYSTEM FOR MEASUREMENT OF TENSILE STRAIN

Figure 10

Typical Frame for Photographic Record

Figure 11

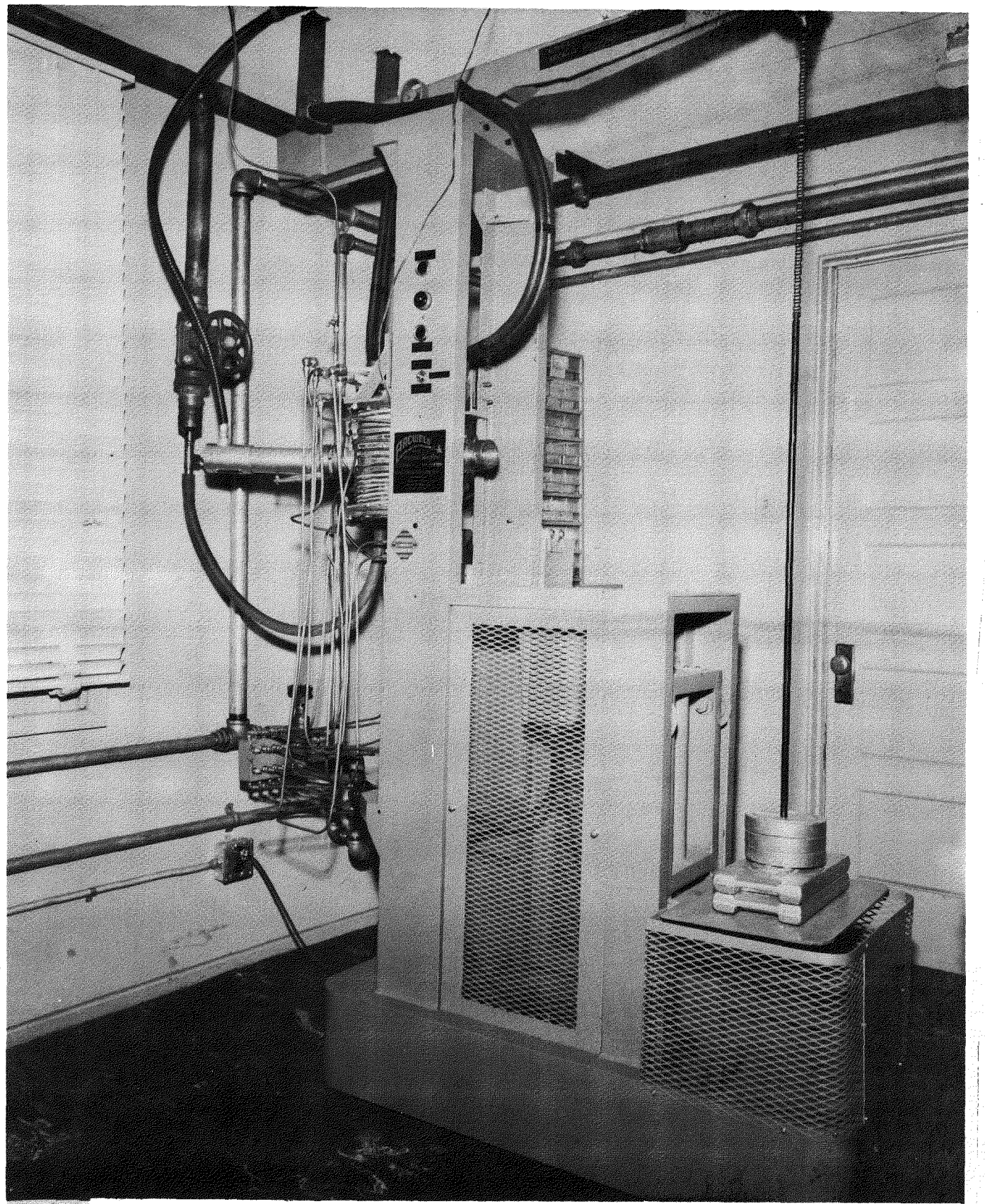

557-615

View of Creep-Test Machine

Figure 12

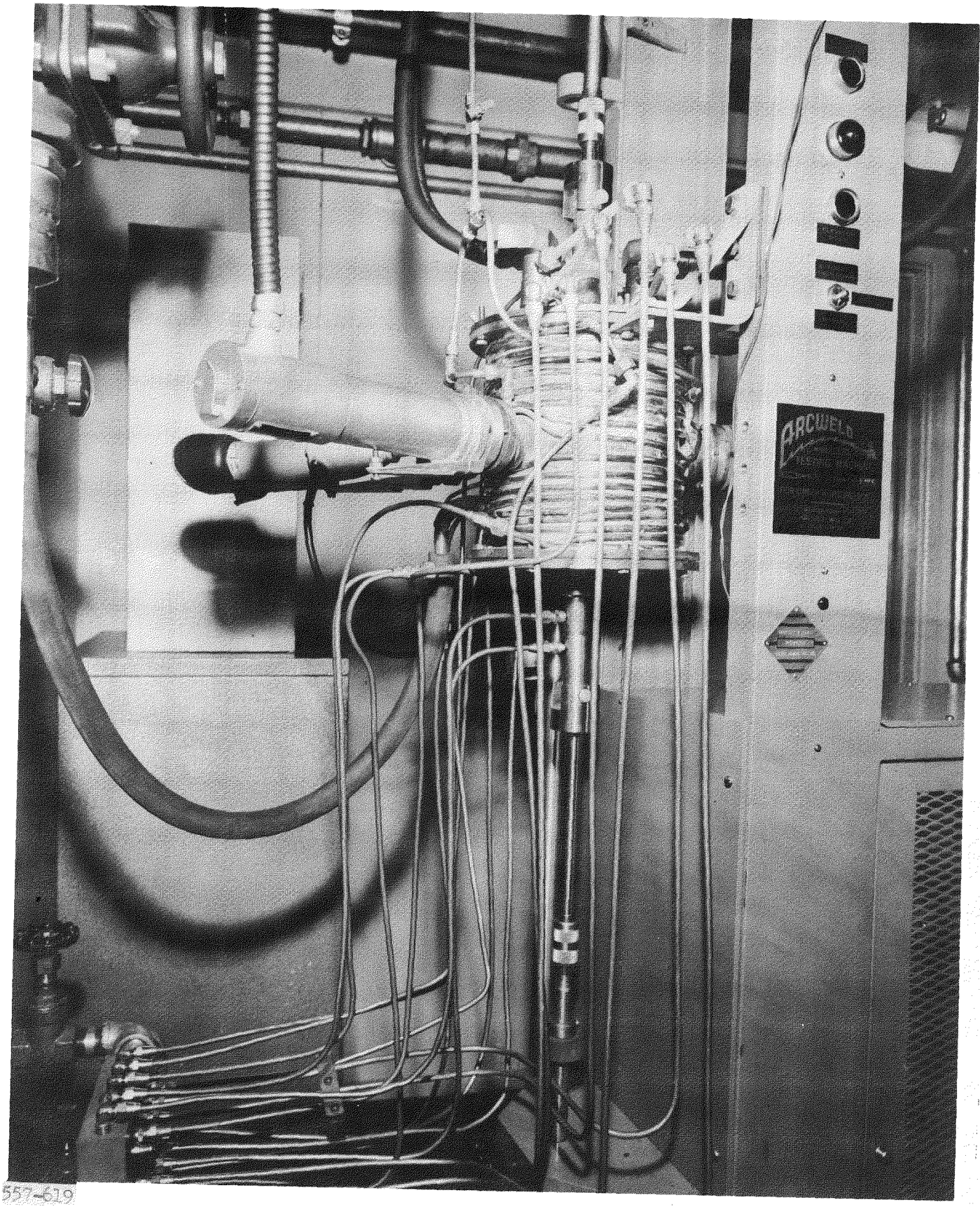

High-Temperature Creep Furnace

Figure 13

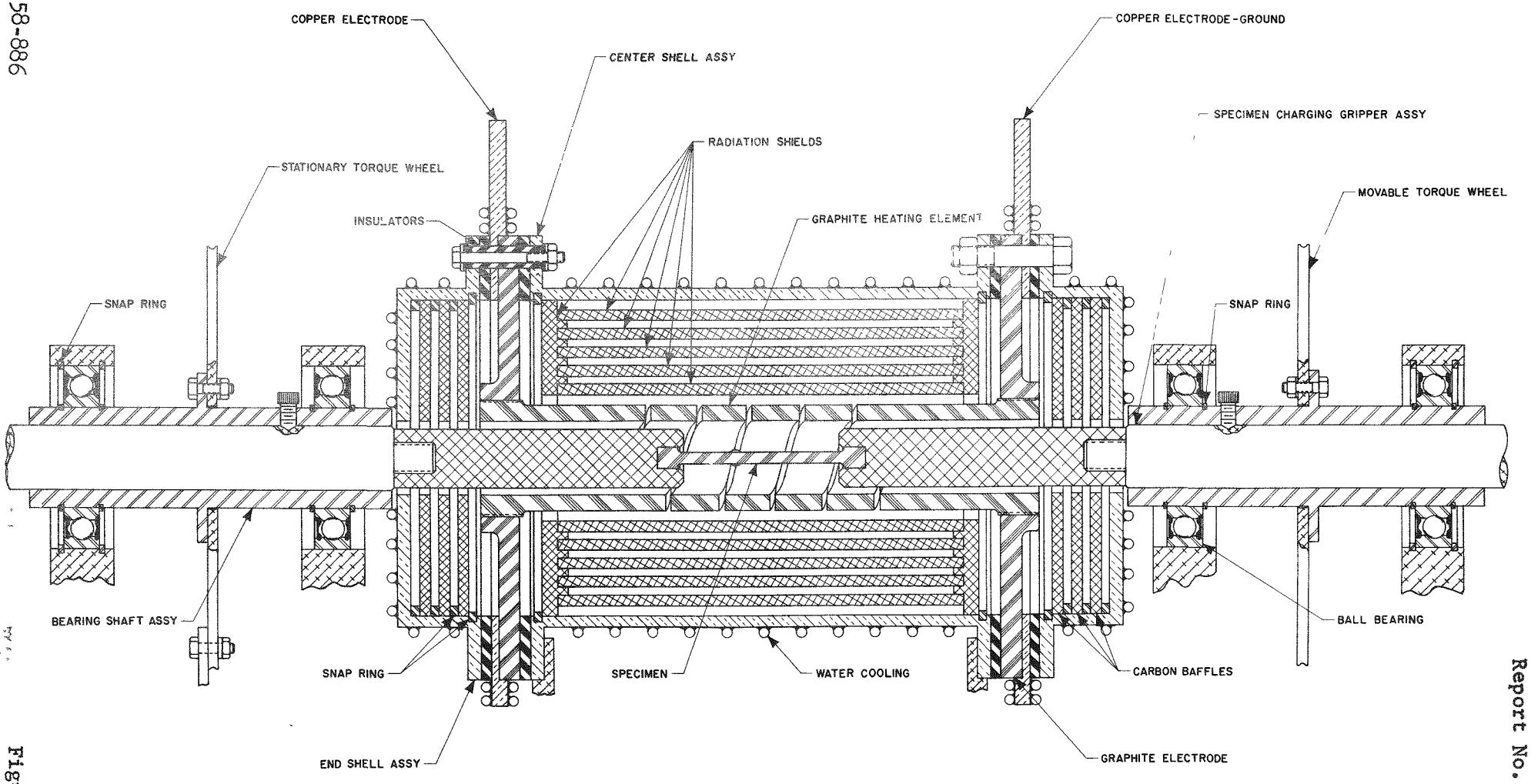

Figure 14

Schematic Diagram of Torsion-Test Furnace

LETTER	DATE	CHANGE	BY	CH'D	
A	12-8-58	SEE CHANGE RECORD	BURNER	LEVIEN 12-9-58	

1-049502 A

COPY

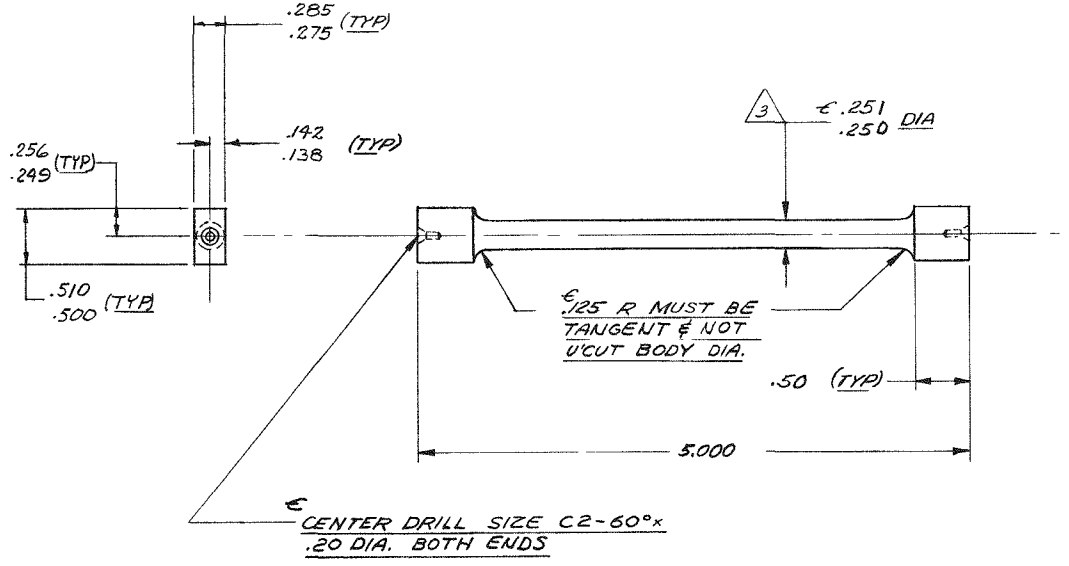

4 MATL. PER COGNIZANT ENGINEER

MATERIAL

4 THIS SPECIMEN MATERIAL & TEST, PER INSTRUCTIONS BY COGNIZANT ENGINEER.

3 NO TOOL MARKS, SCRATCHES, ETC, ALLOWED IN TEST AREA

2. DIAMETERS MARKED ℄ MUST BE CONCENTRIC WITHIN .002 T.I.R.

NOTES: 1. REMOVE ALL BURRS AND SHARP EDGES.

AGC FORM ENG 22-REV-3 2000 2-57

NO. REQD.	NEXT ASSY.	MODEL	
HEAT TREAT	FINISH		
TOLERANCE UNLESS OTHERWISE NOTED			
LINEAR TOL.	.XX	± .03	
	.XXX	± .010	
ANGULAR TOL.		—	

63 INDICATES SURFACE ROUGHNESS
FINISH PER MIL-STD-10 UNLESS OTHERWISE NOTED

		DATE
DRAFTSMAN	YAXLEY	7-29-57
CHECKED	Duncan	11-11-57
STRESS		
ENGINEER	M Stehle	7-29-57
APPROVED	GREEN	12-8-58
PRODUCTION		
CUSTOMER		

SPECIMEN — ROUND CREEP (TORSION)

AEROJET-GENERAL CORPORATION
AZUSA, CALIFORNIA

SIMILAR TO		DWG. SIZE	1-049502
RELEASE DATE	CAL. WEIGHT	B	
11-12-57	ACT. WEIGHT		PART NUMBER

Figure 15

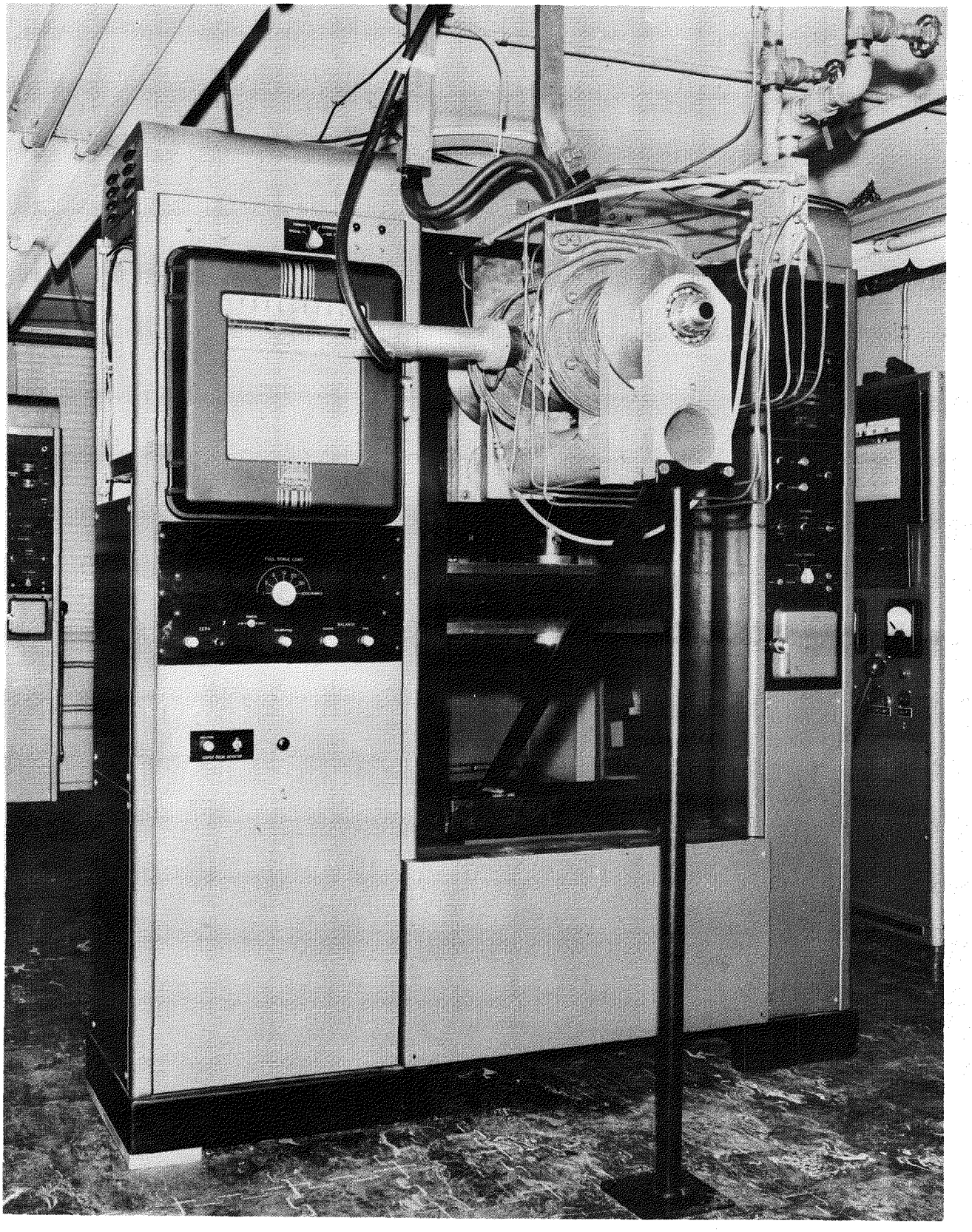

View of Torsion-Test Furnace Mounted on Instron Machine

Figure 16

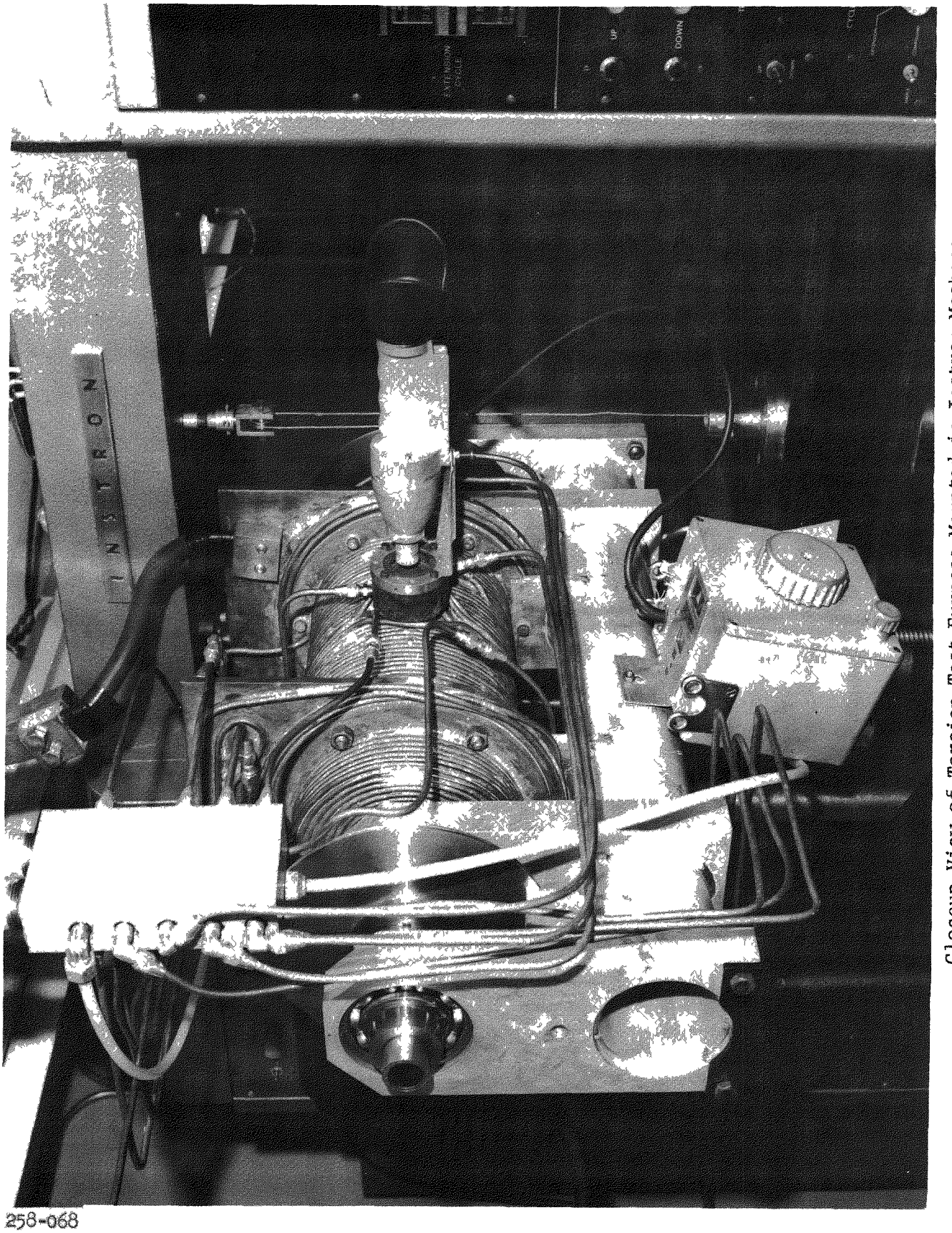

258-068

Closeup View of Torsion Test Furnace Mounted in Instron Machine

Figure 17

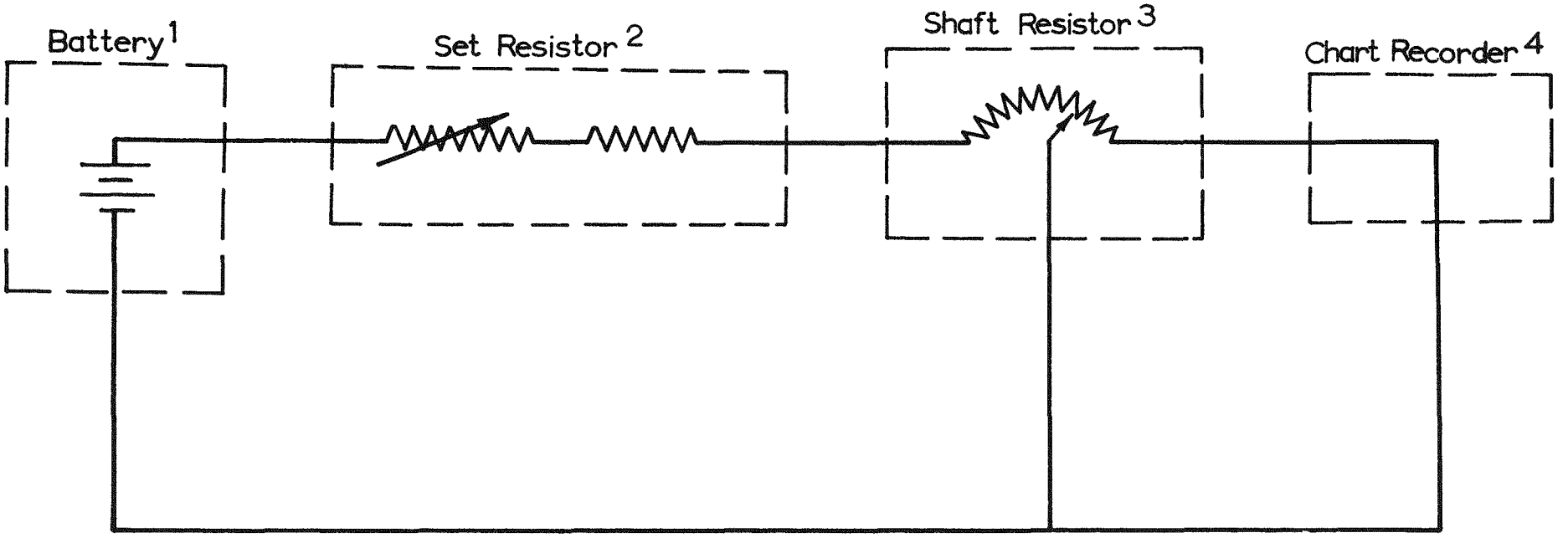

1- 6 volt battery

2- 25 KΩ carbon trimpot 10 turns

30 KΩ carbon resistor

3- 500Ω circular carbon potentiometer

4- 0-10 millivolt recorder

Figure 18

Schematic Diagram of Torsional Strain-Recording System

LETTER	DATE	CHANGE	BY	CHD	
A	1-13 58	① REMOVED .250 "T" DIM Ⓐ .383 R (TYP), 7 PL .375±.250 Ⓐ Rebel			
1.25 IN 2.50		RIGHT SIDE VIEW SHOWN, NOTE Ⓐ DIM 1.250 APPLIES ONLY FOR LENGTH NOTE Ⓐ "T" DIM THIS DIM TO BE DETERMINED BY COGNIZANT ENGINEER. ② CHANGED: 1.25 WAS 50, DRILL 126 DIA THRU WAS DRILL 140 DIA THRU, .925 WAS .545 ③ ADDED .400, 2.00, .25, .06 R (TYP).			

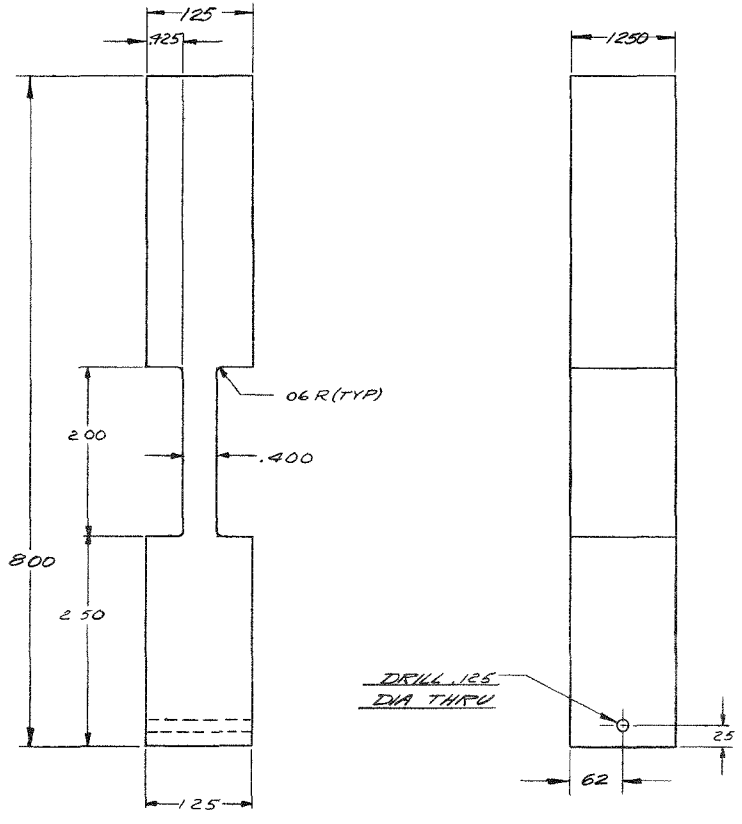

COPY 1-039900 A

NOTES REMOVE ALL BURRS AND SHARP EDGES

1	1-036322		DRAFTSMAN	ELGRAHAM	DATE 11-9-56
NO REQD	NEXT ASSY	MODEL	CHECKED		
HEAT TREAT	FINISH		STRESS		
TOLERANCE UNLESS OTHERWISE NOTED			ENGINEER	Waller	12 7-56
LINEAR TOL.	XX ± .05		APPROVED		
	XXX ± .010		PRODUCTION		
	ANGULAR TOL —		CUSTOMER		
INDICATES SURFACE ROUGHNESS FINISH PER MIL-STD-10 UNLESS OTHERWISE NOTED					

GRAPHITE AS FURNISHED
MATERIAL

SPECIMEN FATIGUE

AEROJET-GENERAL CORPORATION
AZUSA, CALIFORNIA

SIMILAR TO		DWG SIZE
RELEASE DATE 12-6-56	CAL WEIGHT / ACT WEIGHT	C

1-039900
PART NUMBER

AGC FORM ENG 9C REV-3 3M 6-58

Figure 19

Report No. 1537

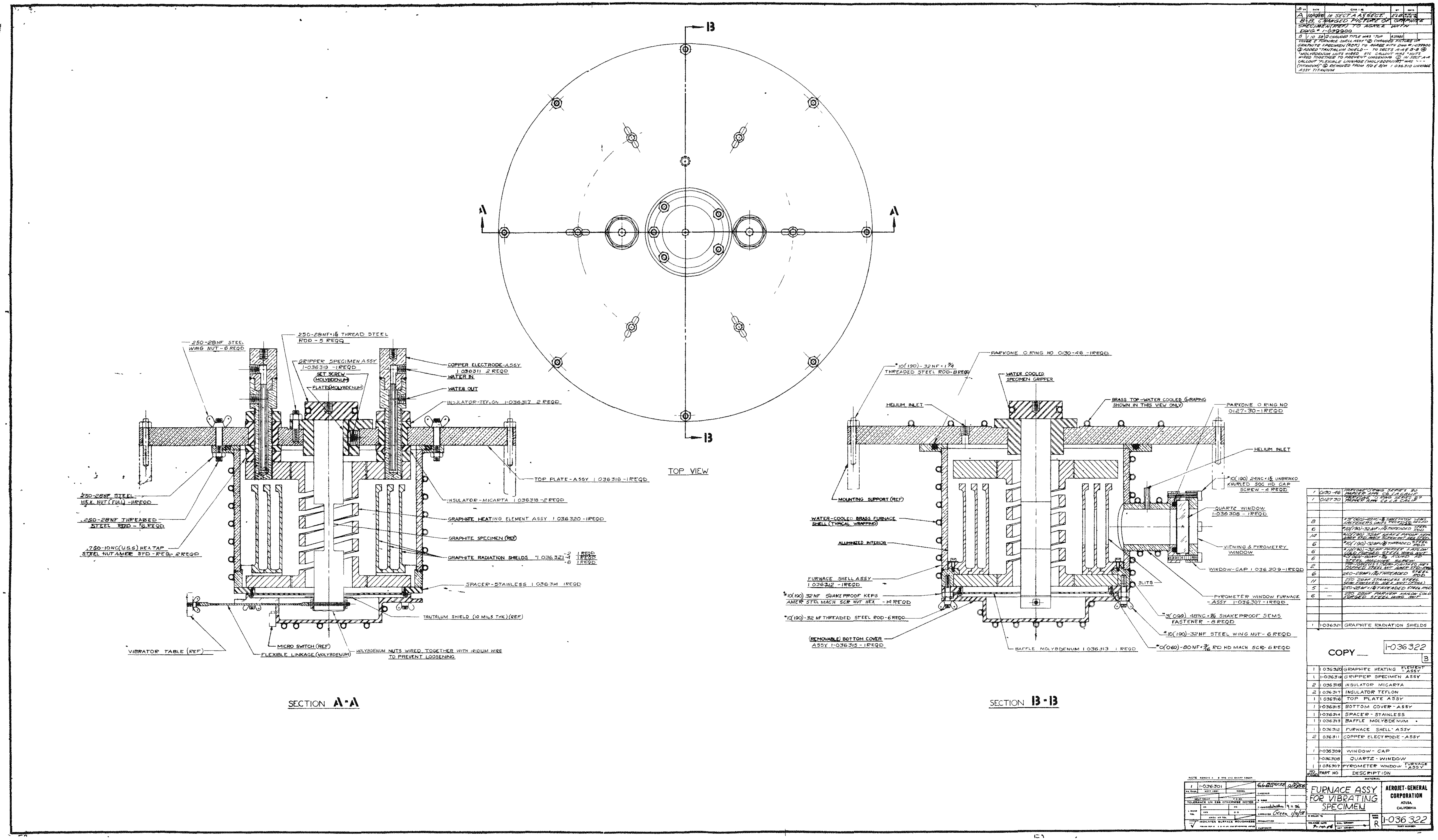
TOP VIEW
SECTION A-A
SECTION B-B
FURNACE ASSY FOR VIBRATING SPECIMEN
AEROJET-GENERAL CORPORATION
AZUSA CALIFORNIA
1-036322
COPY

Figure 20

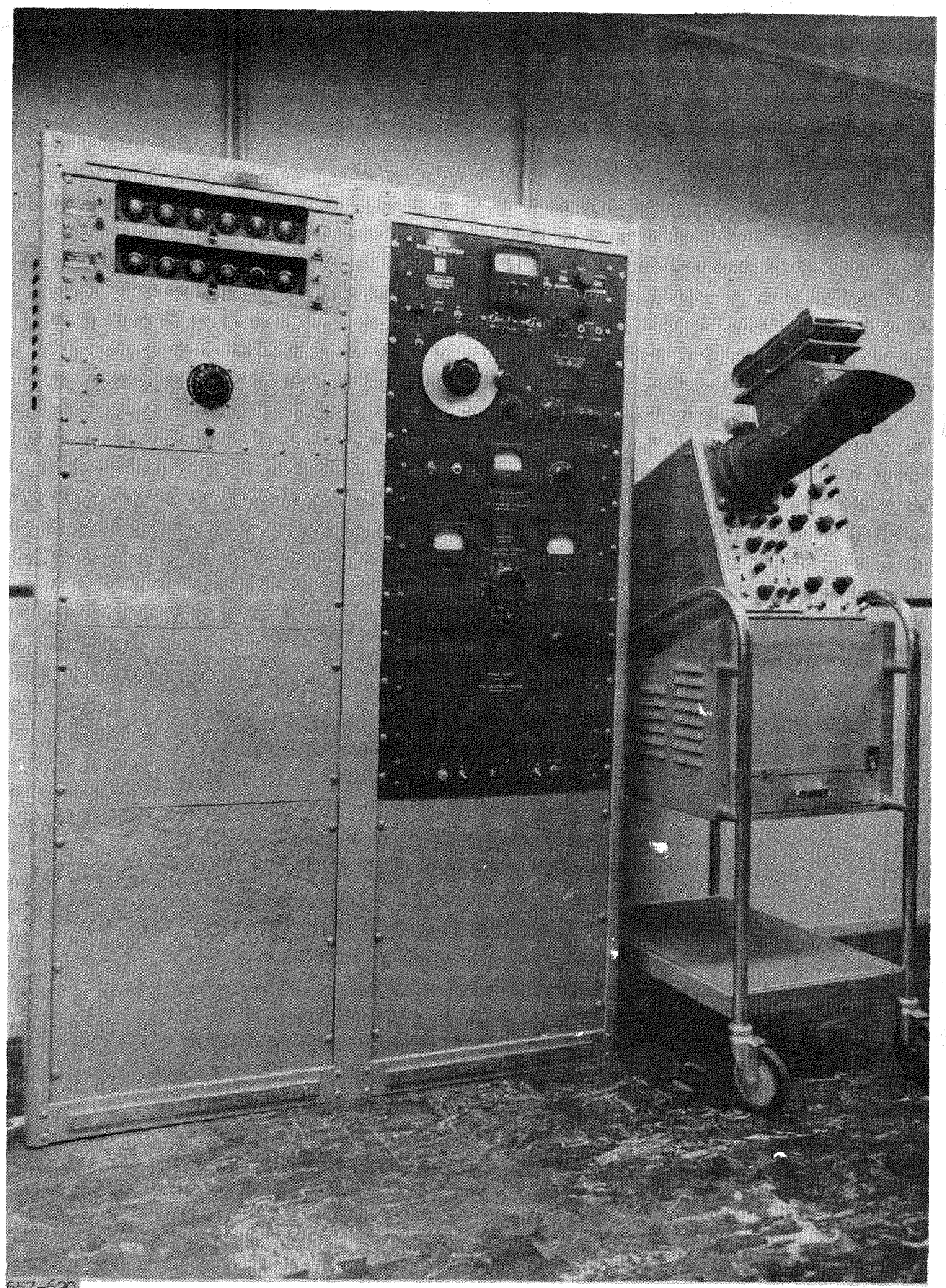

Shaker Console and Accessories

Figure 21

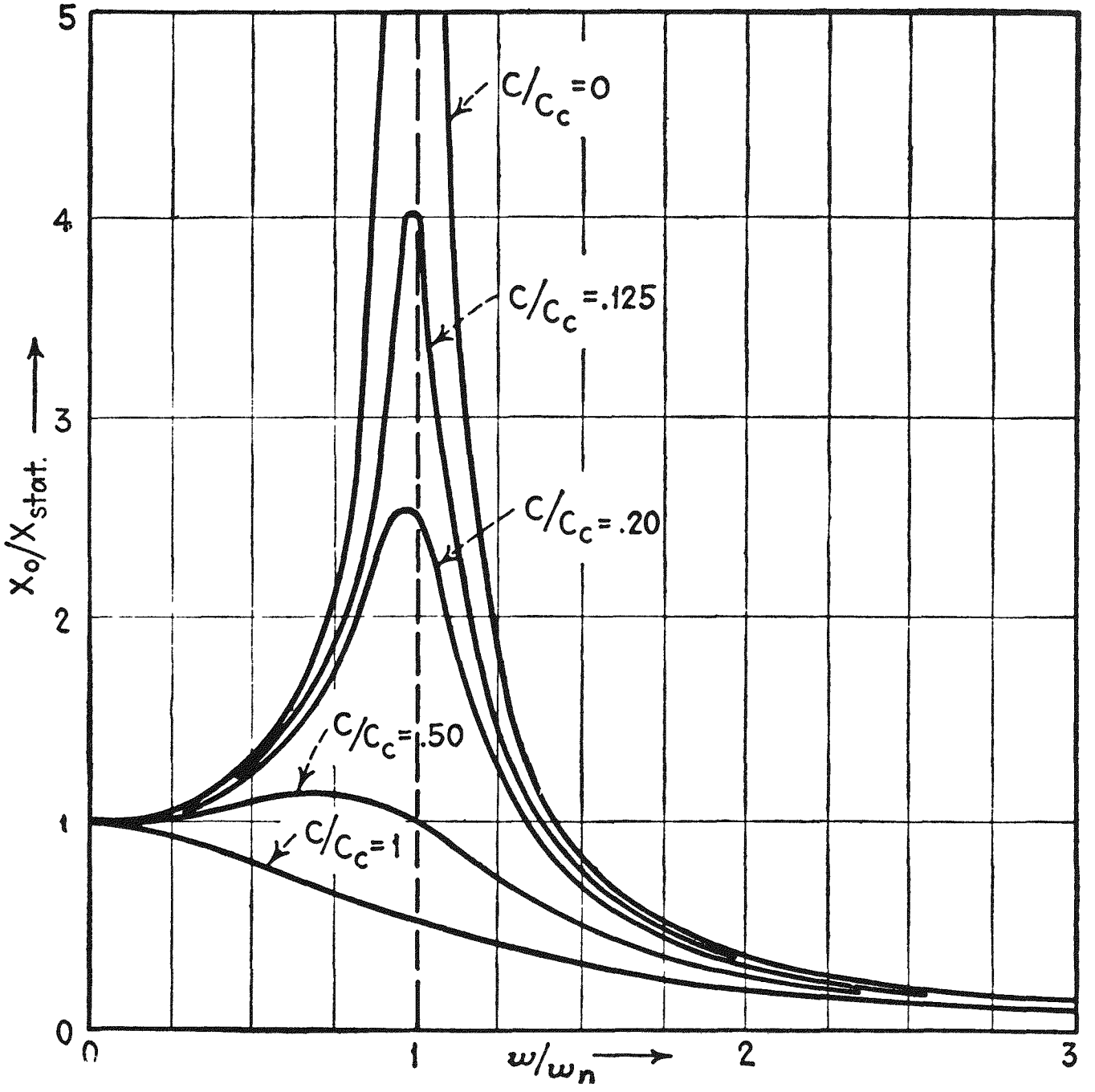

158-052

Resonance Curves for Single-Degree-of-Freedom System

Figure 22

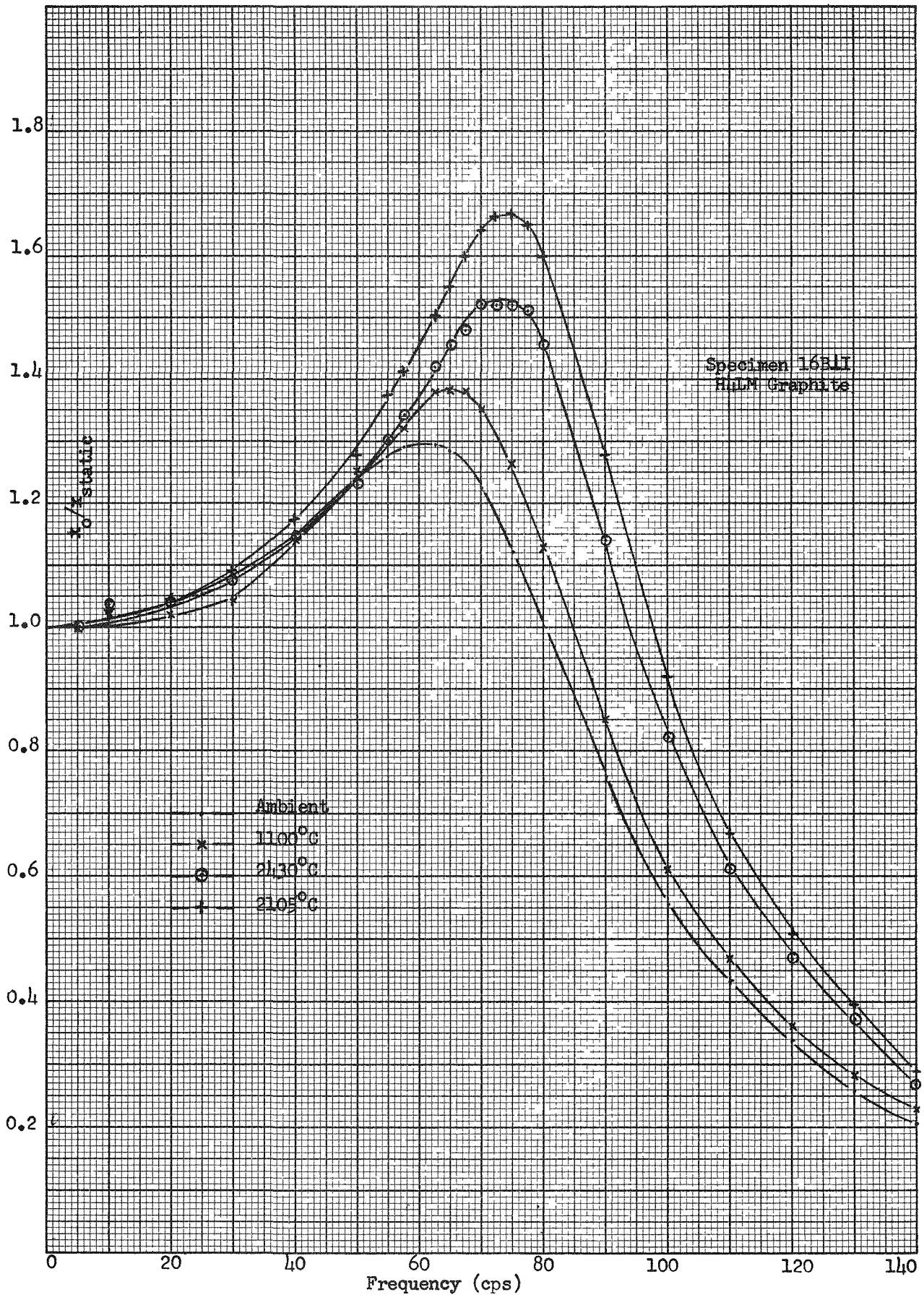

Resonance Curves for Typical Graphite Specimen

Figure 23

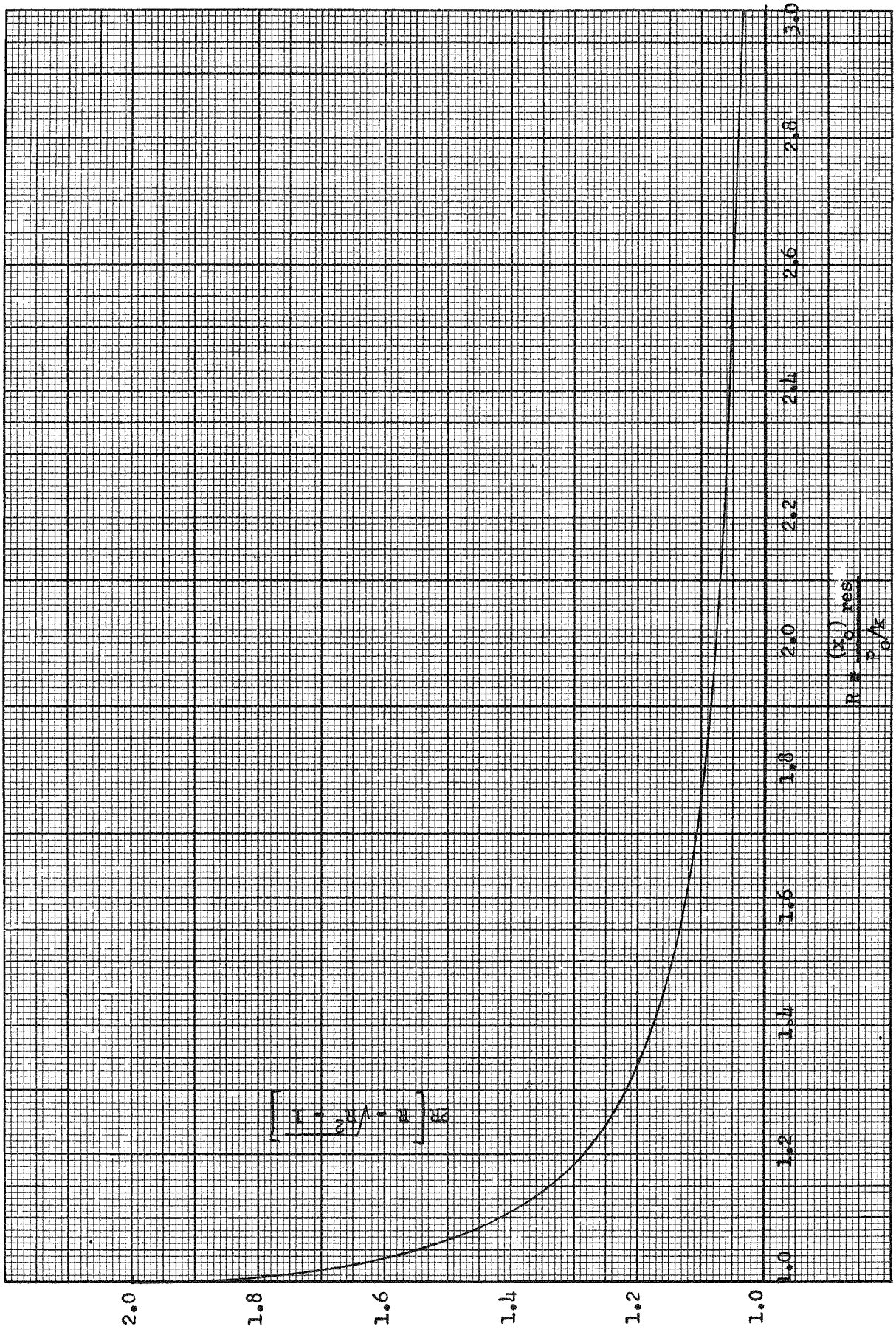

Damping Correction Factor for Calculation of Undamped Natural Frequency

Figure 24

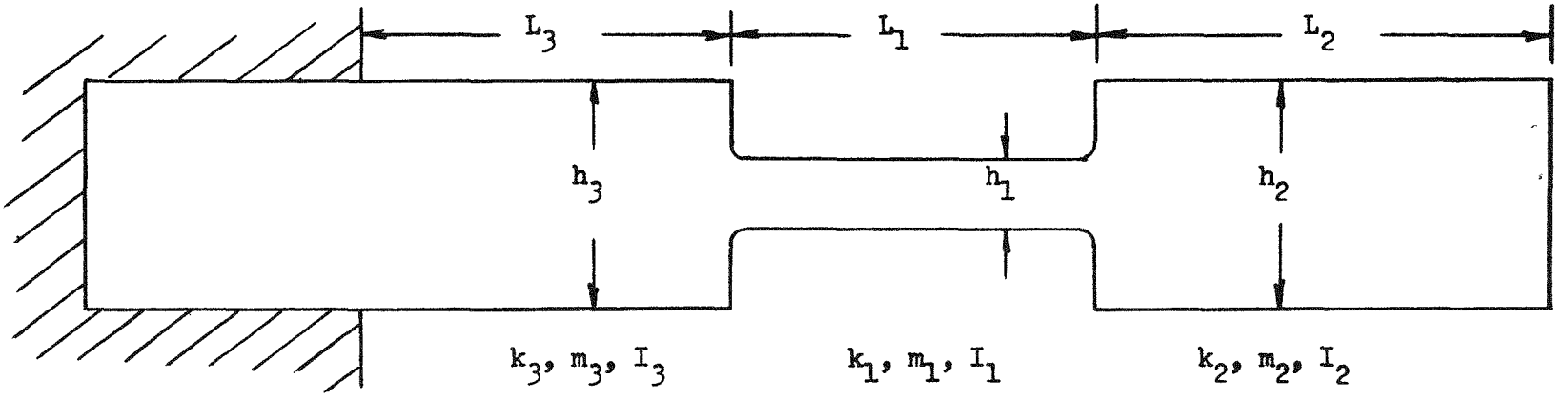

Section	Width, b (in)	Depth, h (in)	$I = bh^3/12$ (in^4)	L (in)	$k = 3EI/L^3$ (lbf/in)
1	1.250	0.400	6.67×10^{-3}	2.00	2.50×10^{-3} E
2	1.250	1.250	0.203	2.50	39.0×10^{-3} E
3	1.250	1.250	0.203	2.00	76.1×10^{-3} E

Total Spring Constant: $\frac{1}{k} = \frac{1}{k_1} + \frac{1}{k_2} + \frac{1}{k_3}$

$$= \frac{400}{E} + \frac{25.6}{E} + \frac{13.1}{E} \cong \frac{439.}{E}$$

$$\therefore \quad k_1 \cong 1.10\ k$$

Figure 25

Properties of Specimen Sections

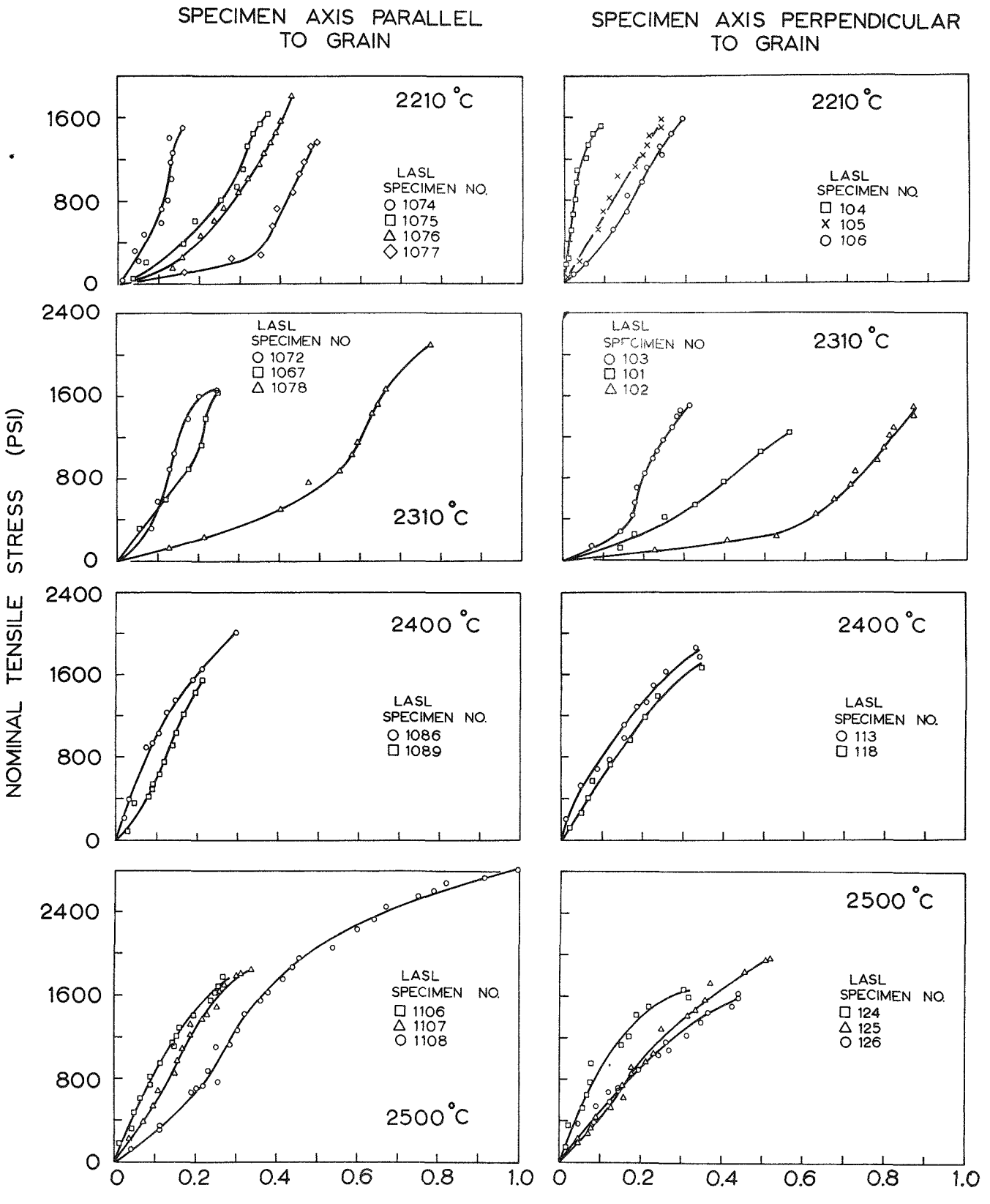

958-1043

Tensile Stress-Strain Curves for Standard H4LM Stock (Platen Rate 0.02 in./min)

Figure 26

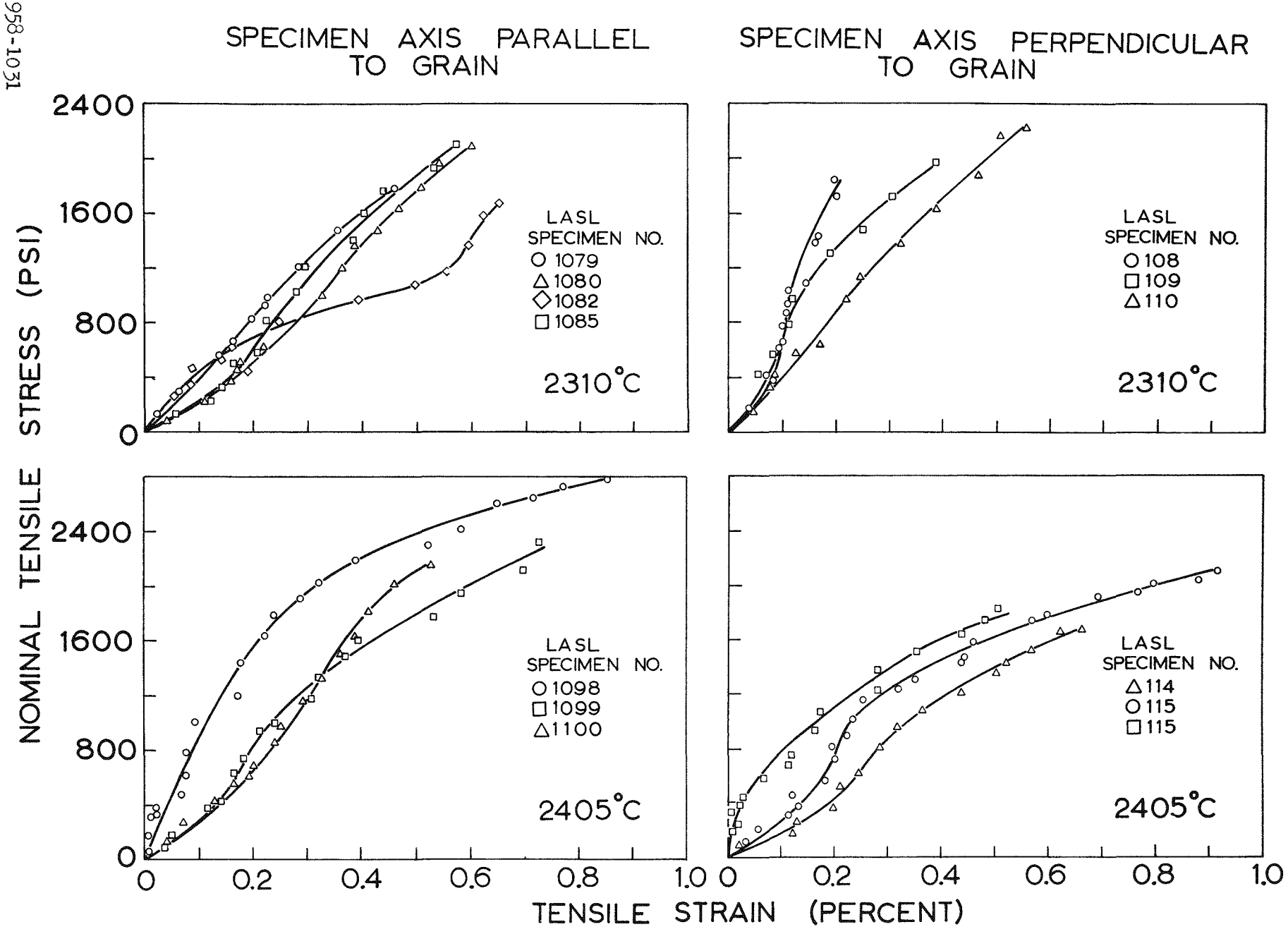

Figure 27

Tensile Stress-Strain Curves for Standard H4LM Stock (Platen Rate 0.002 in./min)

958-1042

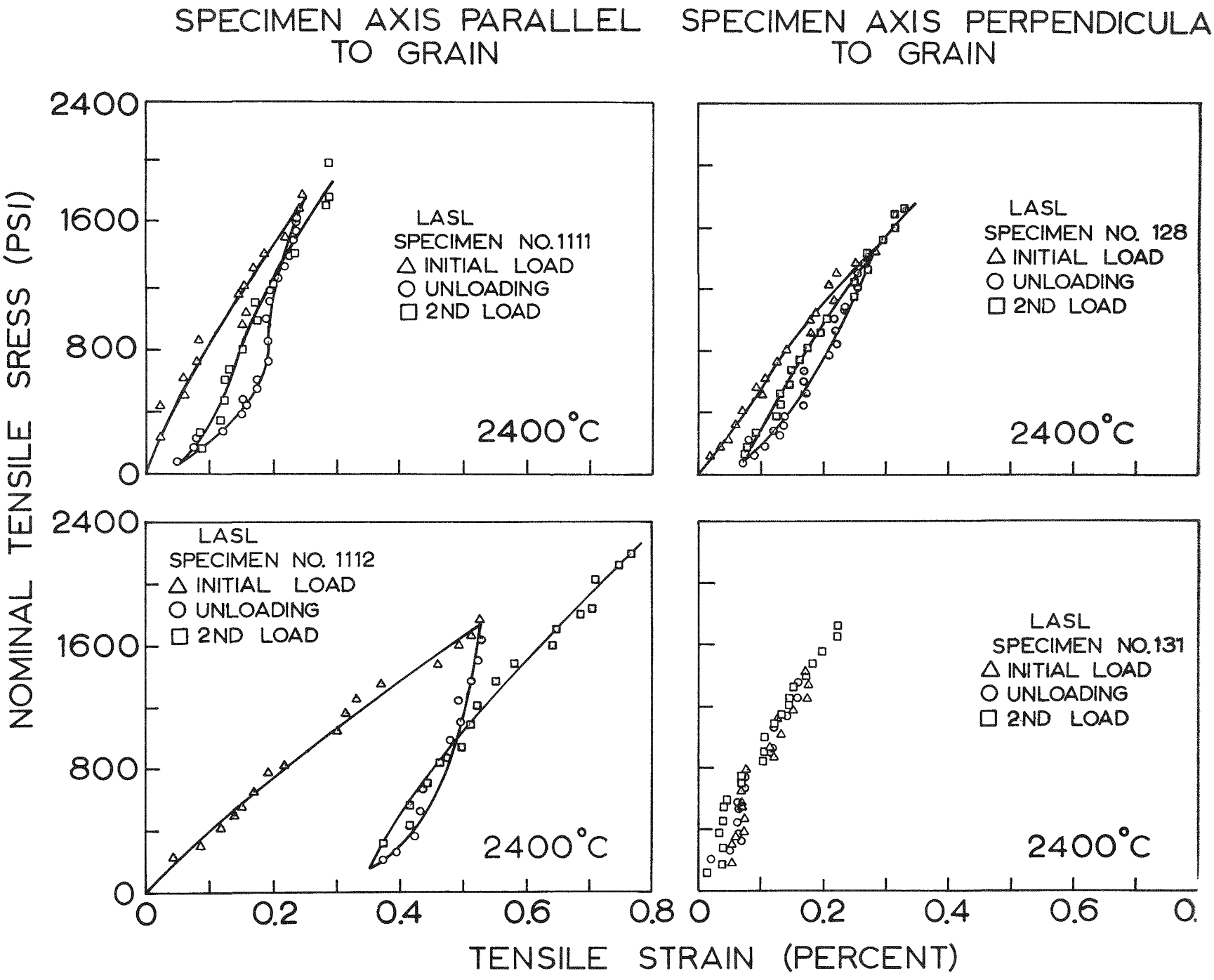

Figure 28

Mechanical-Hysteresis Curves for Standard H4LM Stock

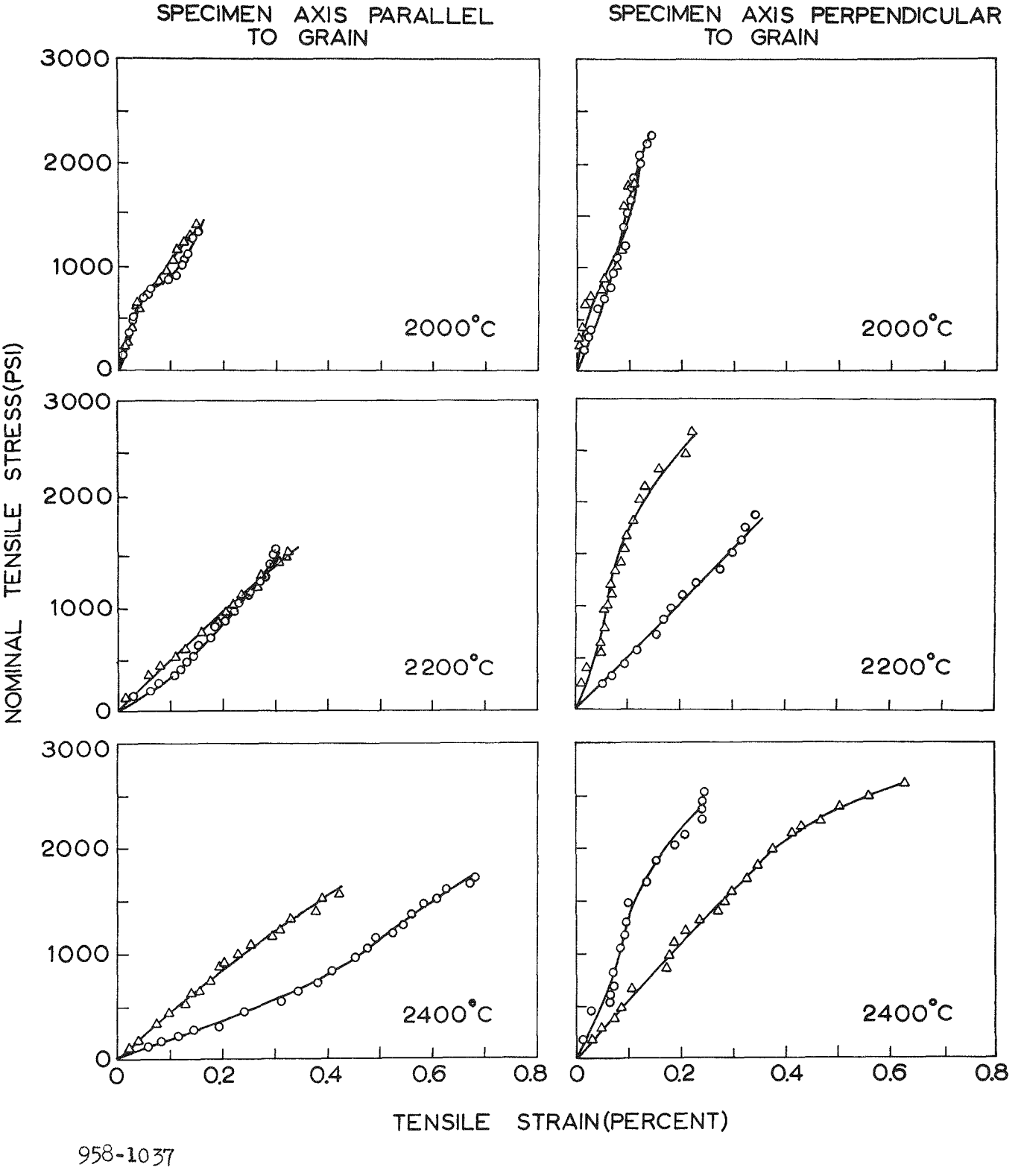

Tensile Stress-Strain Curves for Re-Impregnated H4L= Stock (Platen Rate 0.02 in./min)

Figure 29

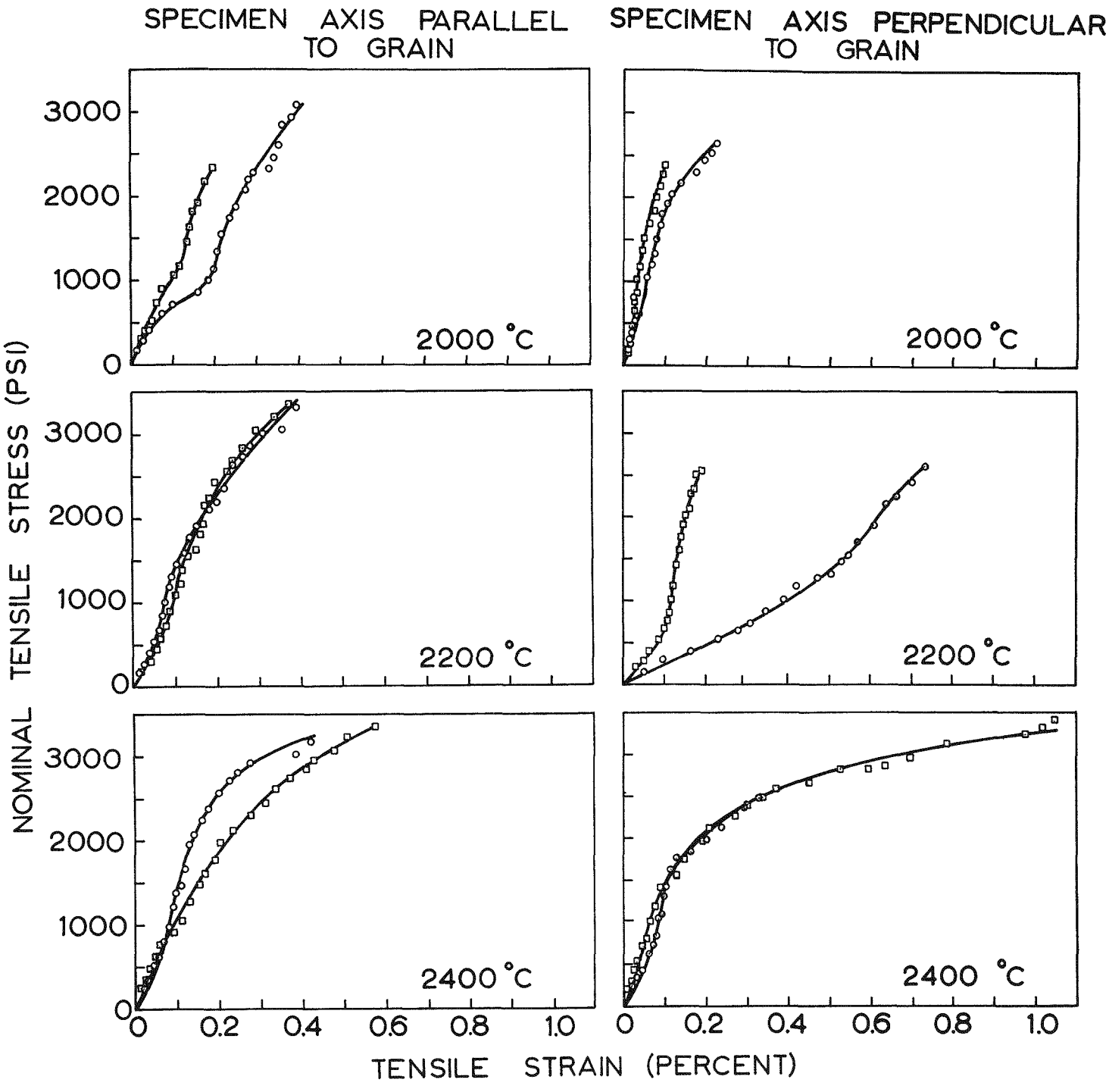

Figure 30

Tensile Stress-Strain Curves for Re-Impregnated H4LM Stock (Platen Rate 0.002 in./min)

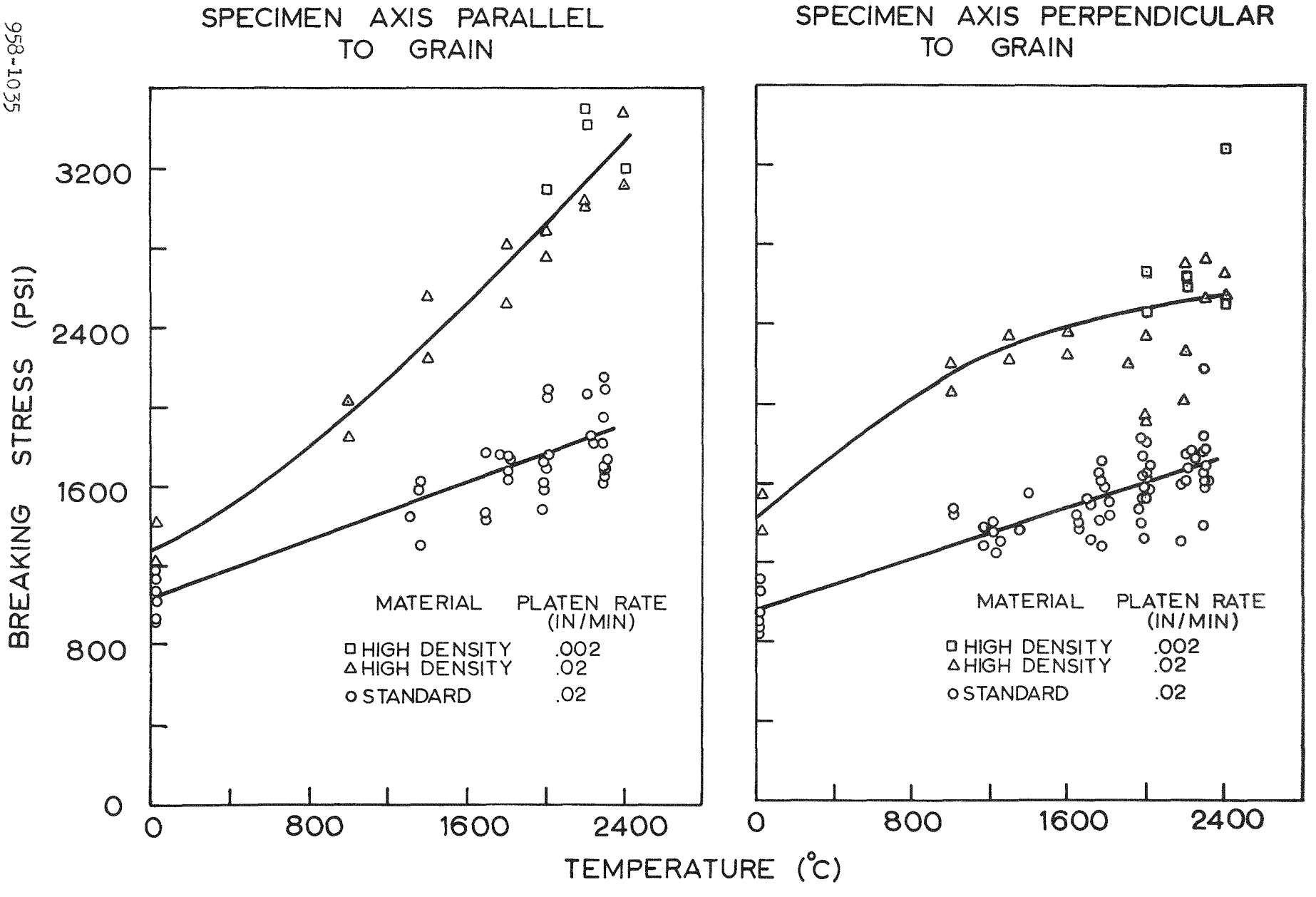

Figure 31

Ultimate Breaking Strength of Structure and Re-Impregnated Stock

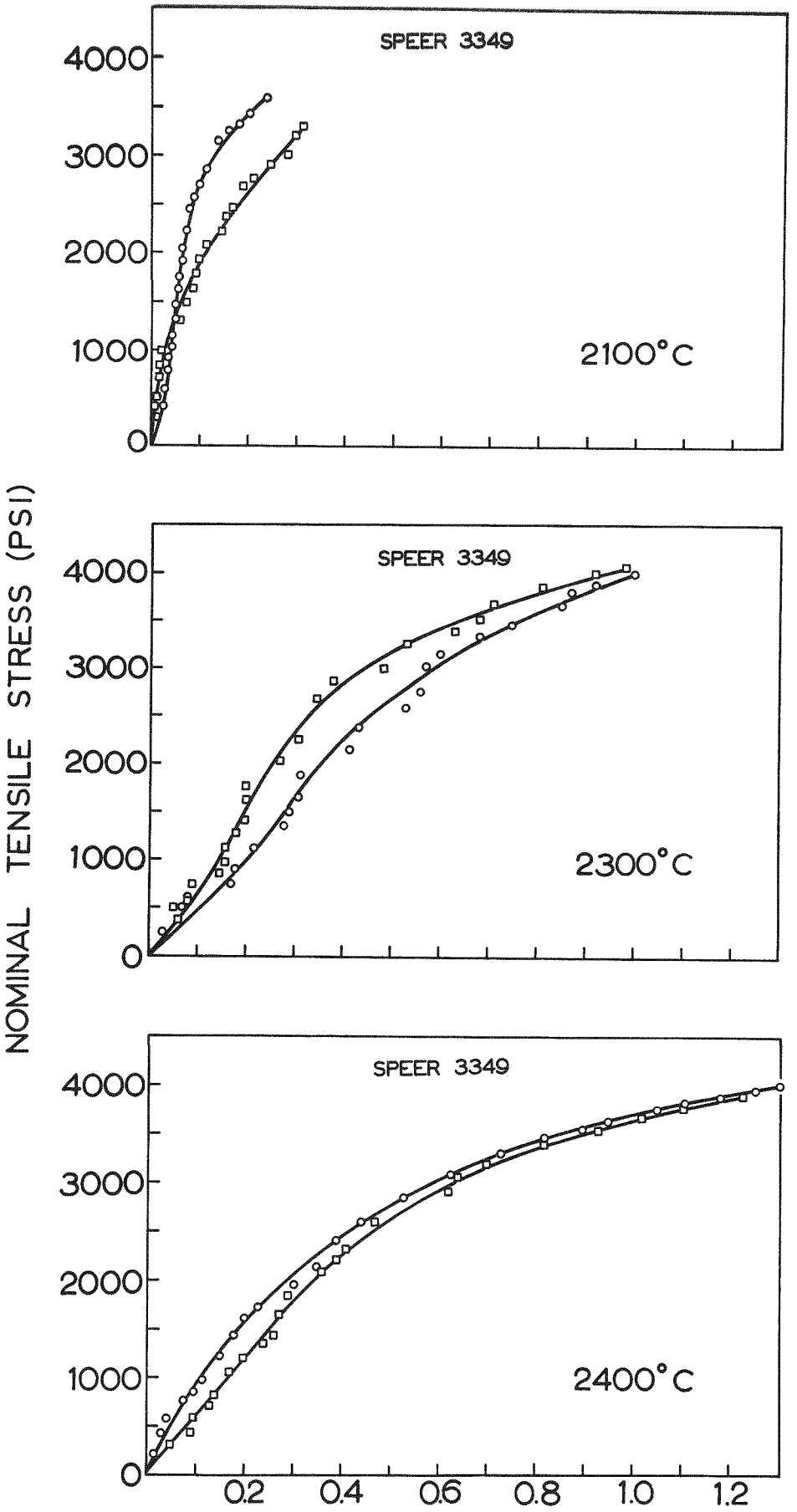

1158-930

30

Figure 32

Tensile Stress-Strain Curves for Spear Carbon, Company Grade 3349 Stock

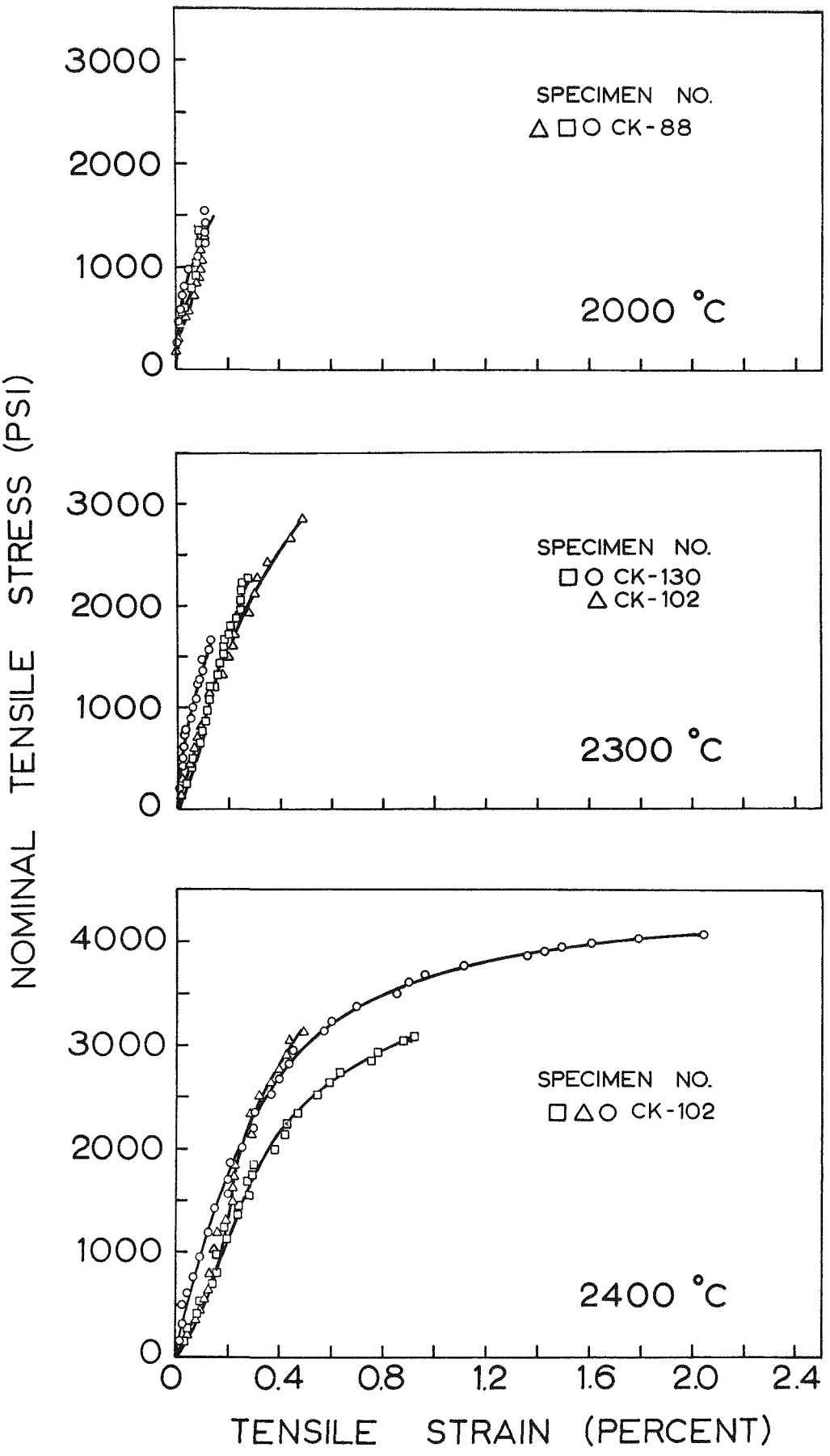

1158-927

Tensile Stress-Strain Curves for CK Stock (Platen Rate 0.02 in./min)

Figure 33

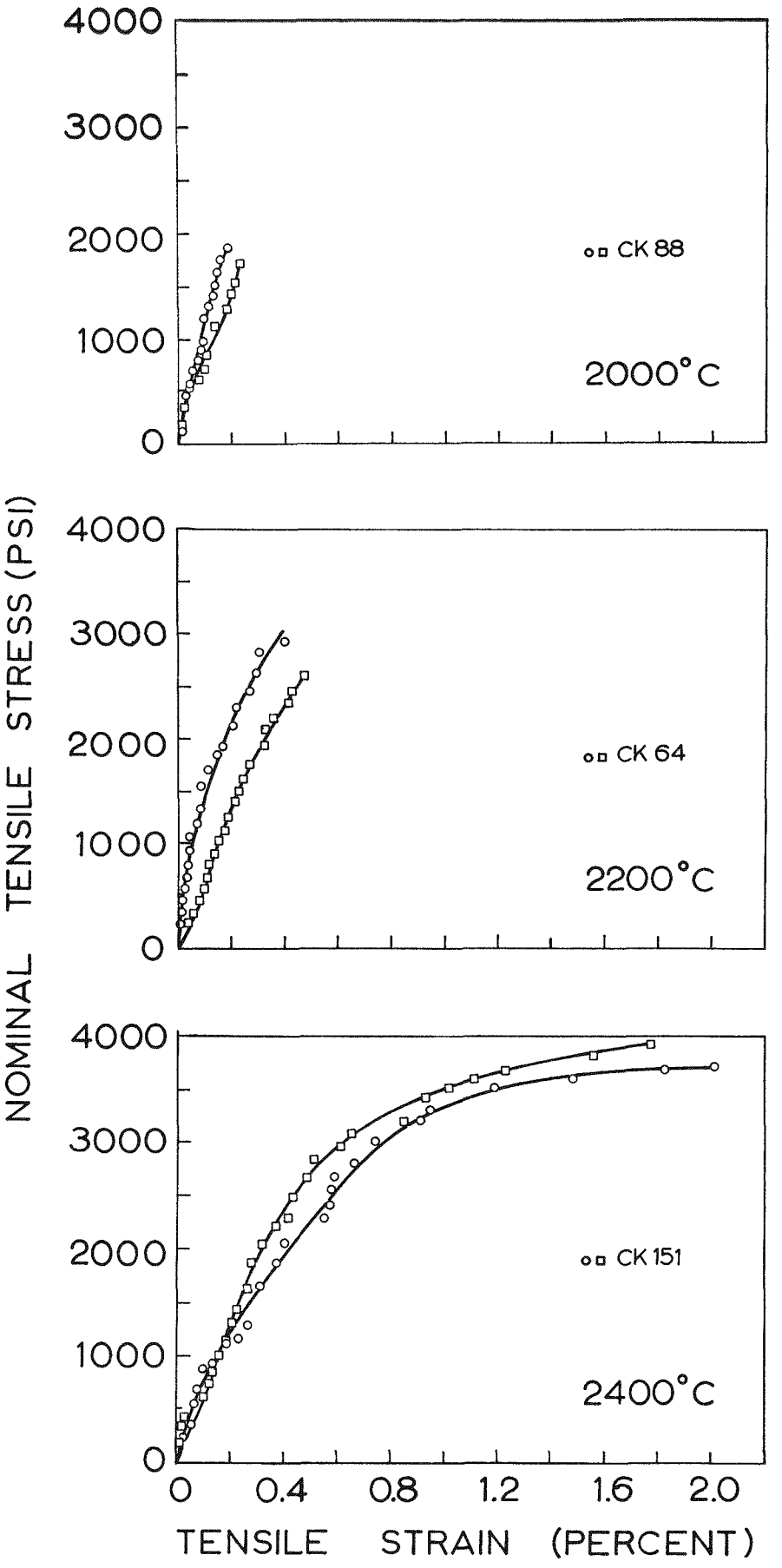

1158-915 Tensile Stress-Strain Curves for CK Stock (Platen Rate 0.002 in./min)

Figure 34

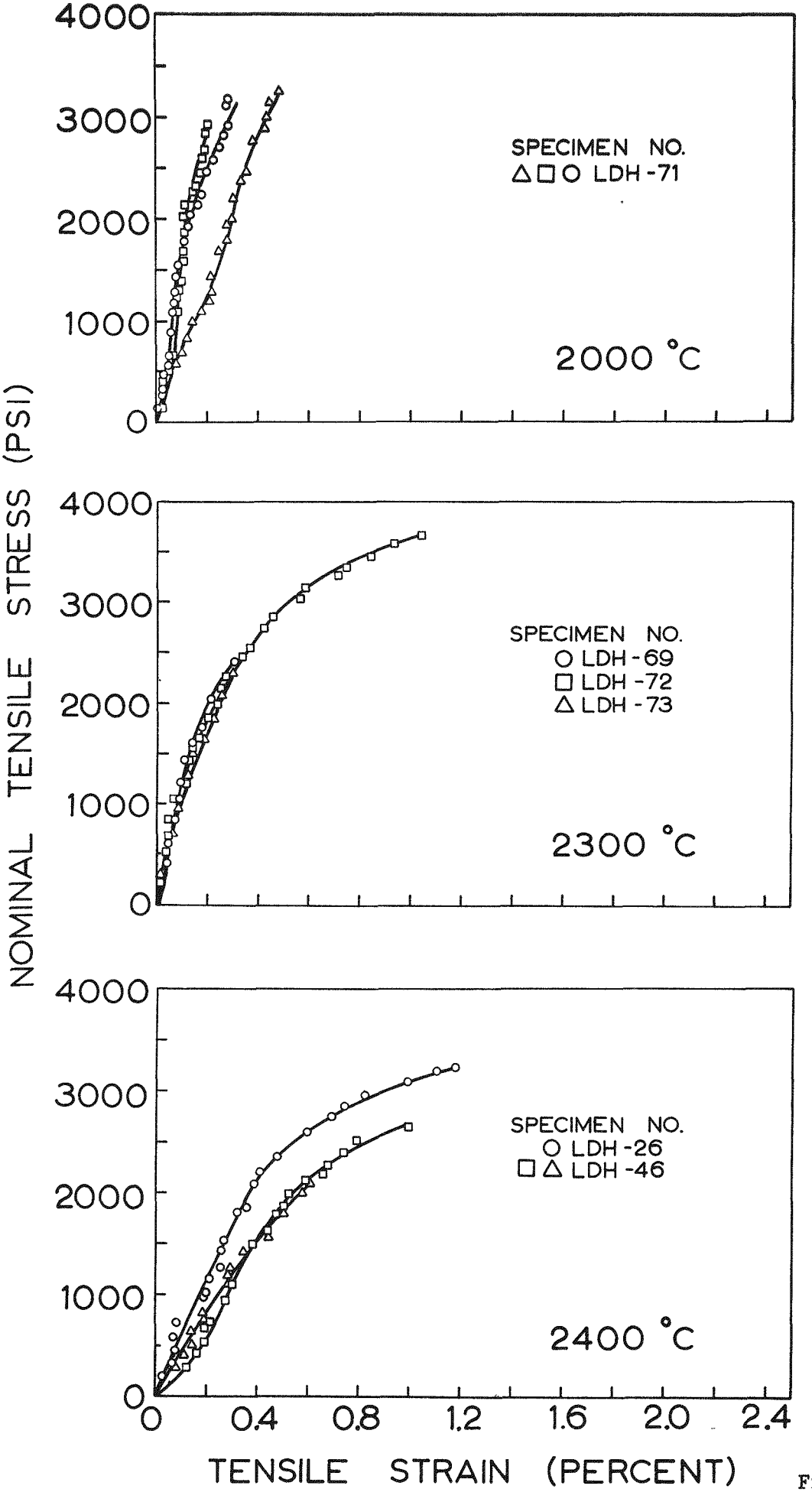

1158-942

Figure 35

Tensile Stress-Strain Curves for LDH Stock (Platen Rate 0.02 in./min)

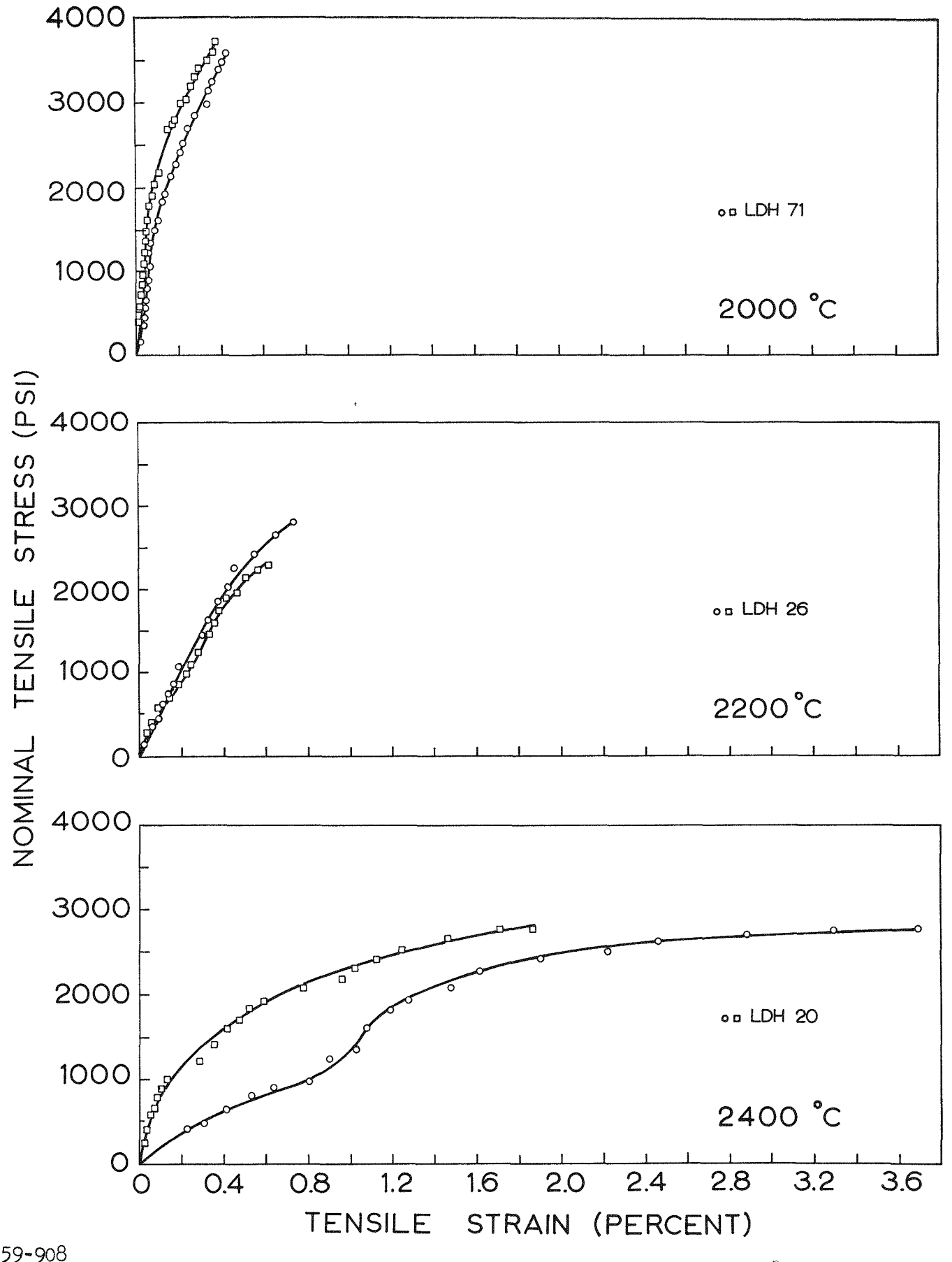

1159-908

Tensile Stress-Strain Curves for LDH Stock (Platen Rate 0.002 in./min) Figure 36

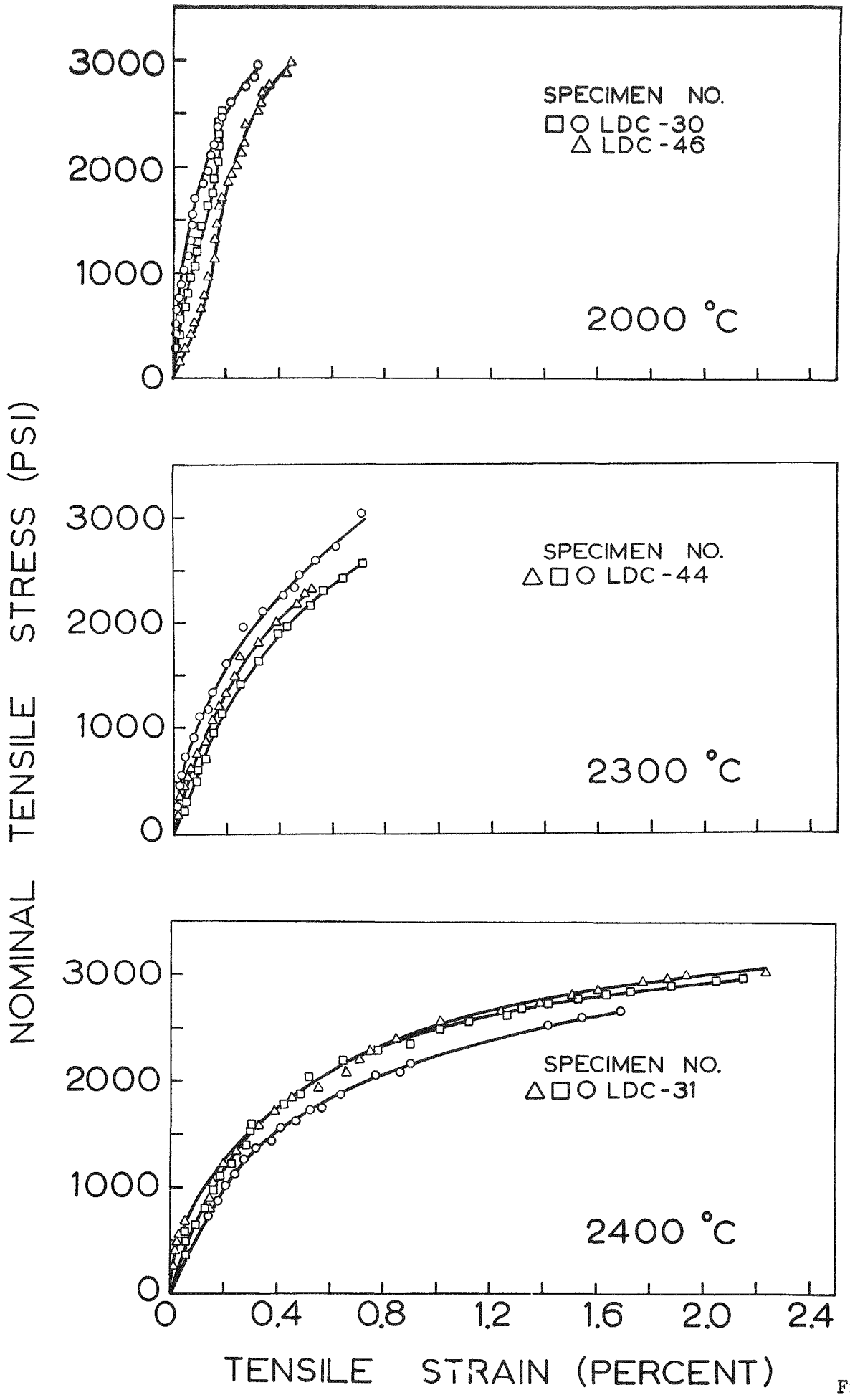

1158-941

Figure 37

Tensile Stress-Strain Curv3s for LDC Stock (Platen Rate 0.02 in./min

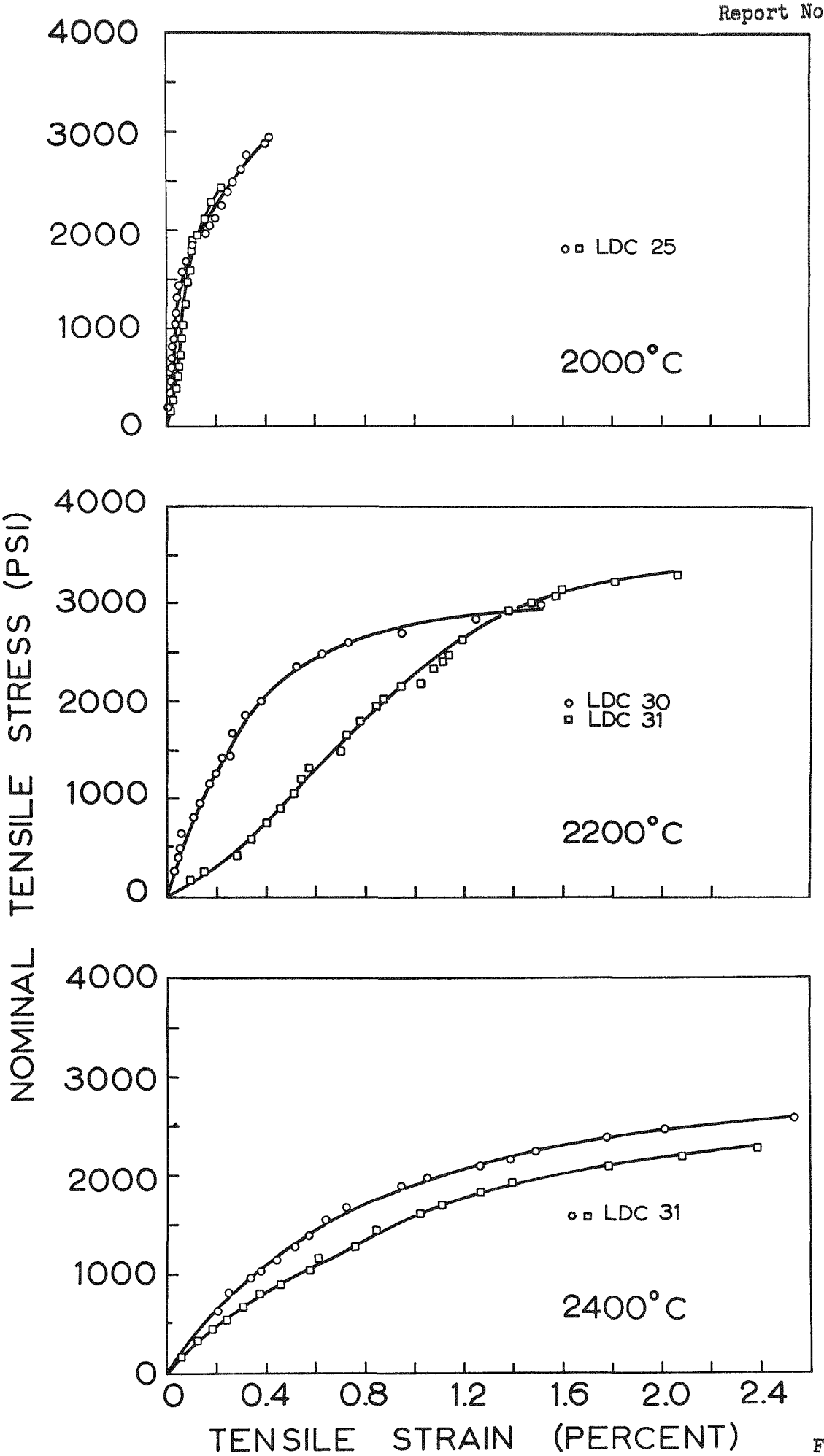

1158-912

Figure 38

Tensile Stress-Strain Curves for LDC Stock (Platen Rate 0.002 in./min

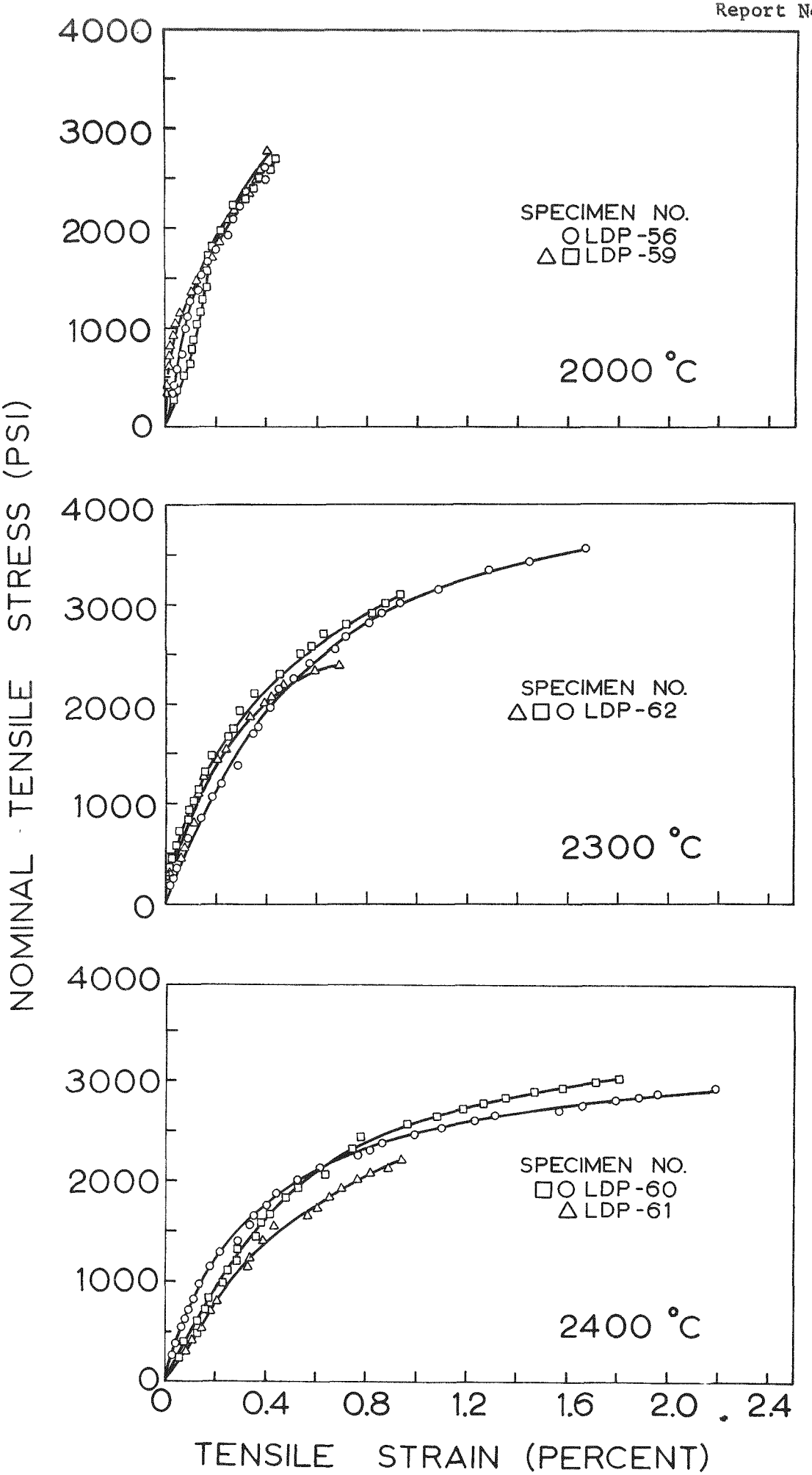

1158-901

Figure 39

Tensile Stress-Strain Curves for LDP Stock (Platen Rate 0.02 in./min)

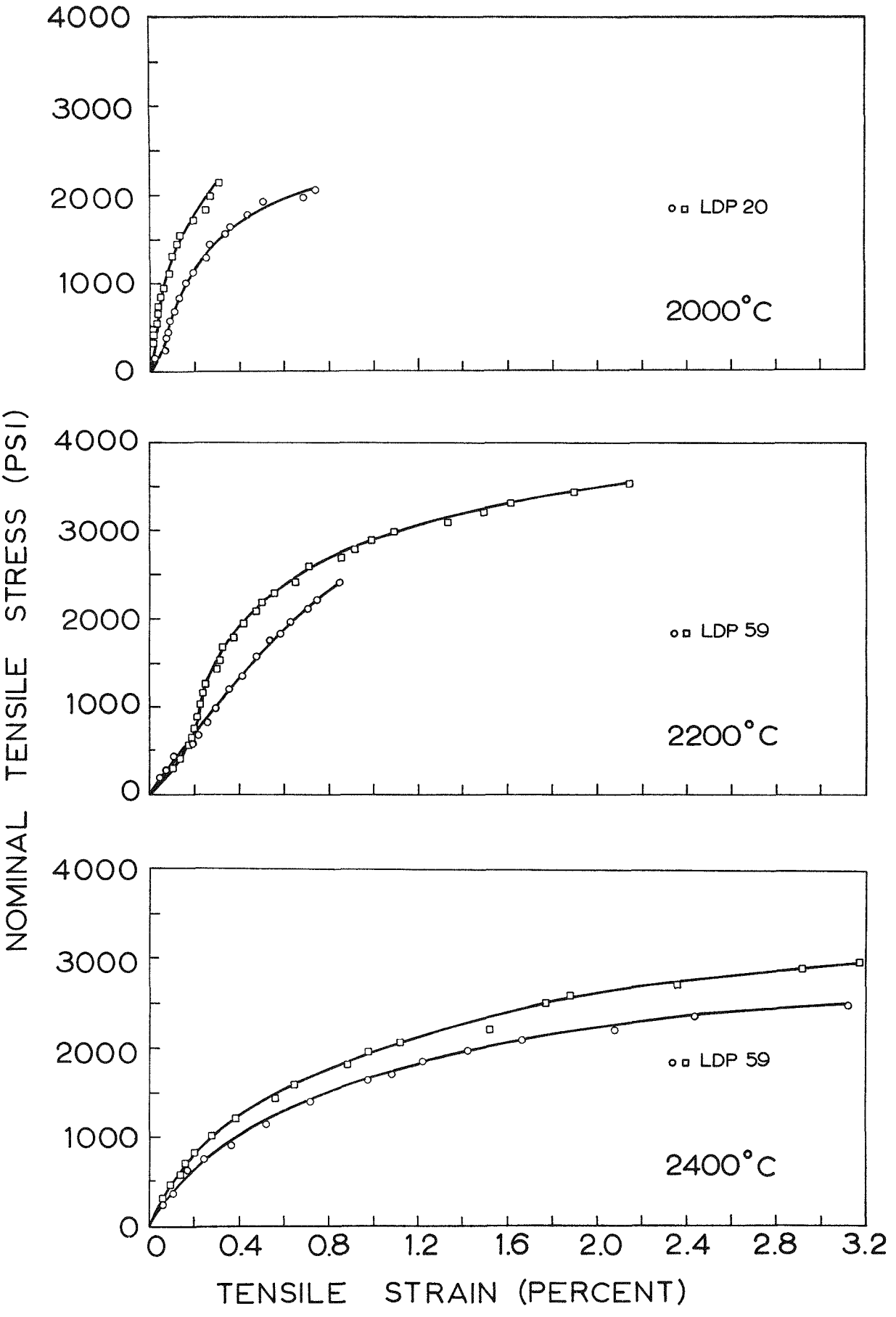

1158-916

Figure 40

Tensile Stress-Strain Curves for LDP Stock (Platen Rate 0.002 in./min)

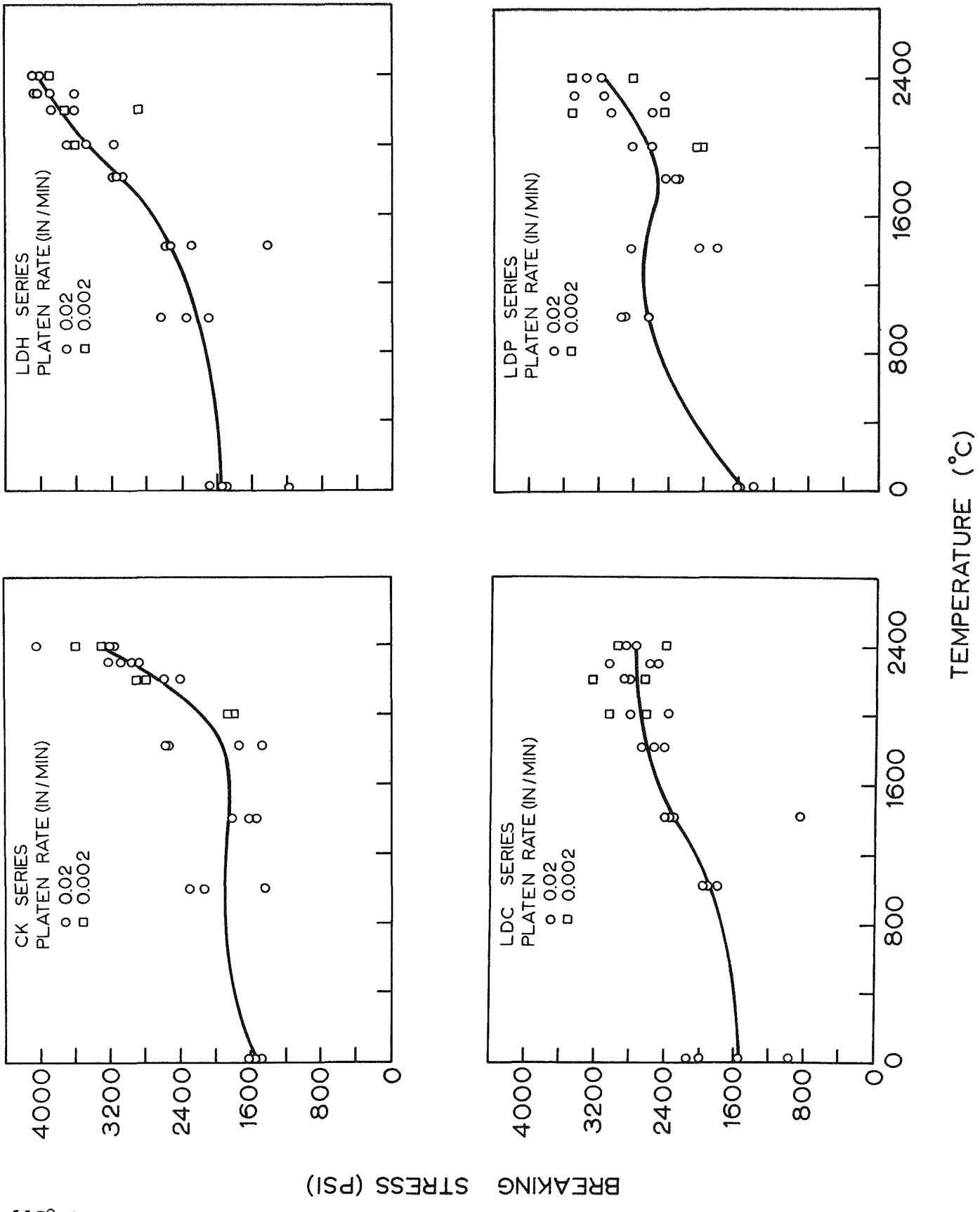

1158-900

Ultimate Tensile Breaking Strength of Los Alamos Grades

Figure 41

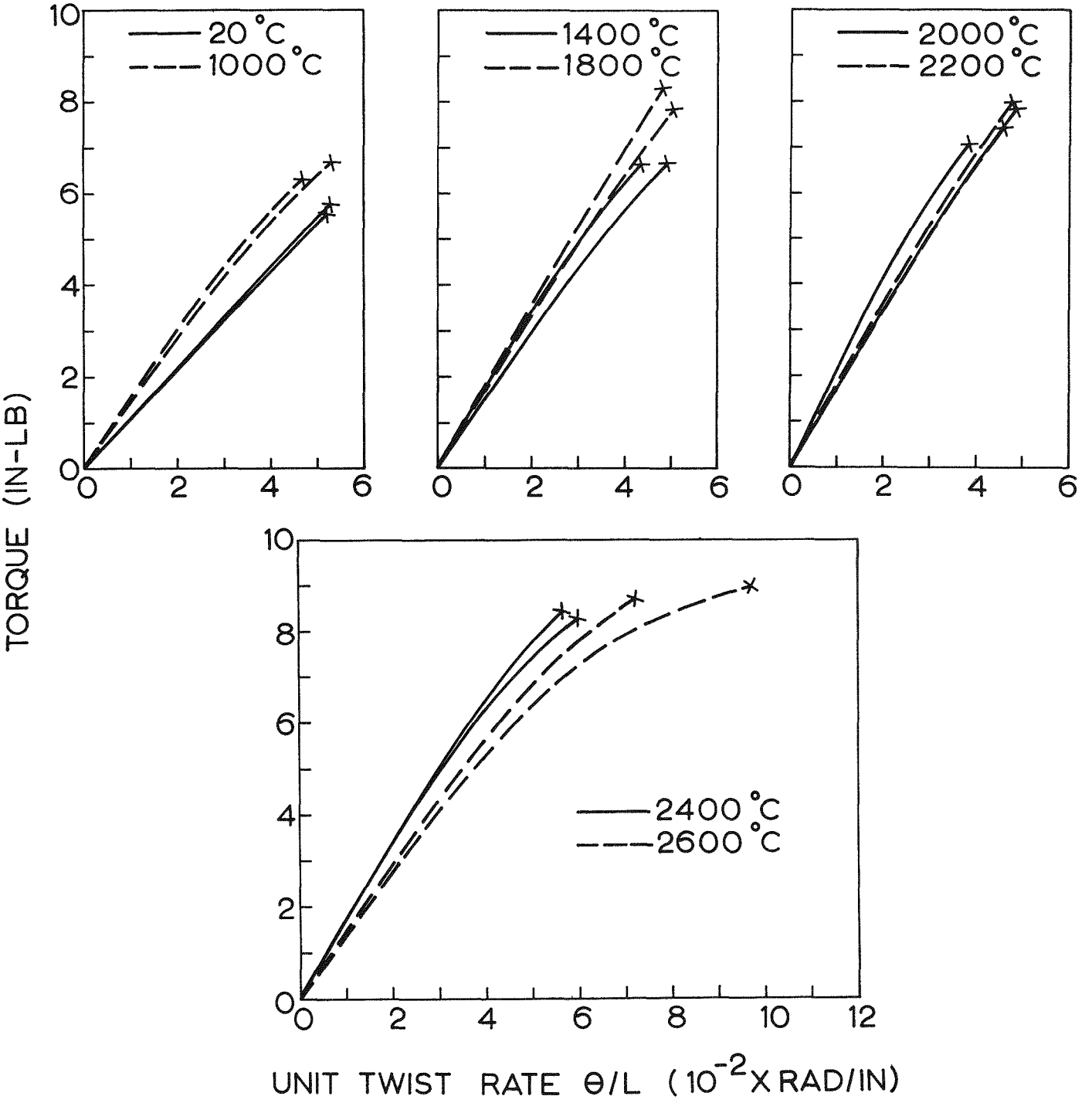

Torque-Twist Curves for Re-Impregnated H4LM Stock (Specimen Axis Paralled to Grain, Rate of Twist 0.5 rad/min)

Figure 42

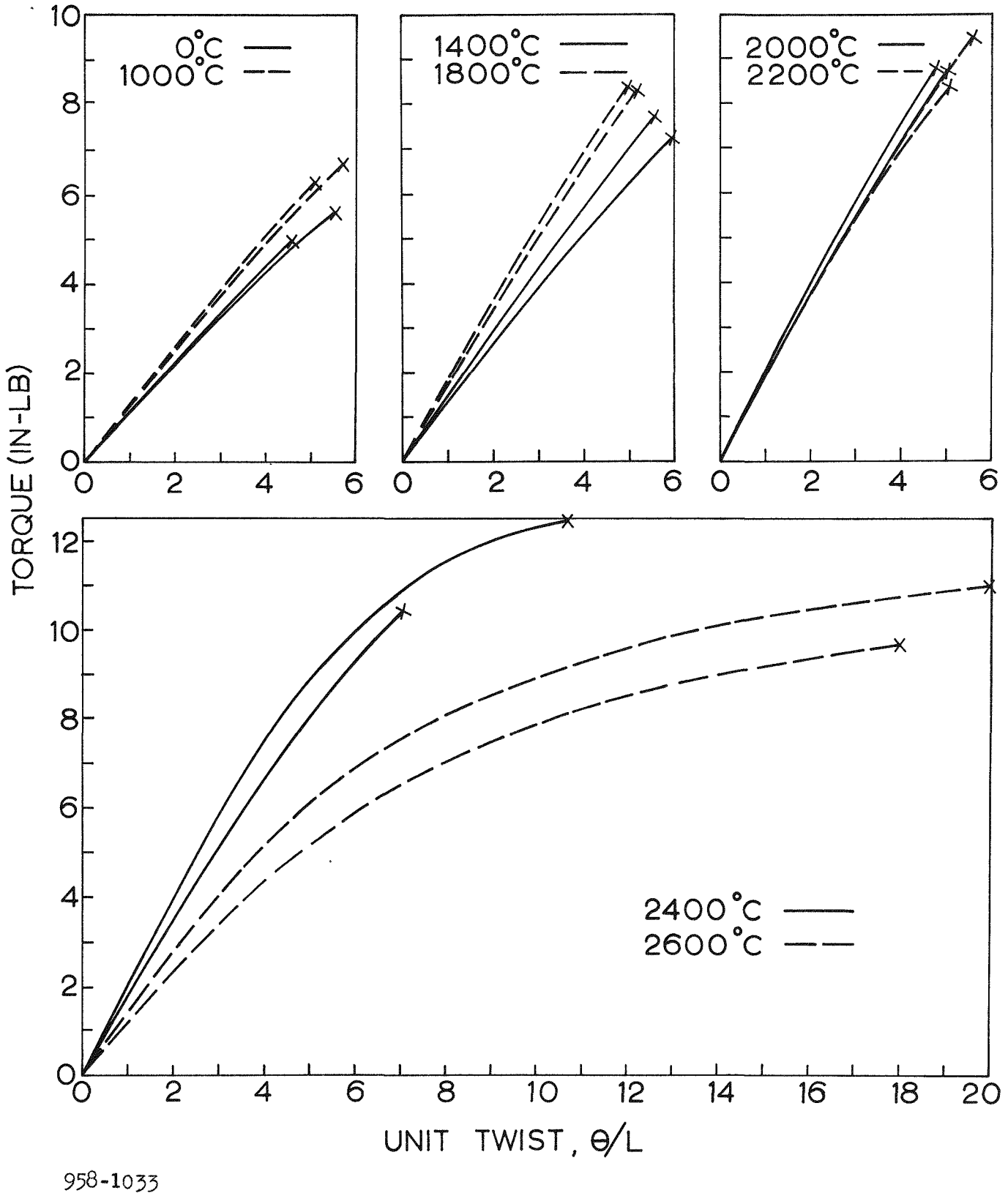

Torque-Twist Curves for Re-Impregnated H4LM Stock (Specimen Axis Parallel to Grain, Rate of Twist 0.1 rad/min)

Figure 43

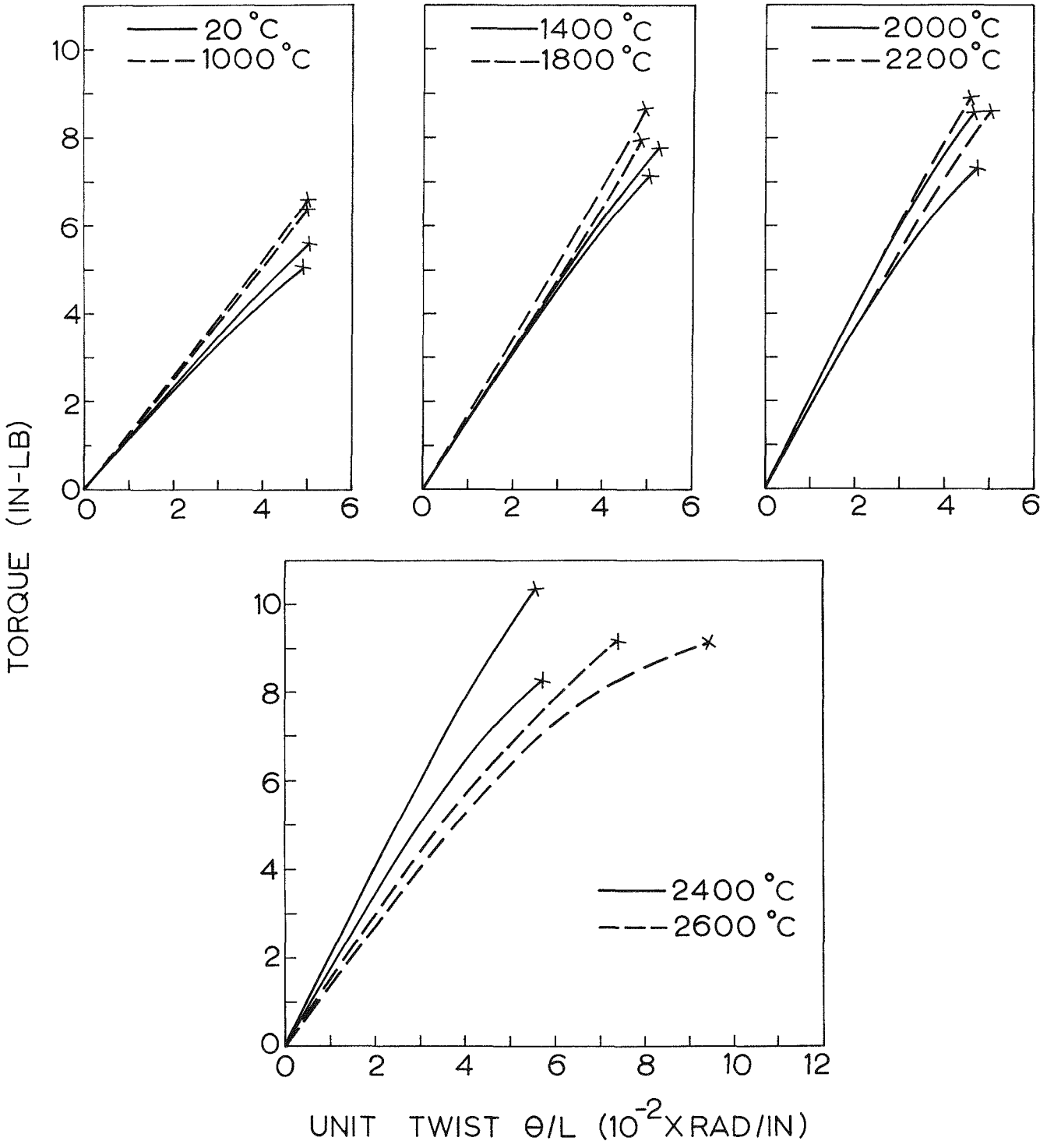

1158-888

Torque-Twist Curves for Re-Impregnated H4LM Stock (Specimen Axis Perpendicular to Grain, Unit-Twist Rate 0.5 rad/min)

Figure 44

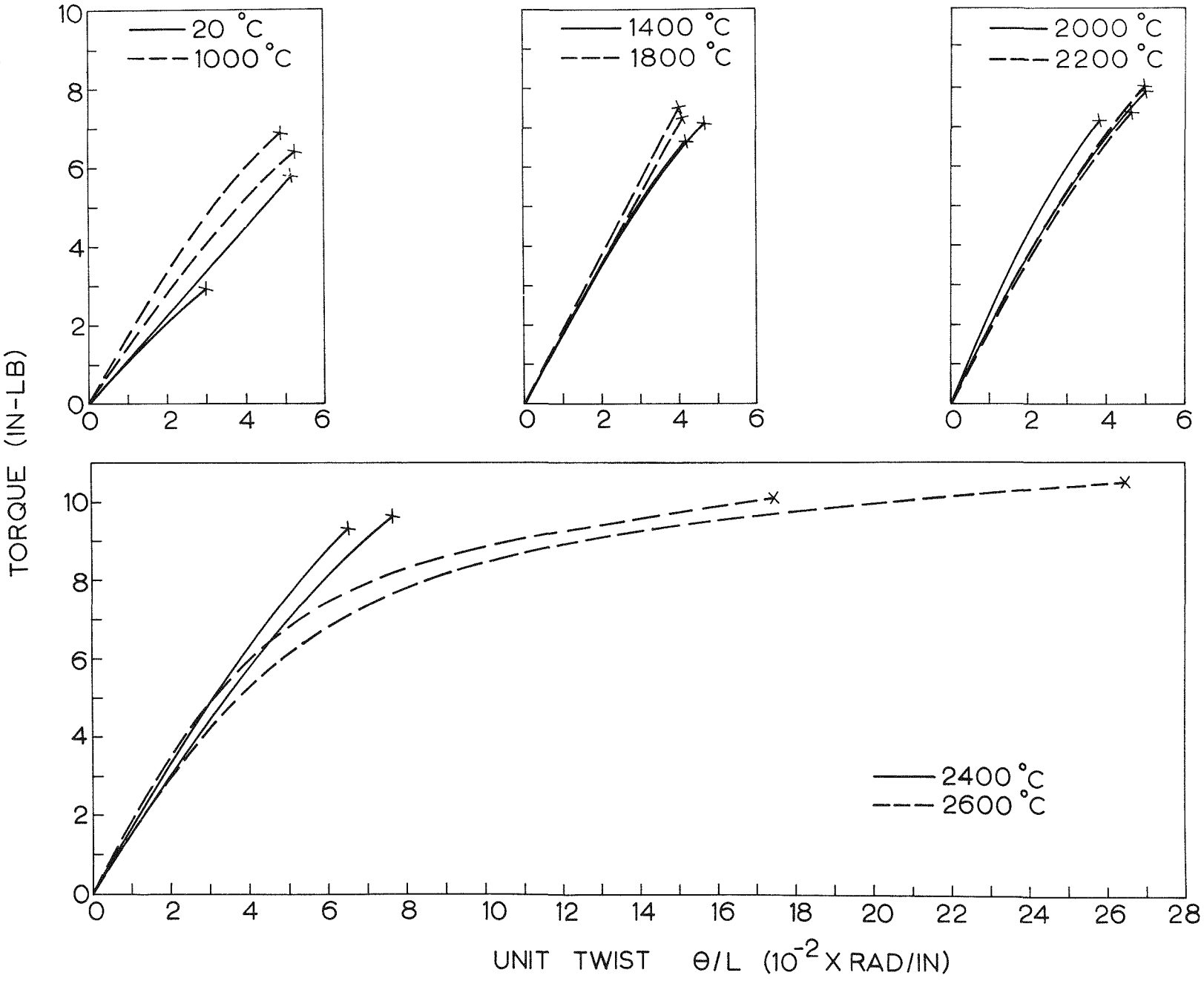

Figure 45

Torque-Twist Curves for Re-Impregnated H4LM Stock (Specimen Axis Perpendicular to Grain, Unit-Twist Rate 0.1 rad/min)

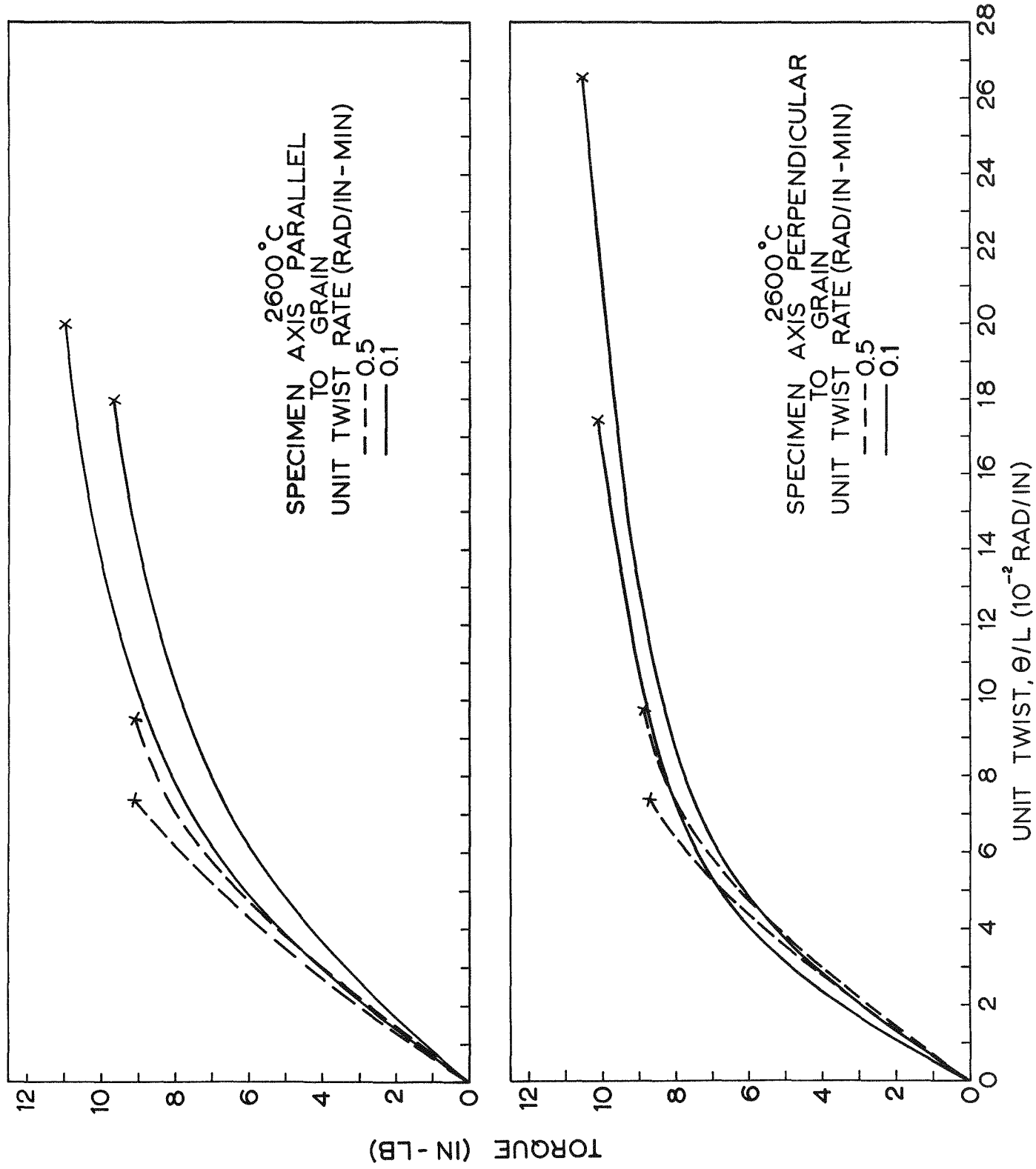

958-1041

Effect of Unit-Twist Rate of Torque-Twist Curves on Torque-Twist Curves for Re-Impregnated H4LM Stock at 2600°C

Figure 46

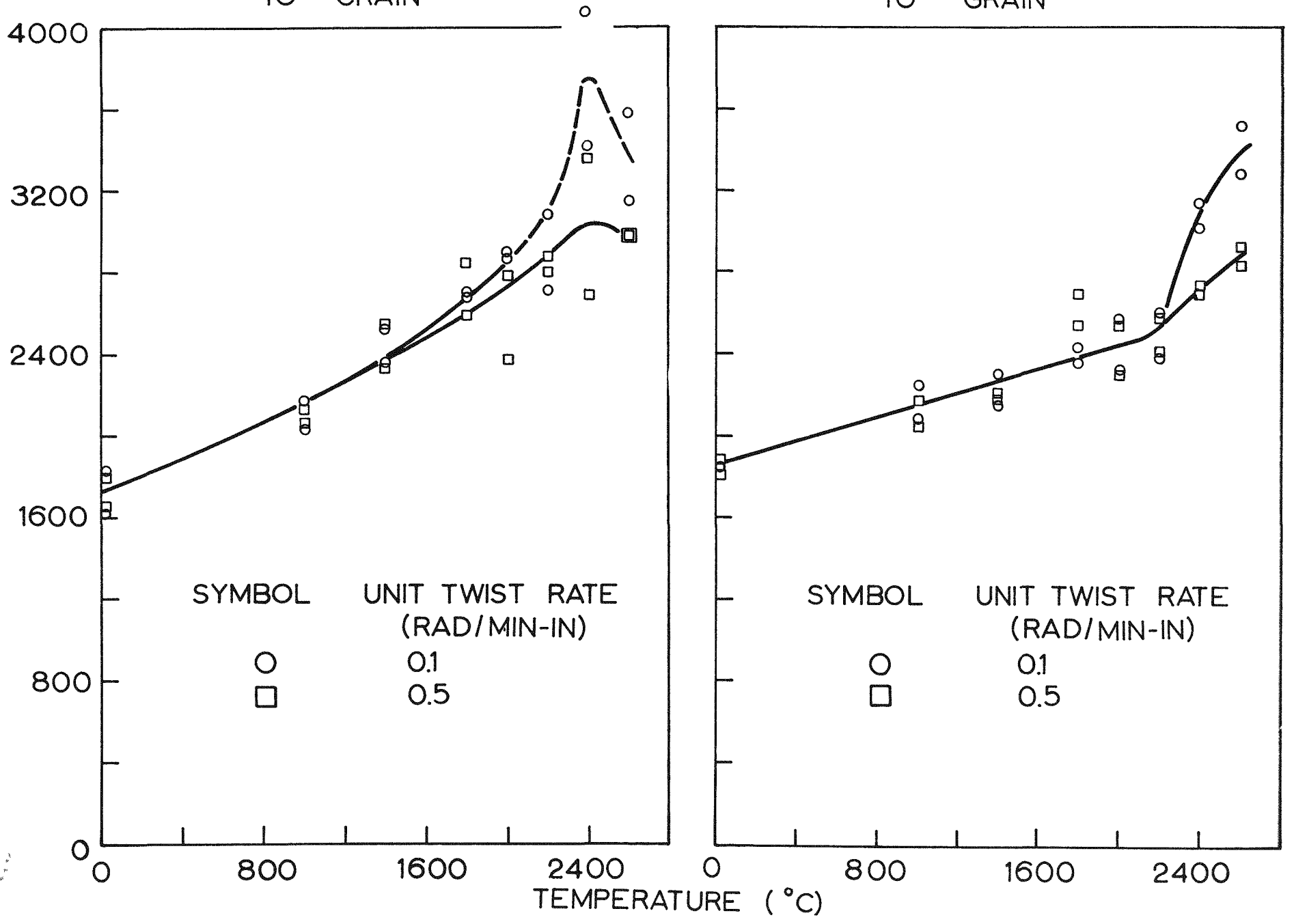

Figure 47

Maximum Shear Stress at Fracture for Re-Impregnated H4LM Stock

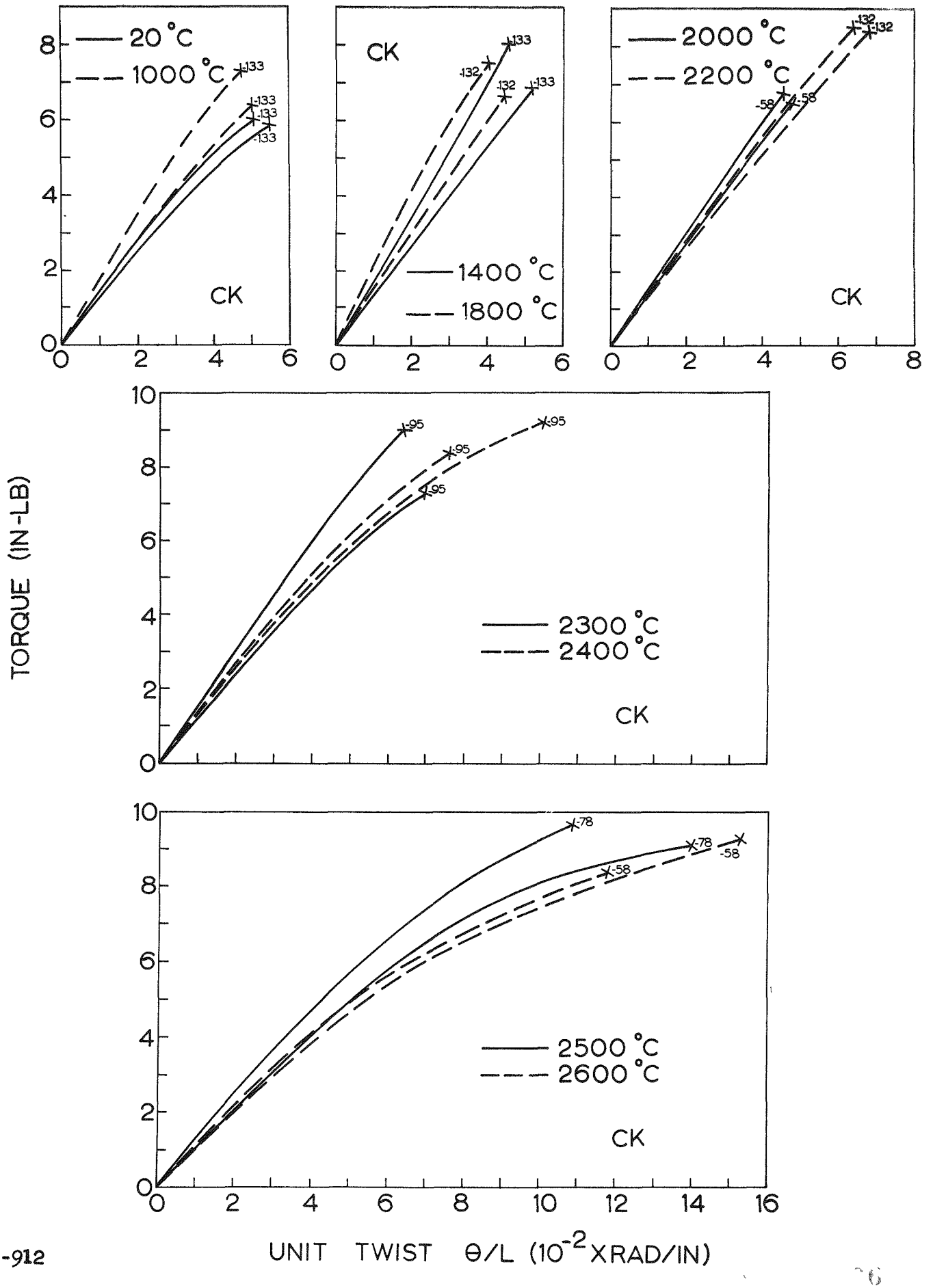

1158-912

Torque-Twist Curves for CK Stock (Unit Twist Rate 0.05 rad/min)

Figure 48

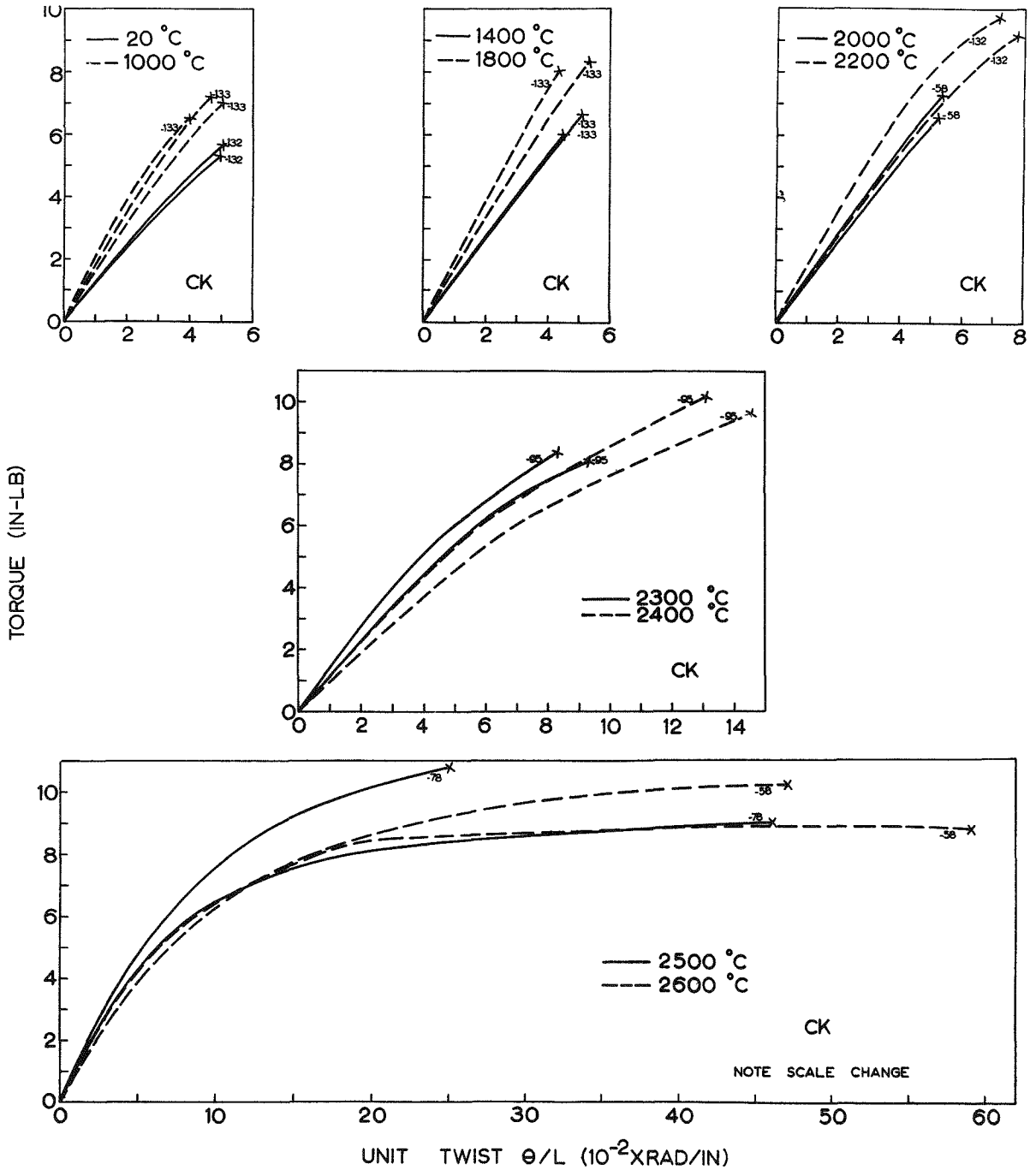

Figure 49

Torque-Twist Curves for CK Stock (Unit Twist Rate 0.1 rad/min)

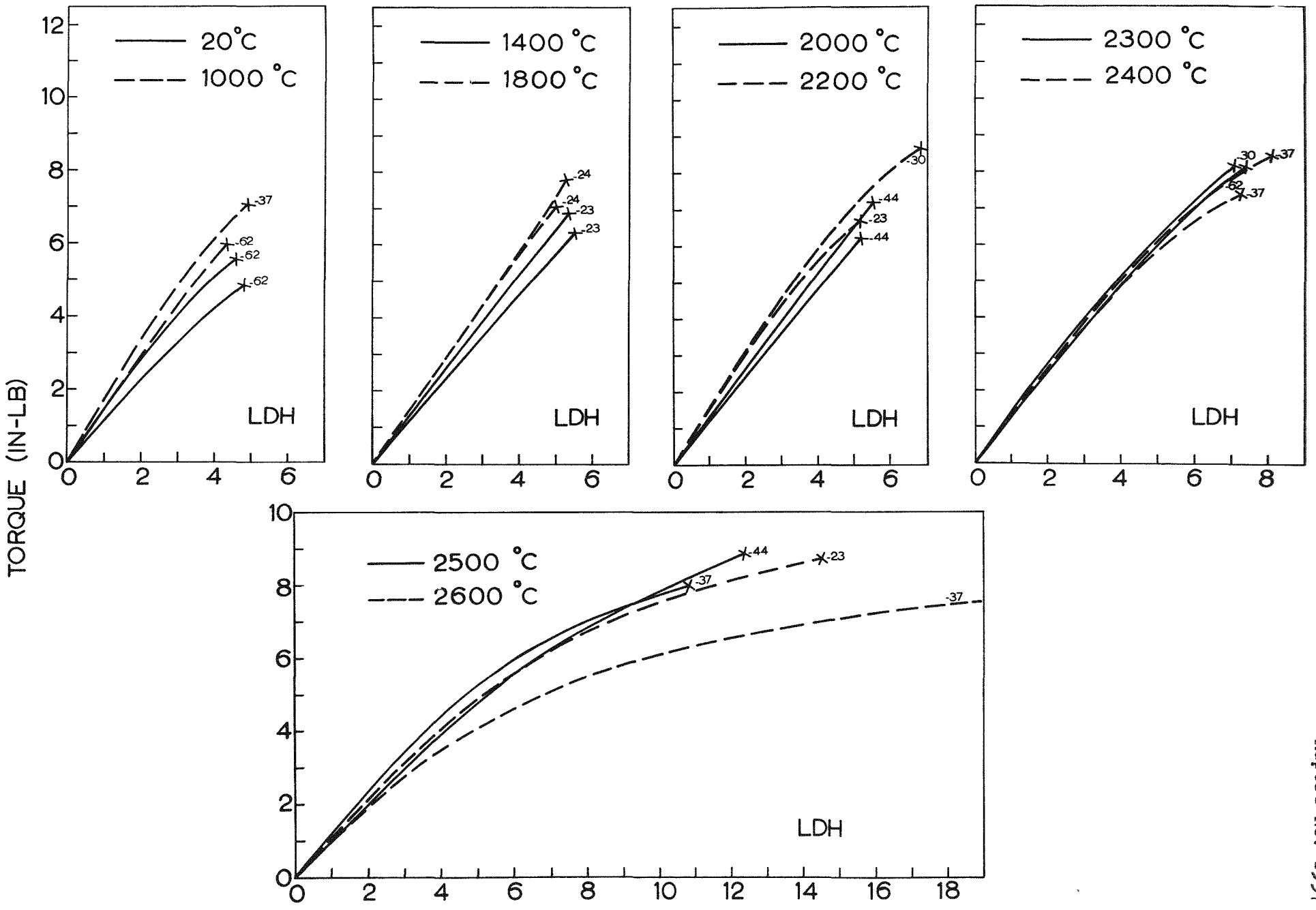

Torque-Twist for LDH Stock (Unit Twist Rate 0.5 rad/min)

Figure 50

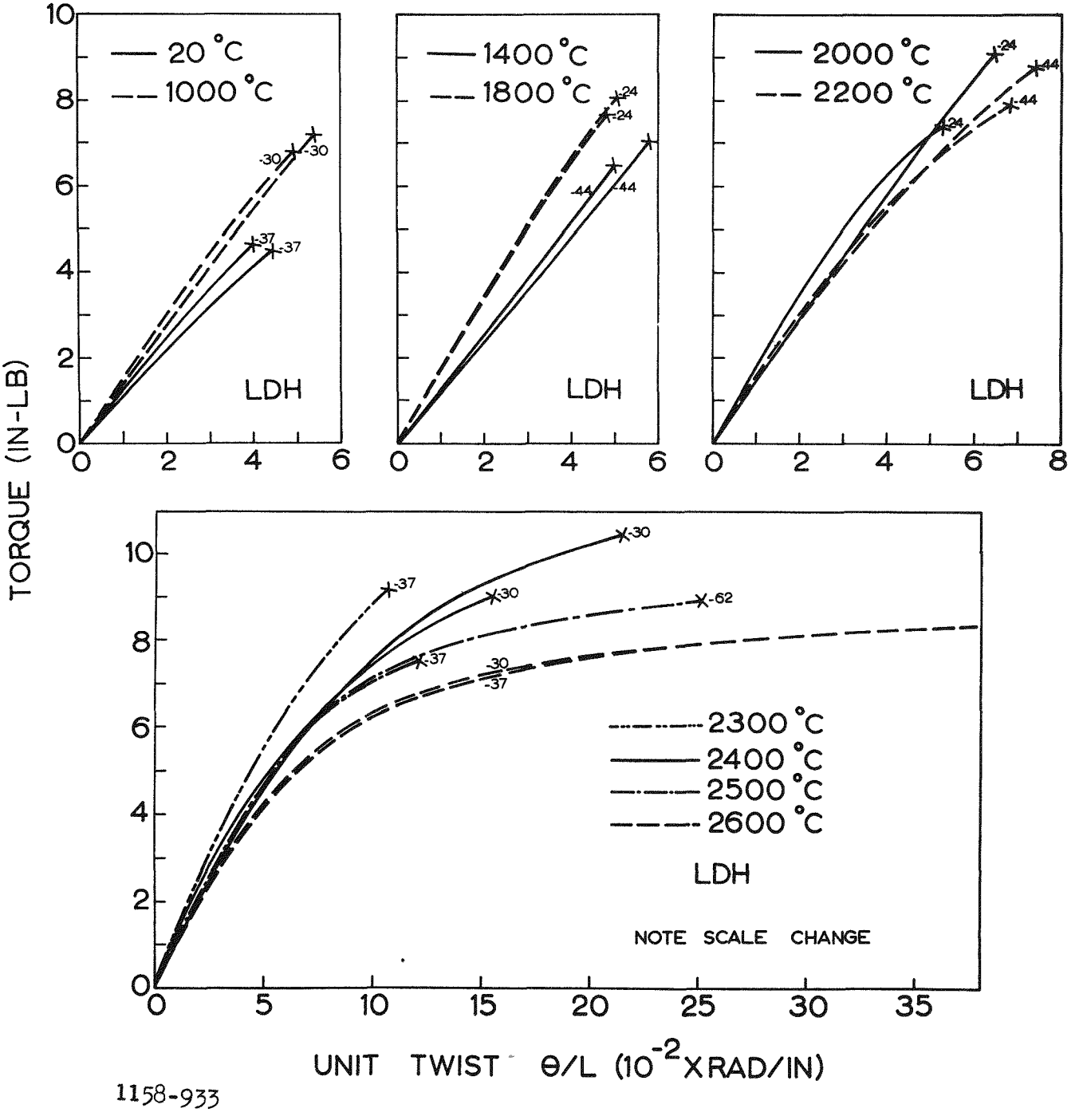

Torque-Twist for LDH Stock (Unit Twist Rate 0.1 rad/min)

Figure 51

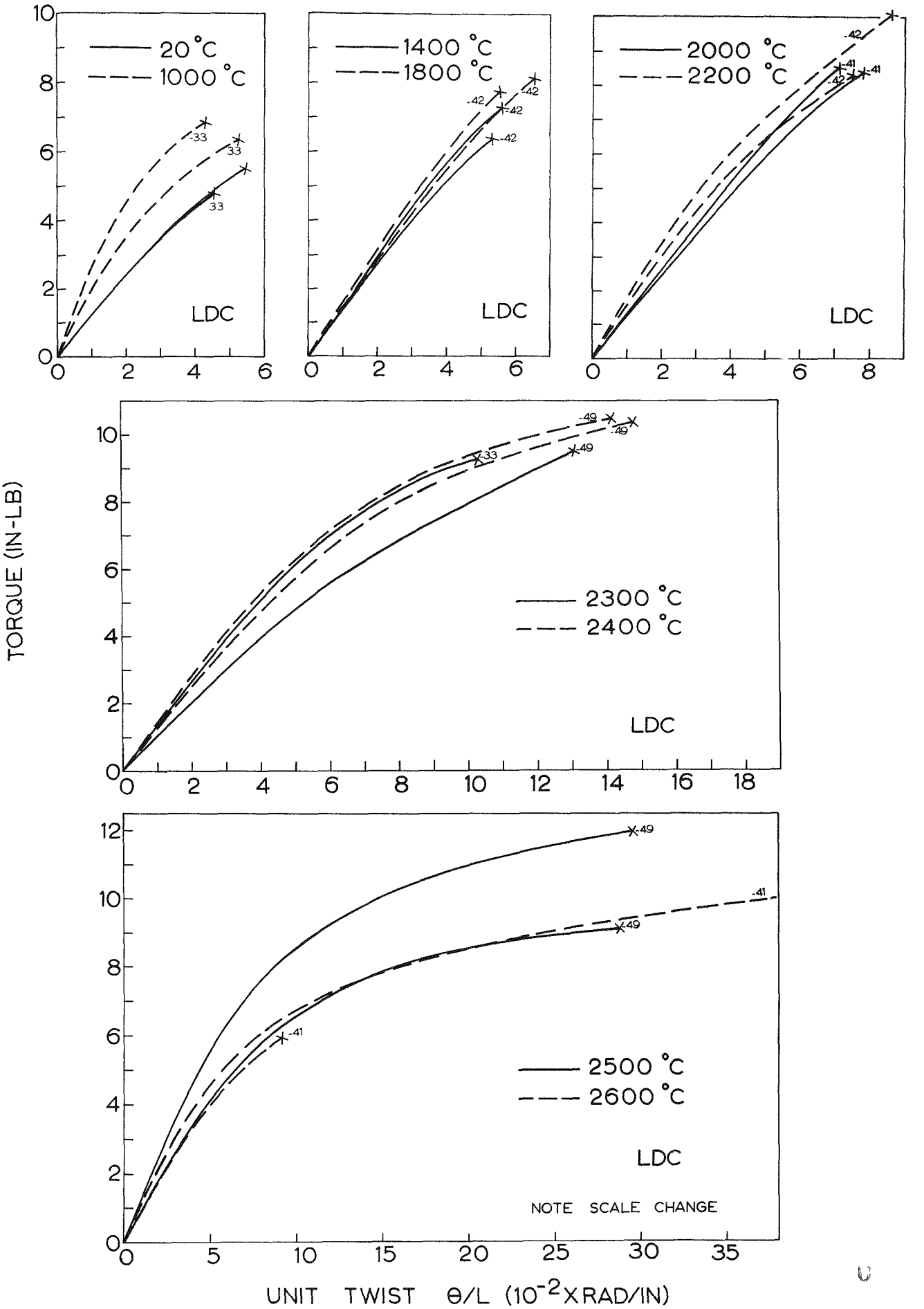

Figure 52

Torque-Twist Curves for LDC Stock (Unit-Twist Rate 0.5 rad/min)

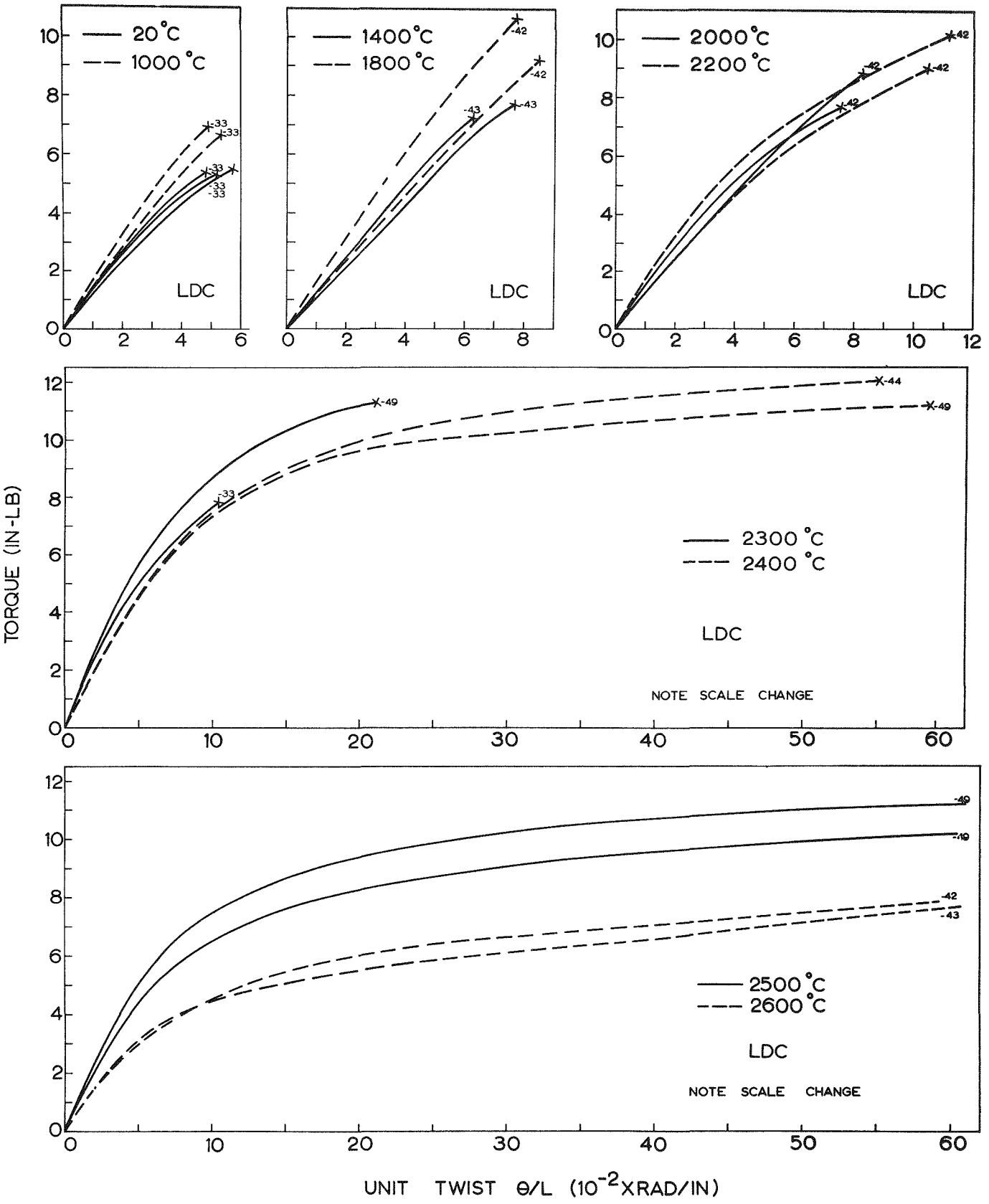

1158-910

Torque-Twist Curves for LDC Stock (Unit-Twist Rate 0.1 rad/min)

Figure 53

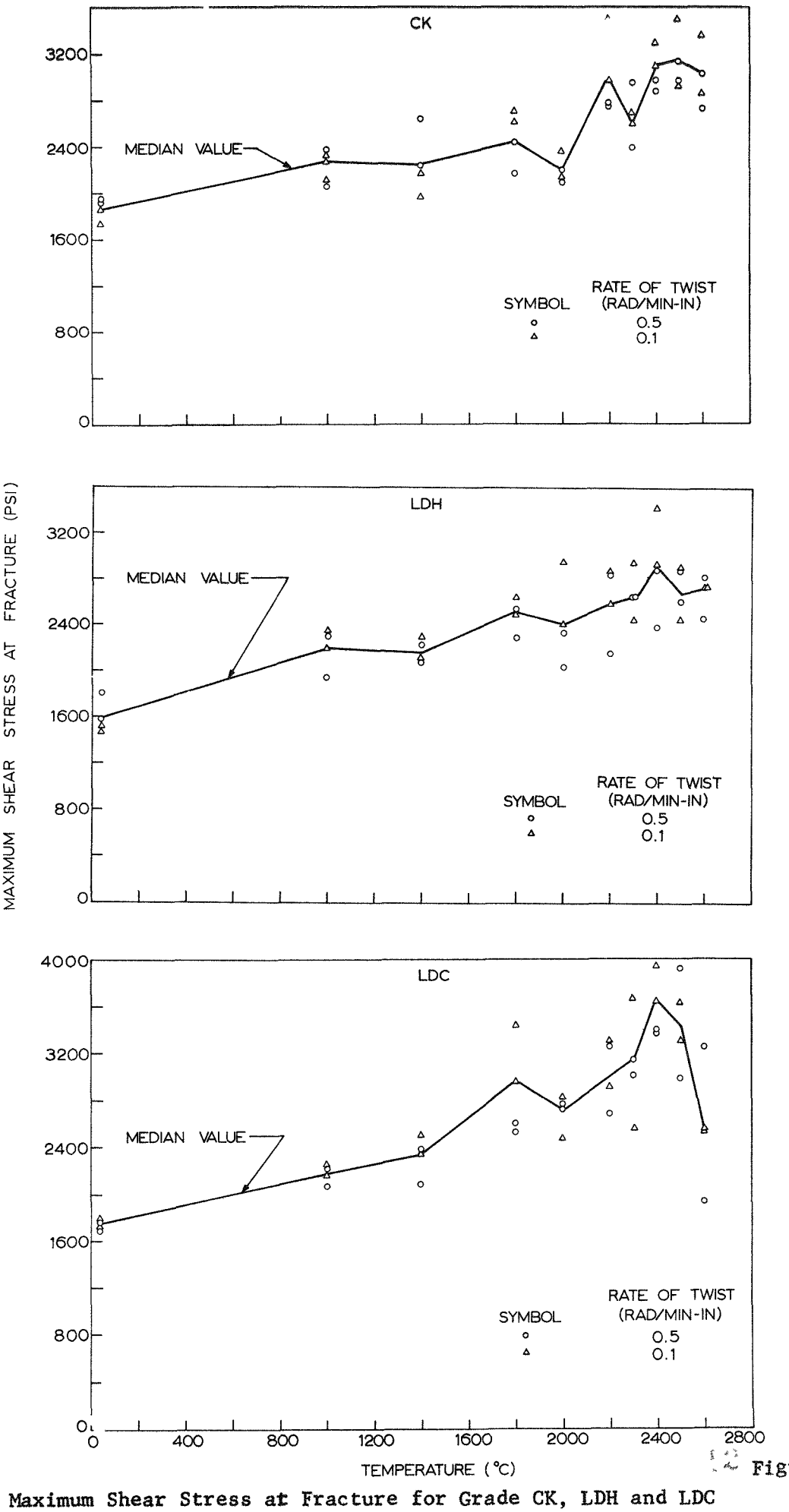

1158-894

Figure 54

Maximum Shear Stress at Fracture for Grade CK, LDH and LDC

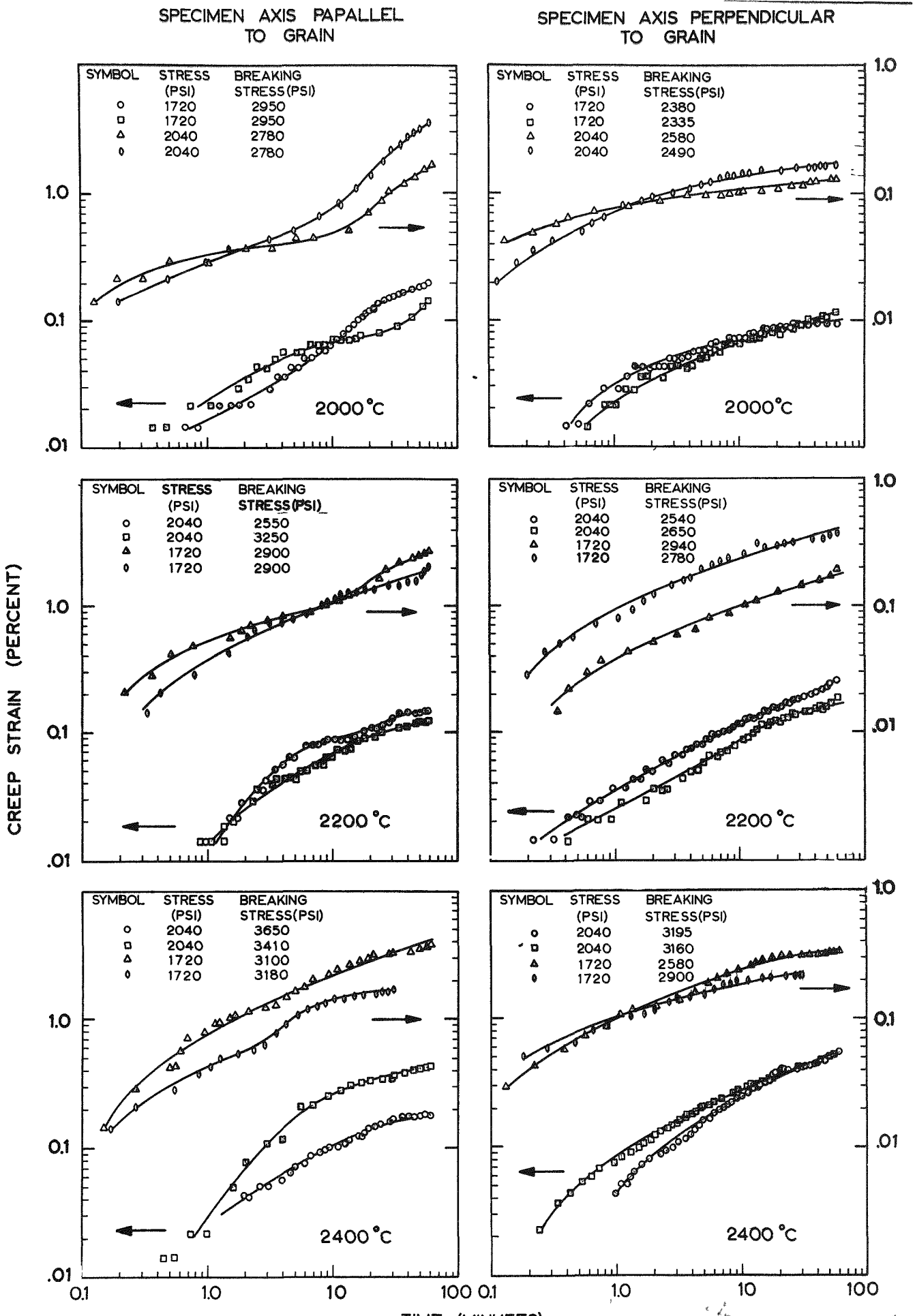

958-1044

Figure 56

Tensile Creep of Re-Impregnated H4LM Stock

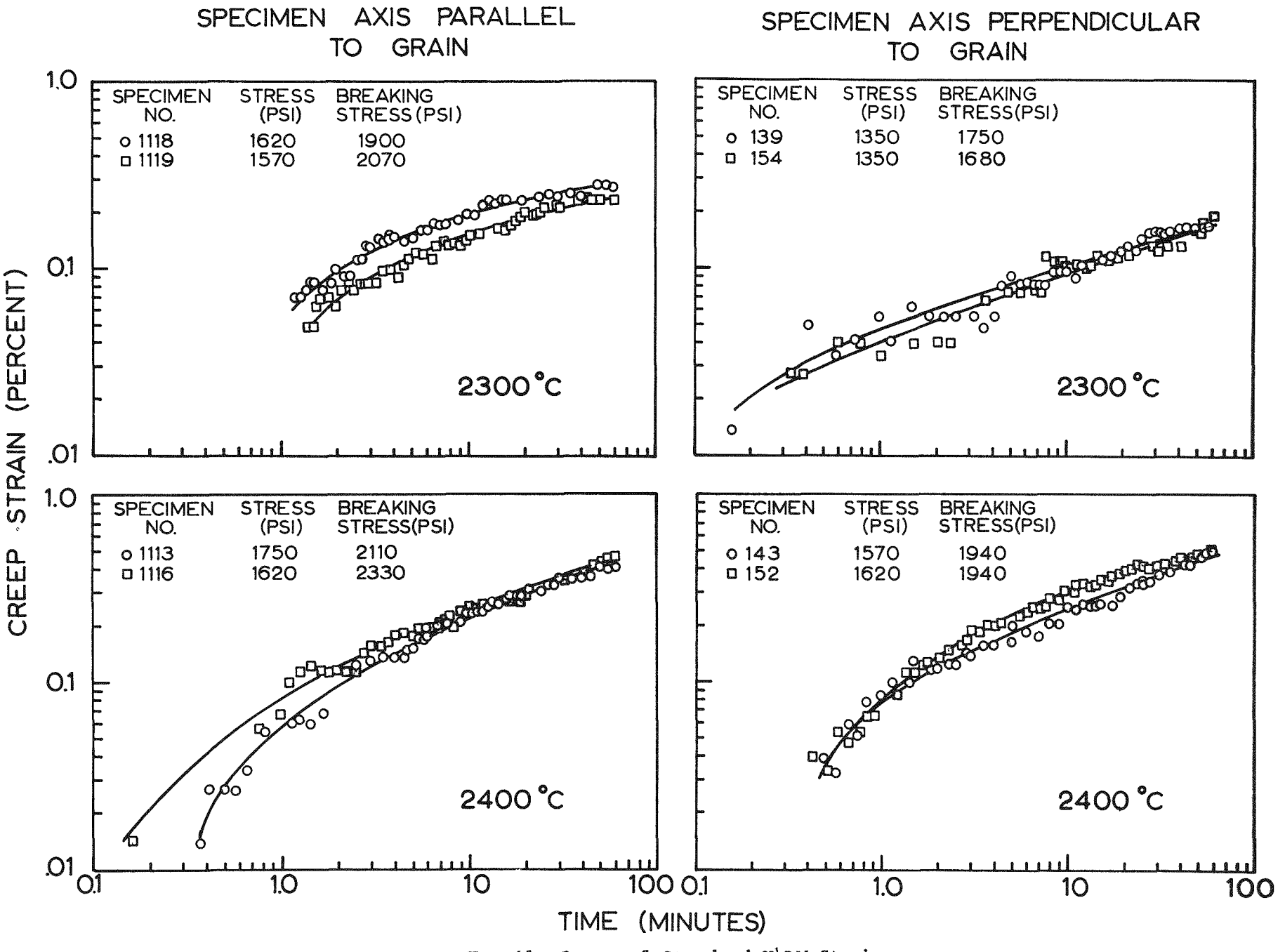

Figure 55

Tensile Creep of Standard H4LM Stock

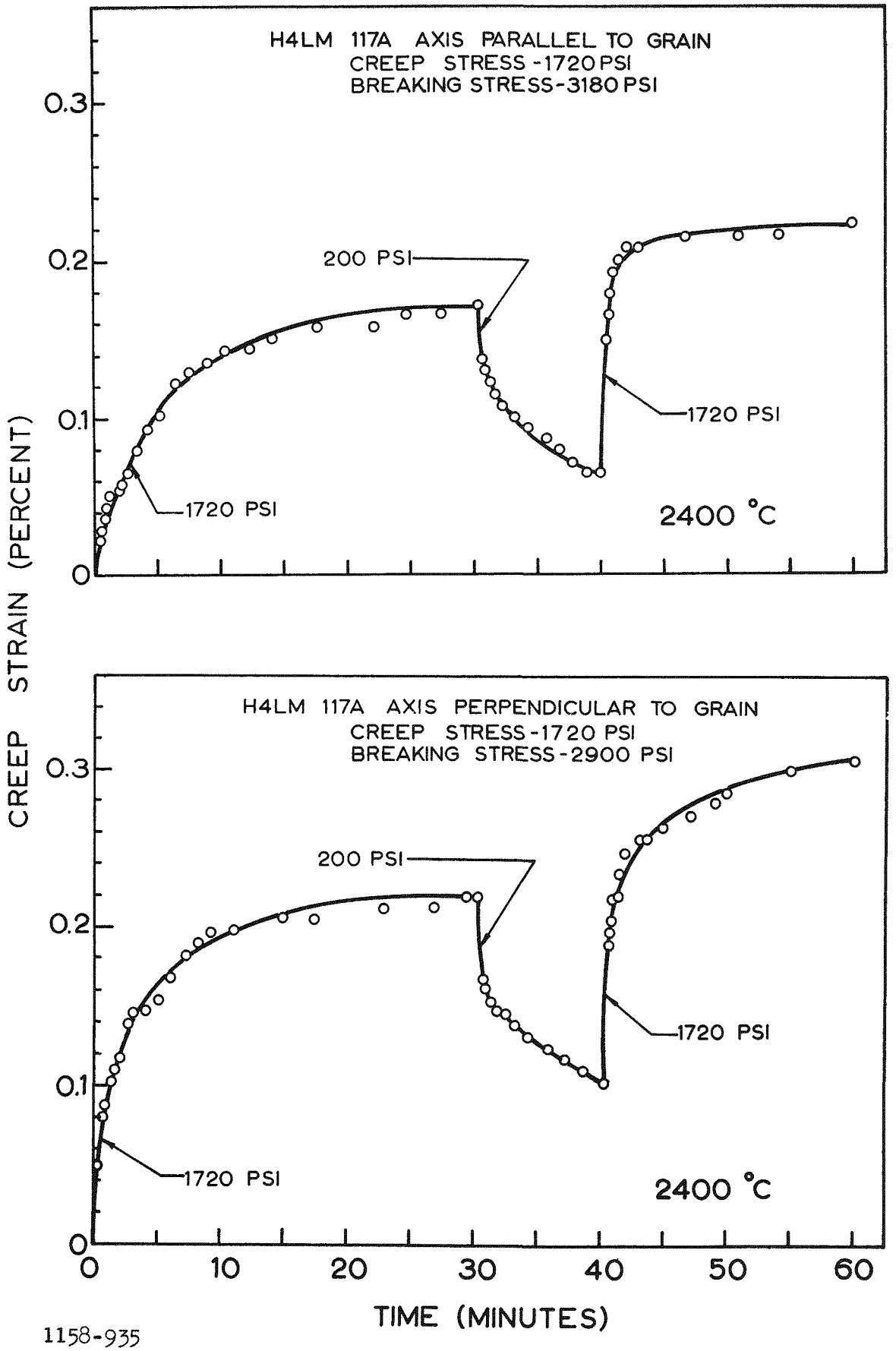

Creep Curves for Re-Impregnated Stock at 2400°C

Figure 57

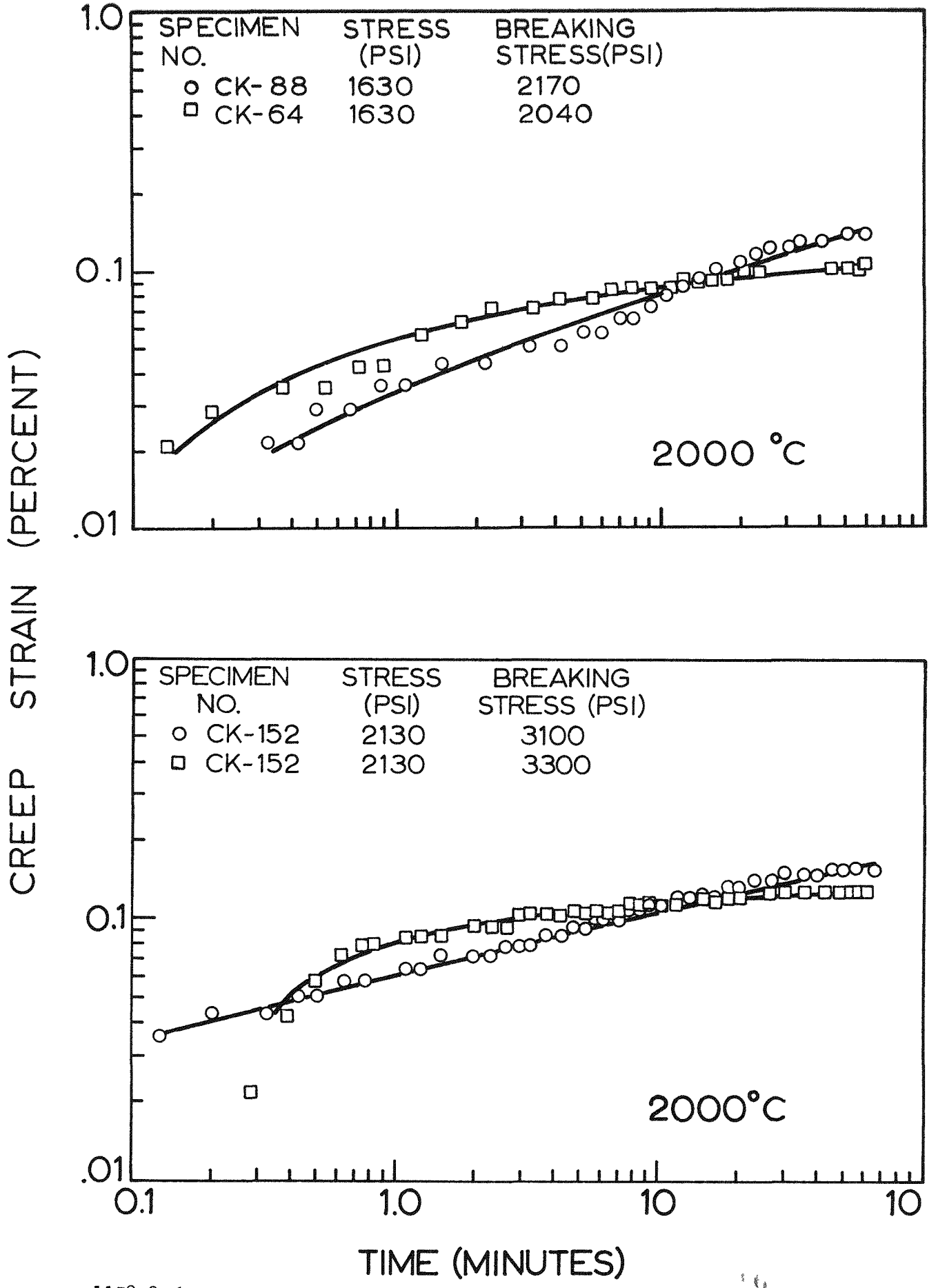

1158-896

Tensile Creep of CK Stock at 2000°C

Figure 58

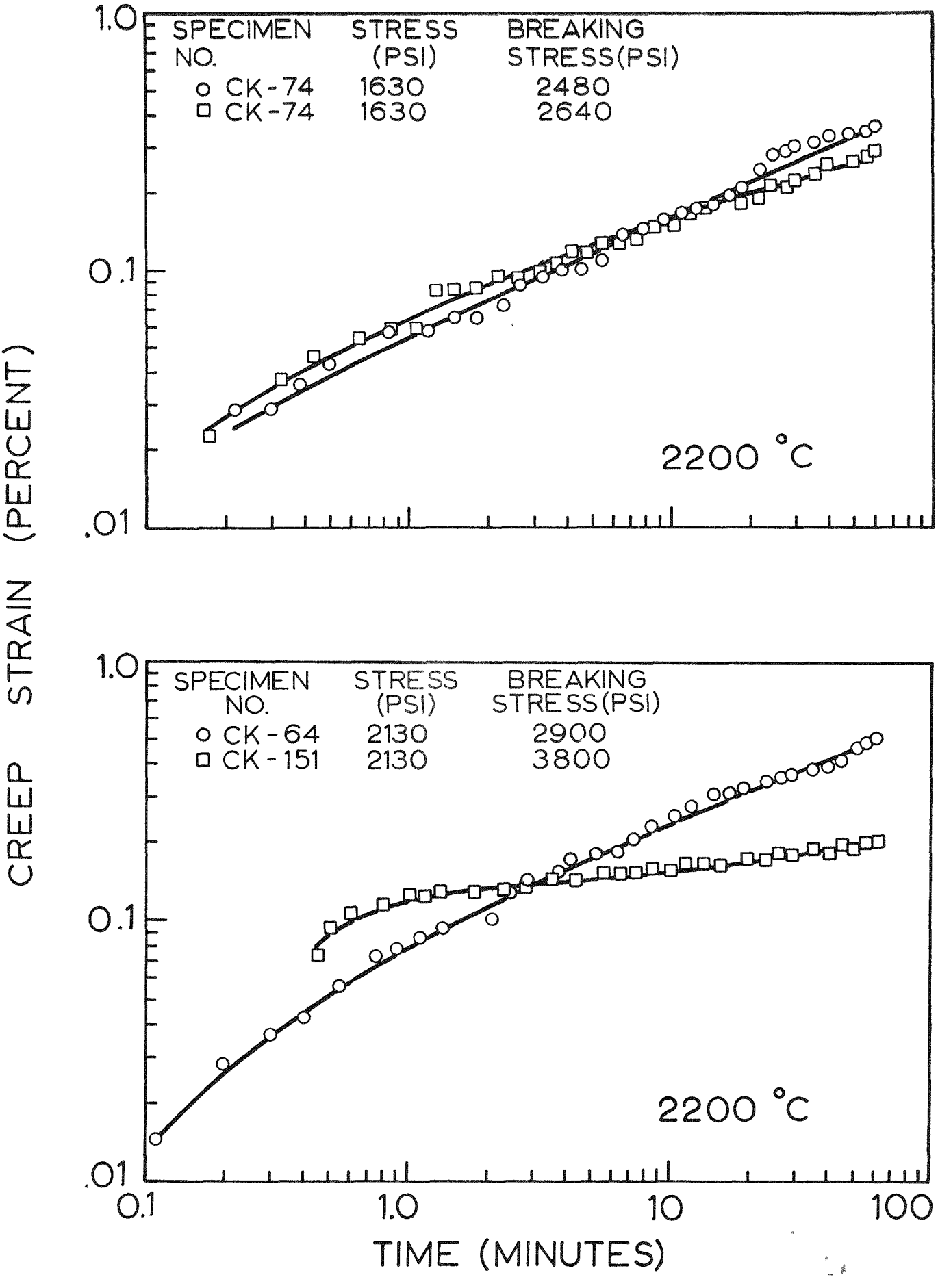

1158-895

Tensile Creep of CK Stock at 2200°C

Figure 59

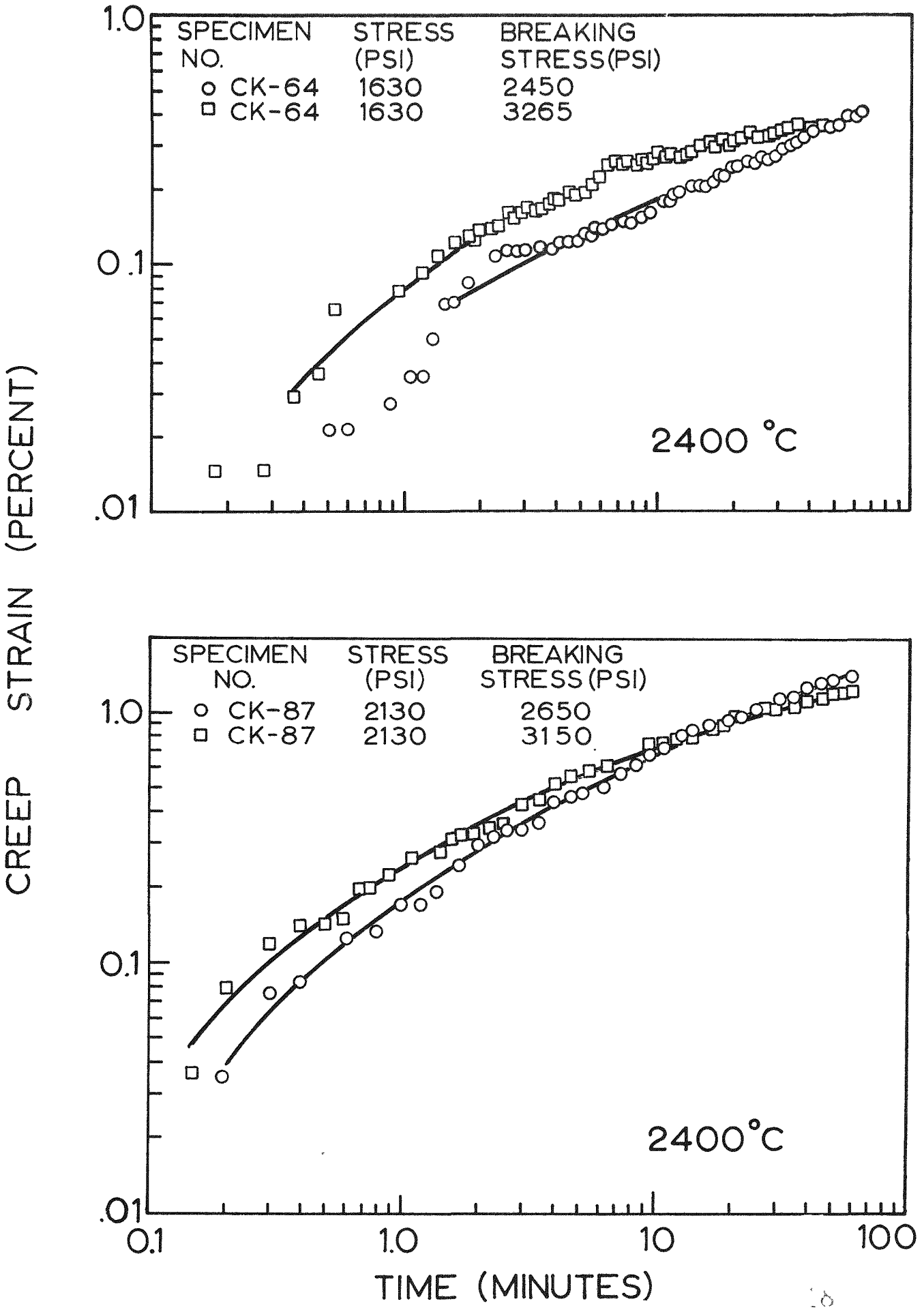

1158-893

Tensile Creep of CK Stock at 2400°C

Figure 60

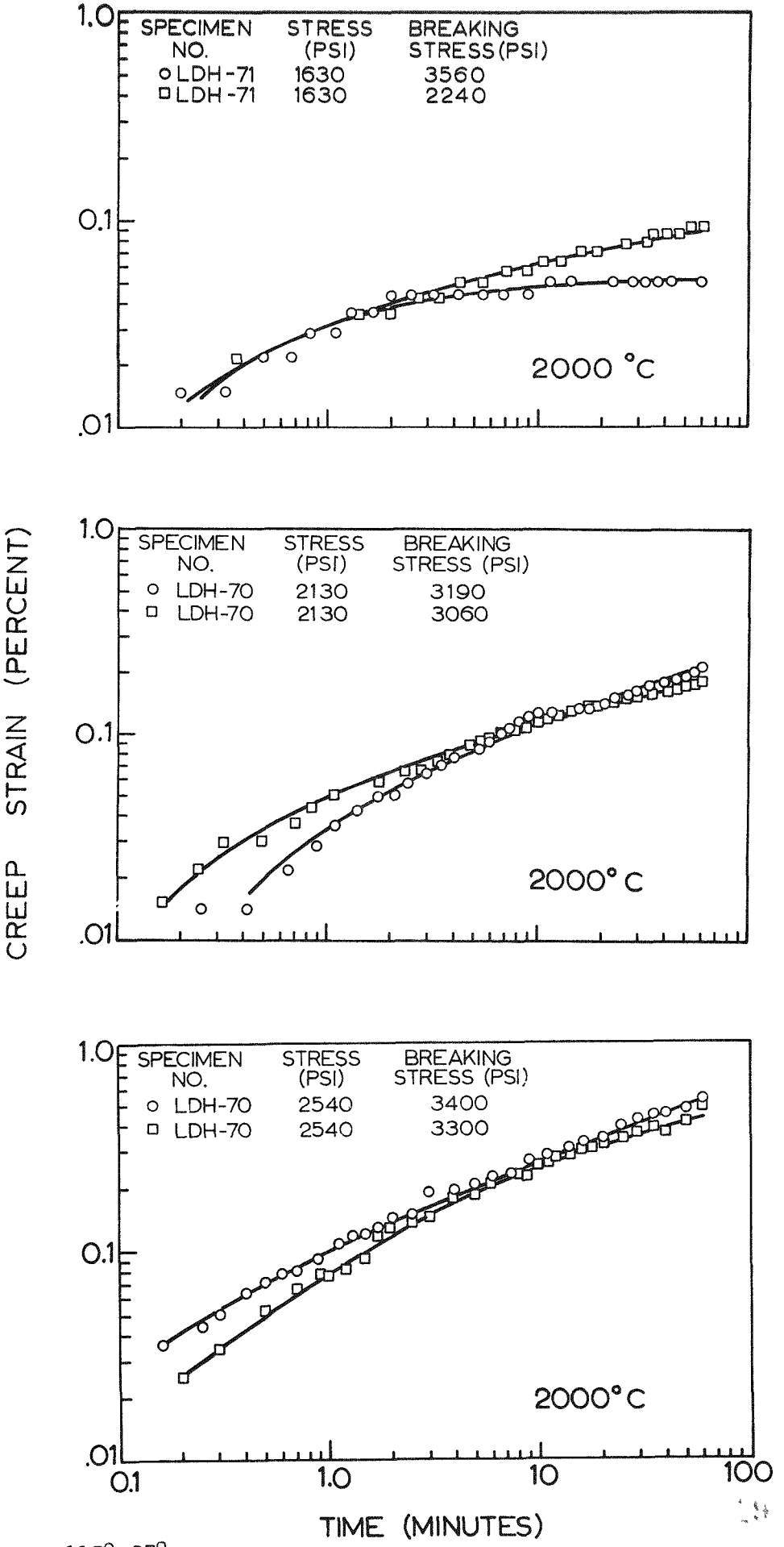

1158-938

Tensile Creep of LDH Stock at 2000°C

Figure 61

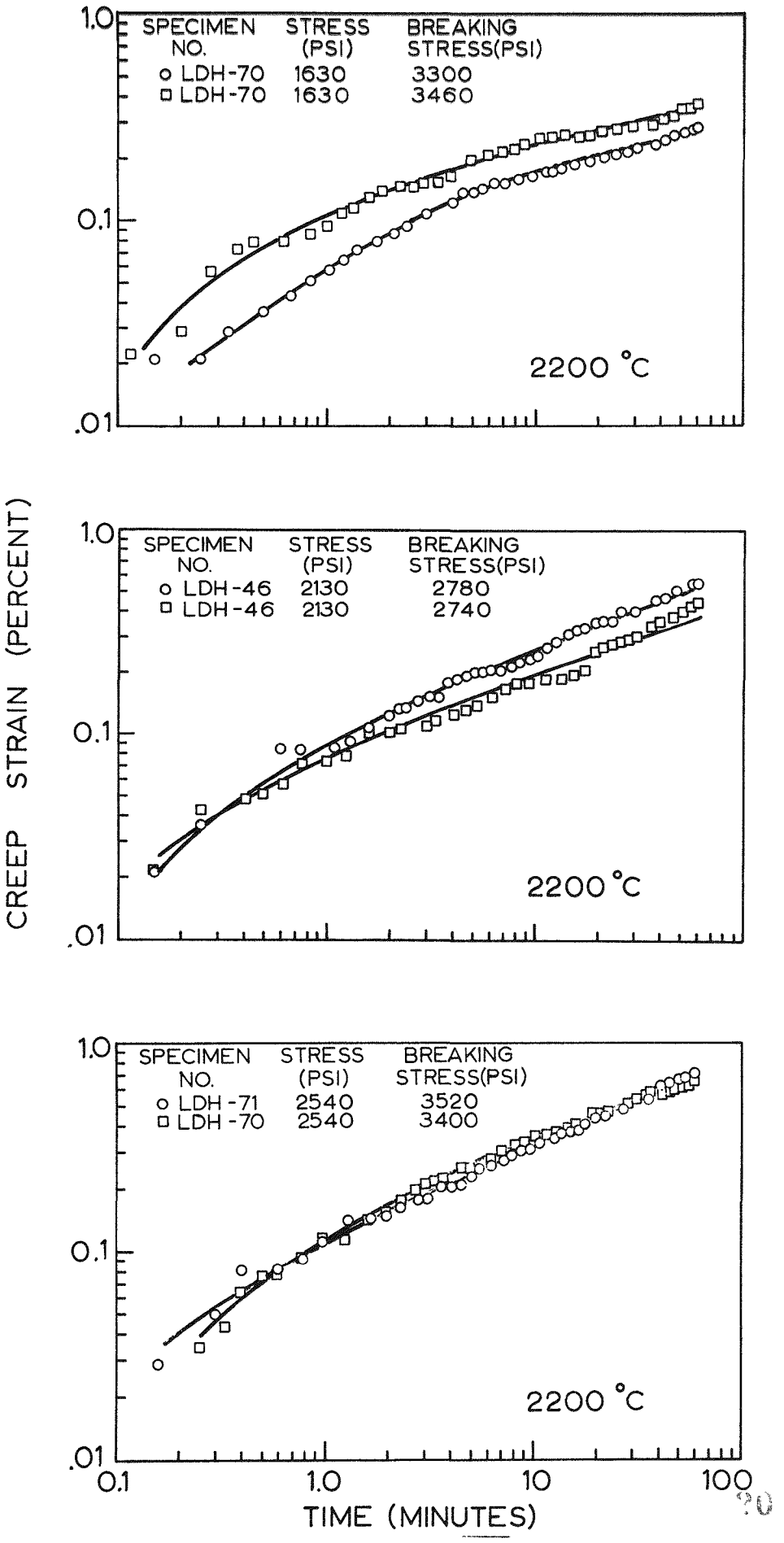

1158-905

Tensile Creep of LDH Stock at 2200°C

Figure 62

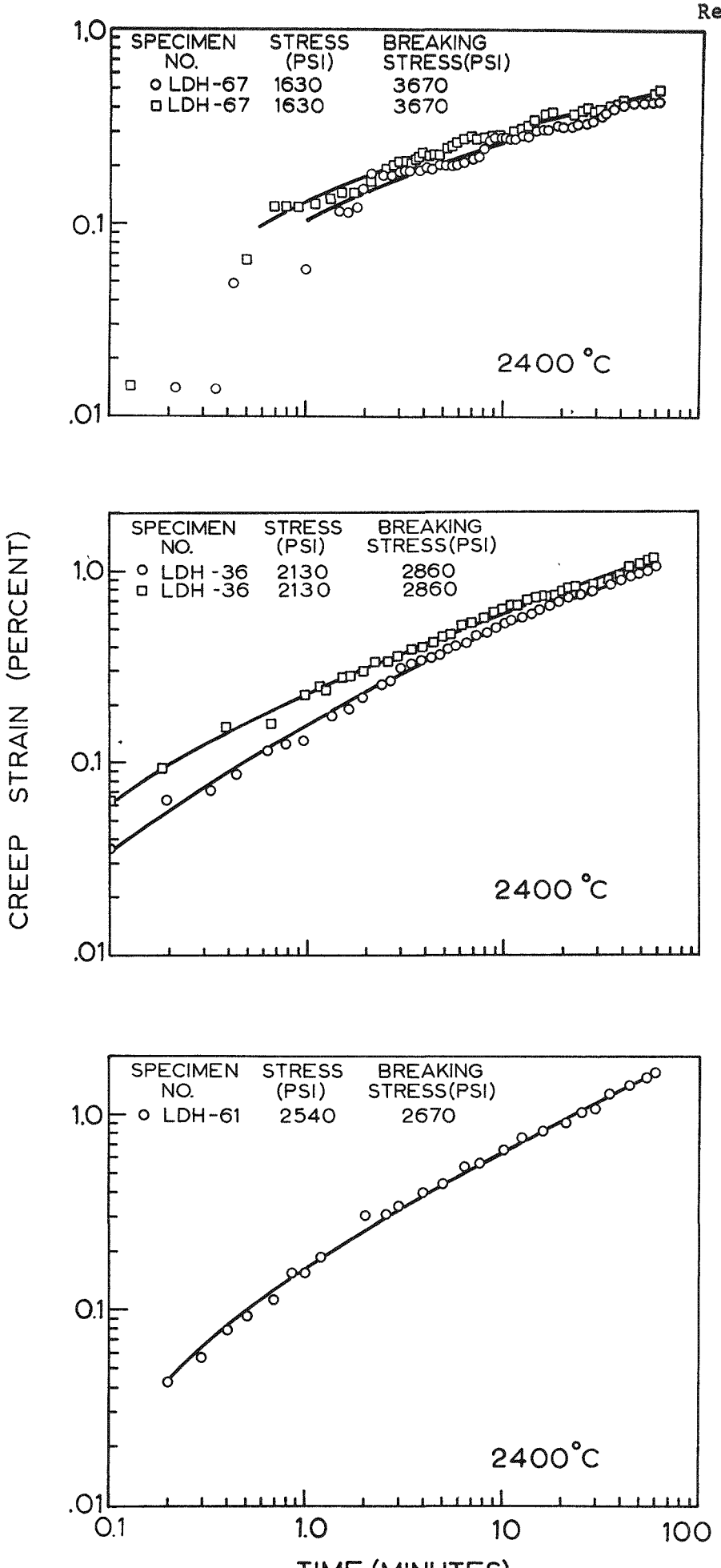

Figure 63

1158-907 Tensile Creep of LDH Stock at 2400°C

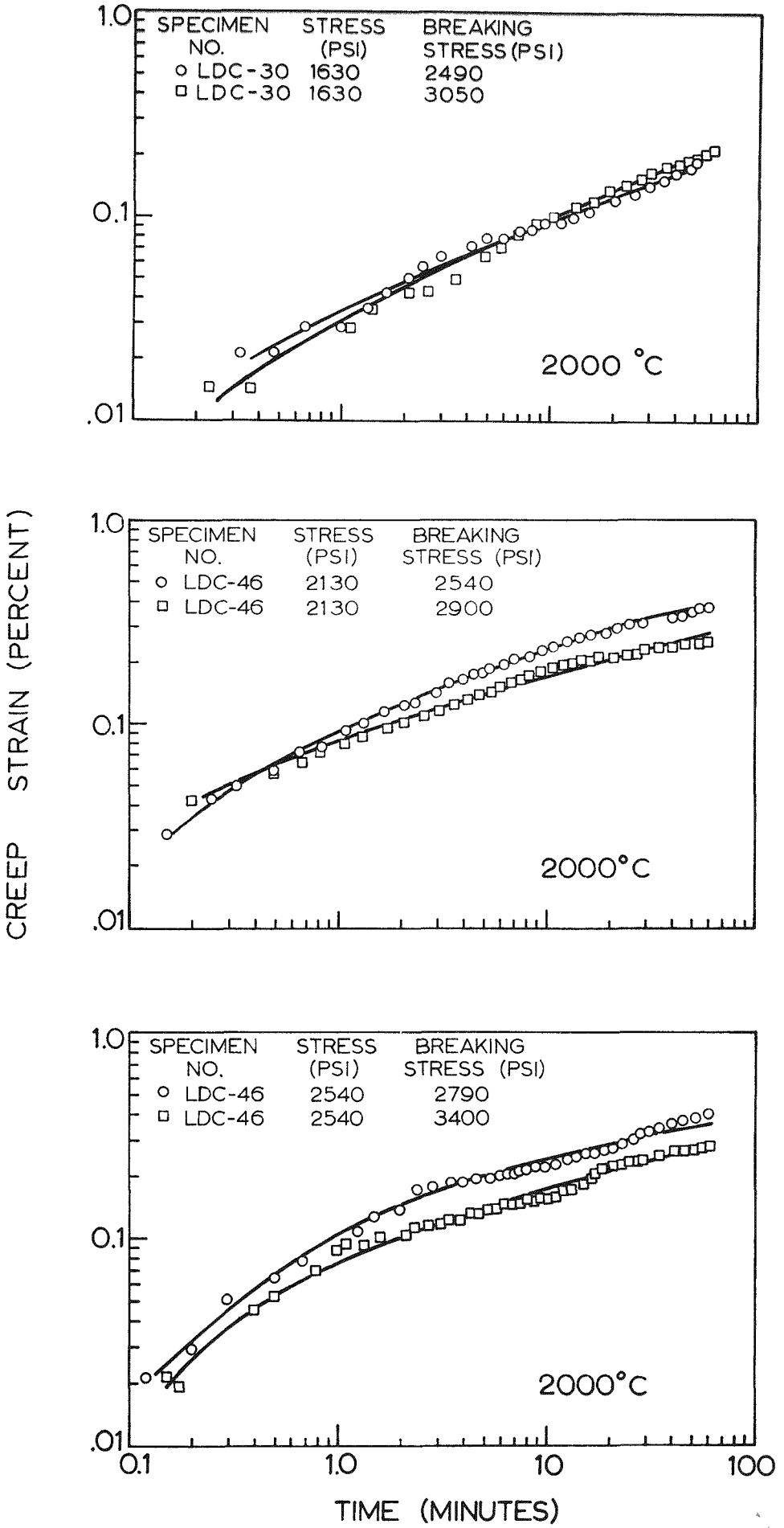

Tensile Creep of LDC Stock at 2000°C

Figure 64

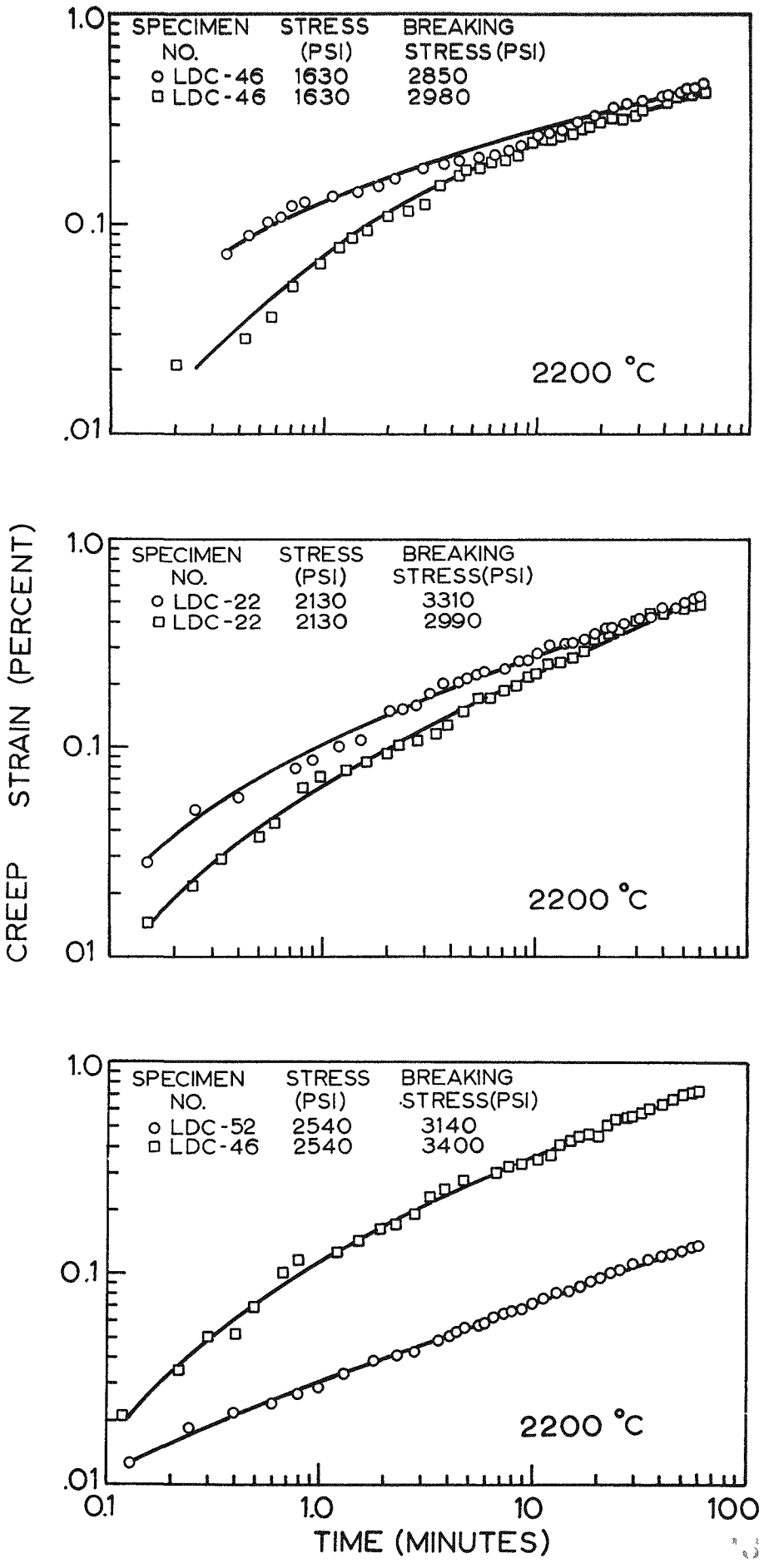

1158-939

Figure 65

Tensile Creep of LDC Stock at 2200°C

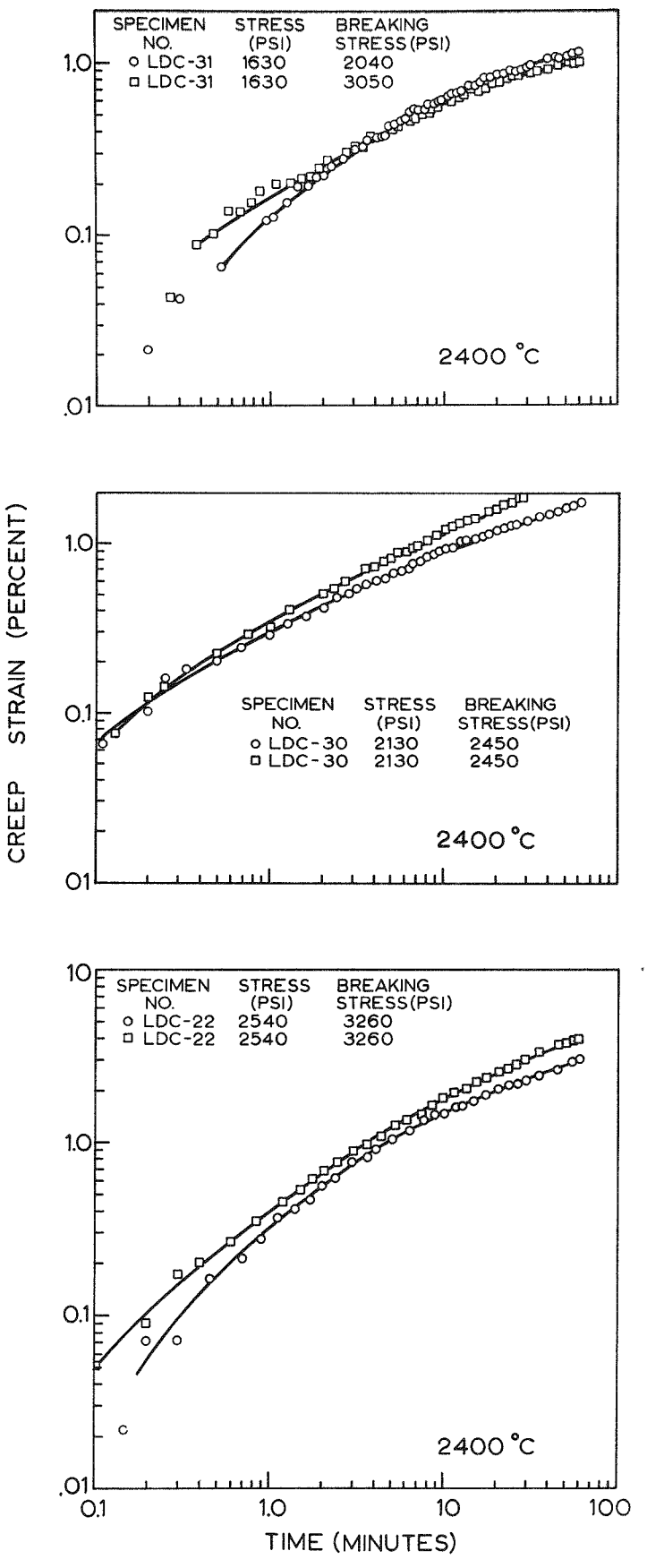

1158-928

Tensile Creep of LDC Stock at 2400°C

Figure 66

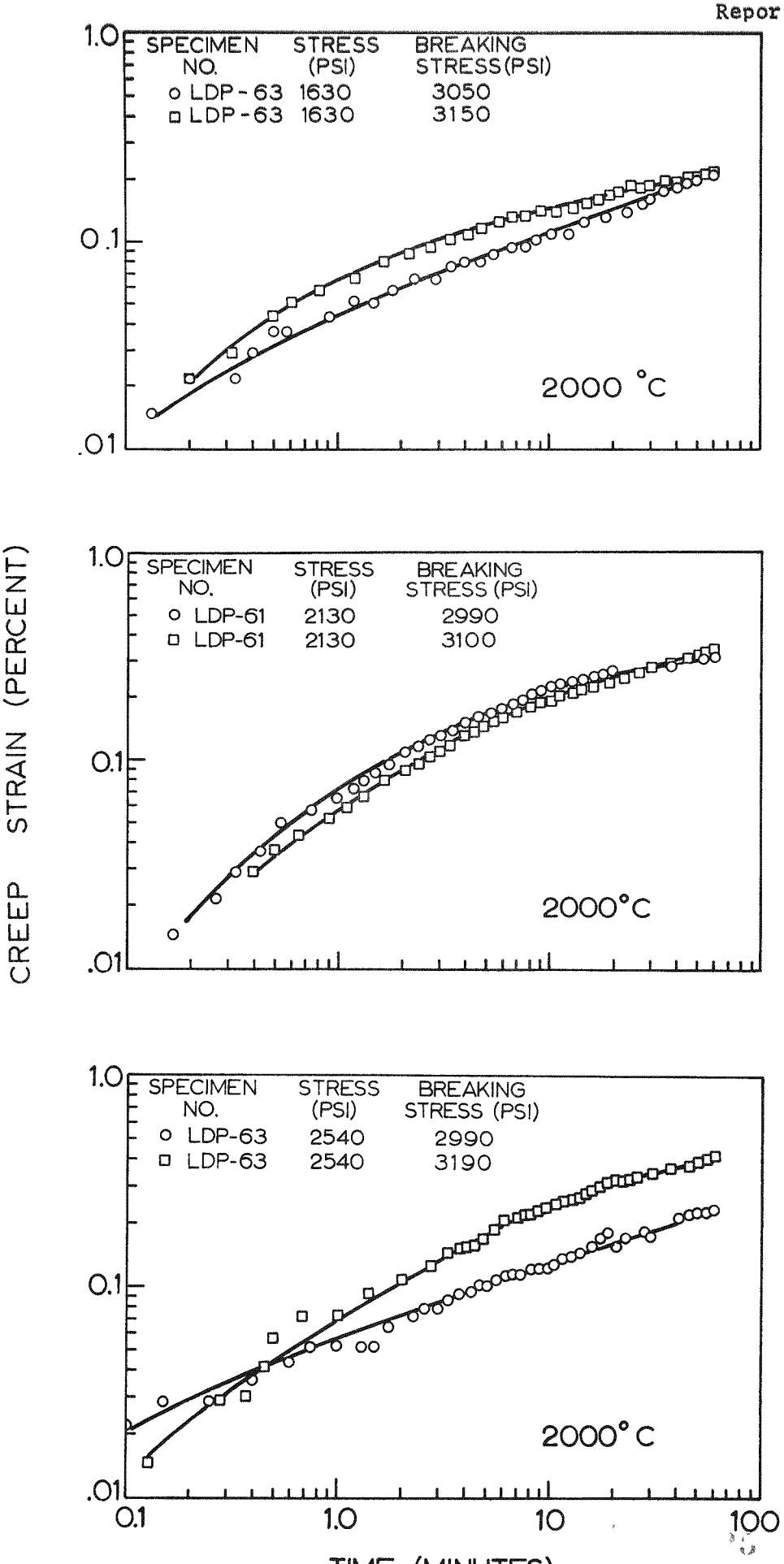

1158-940

Tensile Creep of LDP Stock at 2000°C

Figure 67

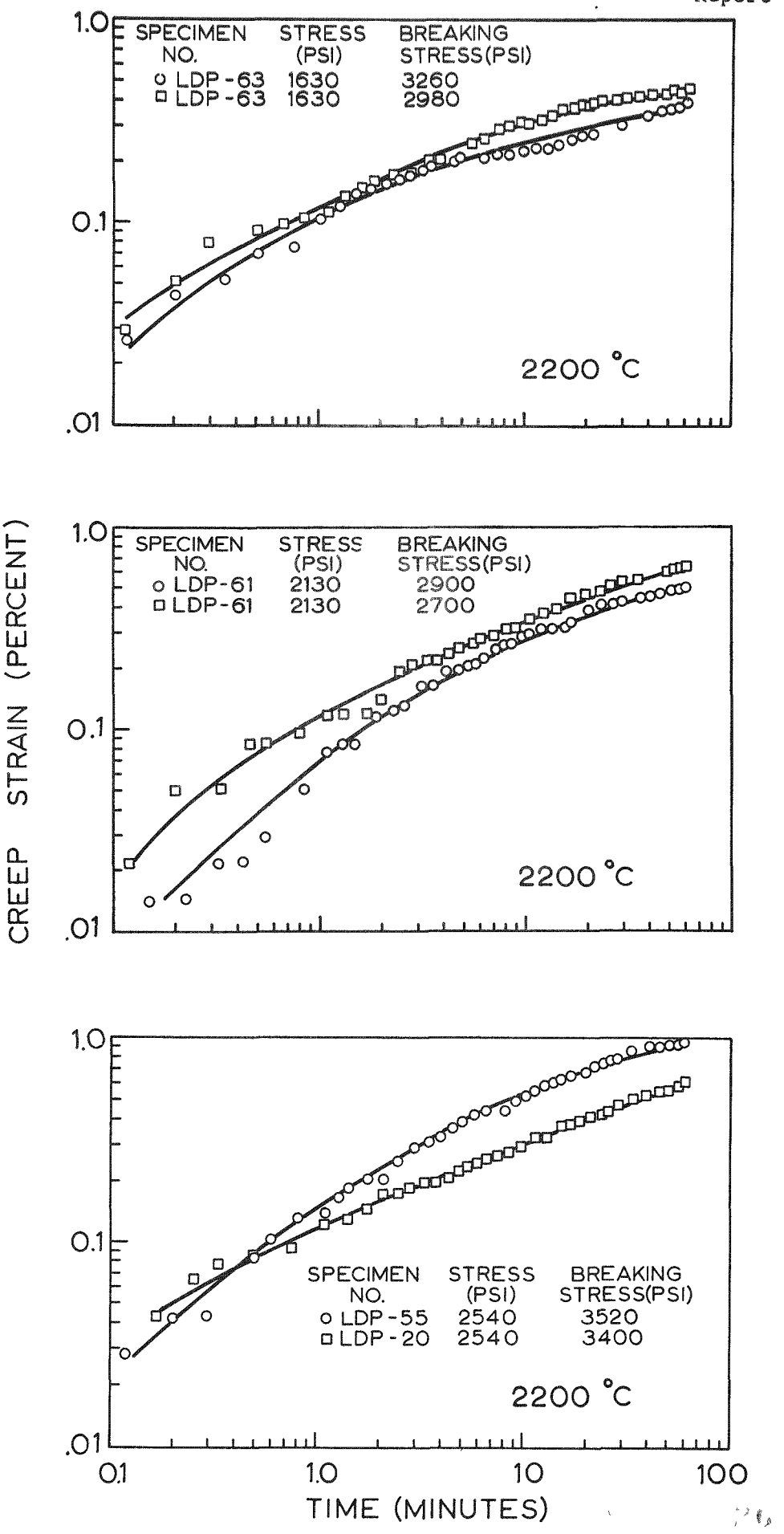

1158-903 Tensile Creep of LDP Stock at 2200°C Figure 68

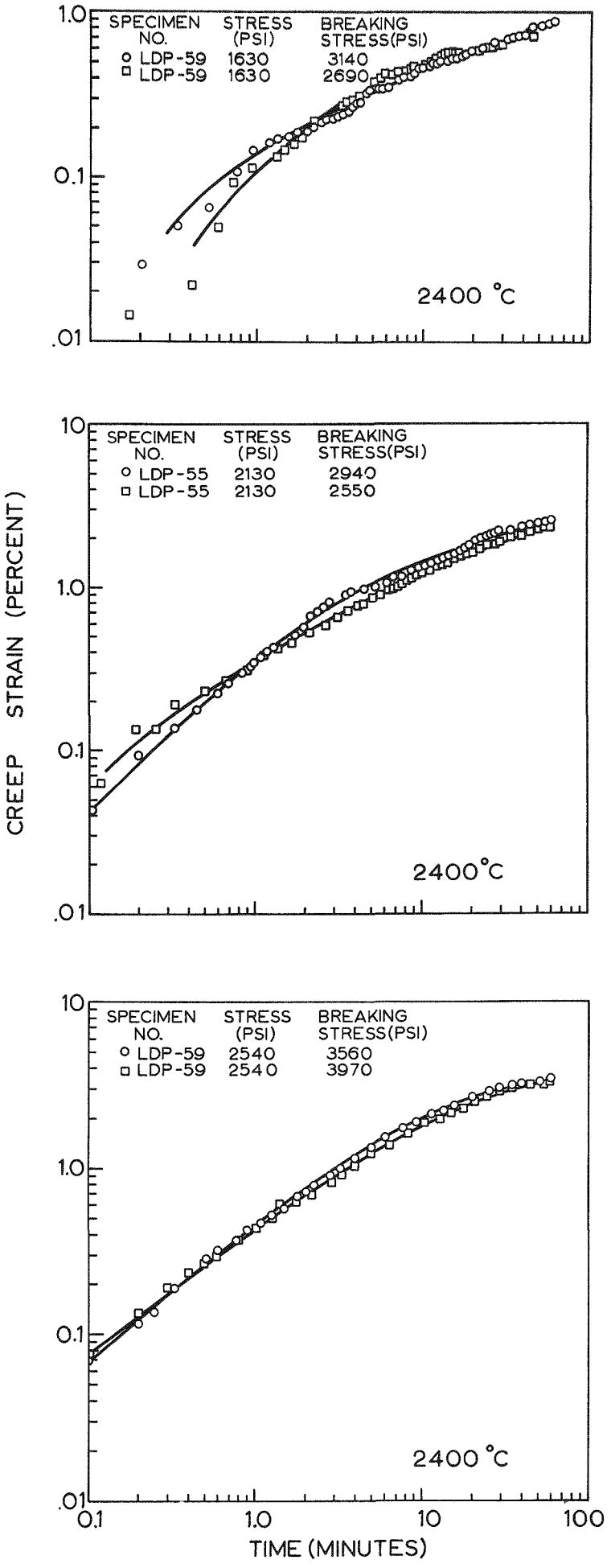

1158-409

Tensile Creep of LDP Stock at 2400°C

Figure 69

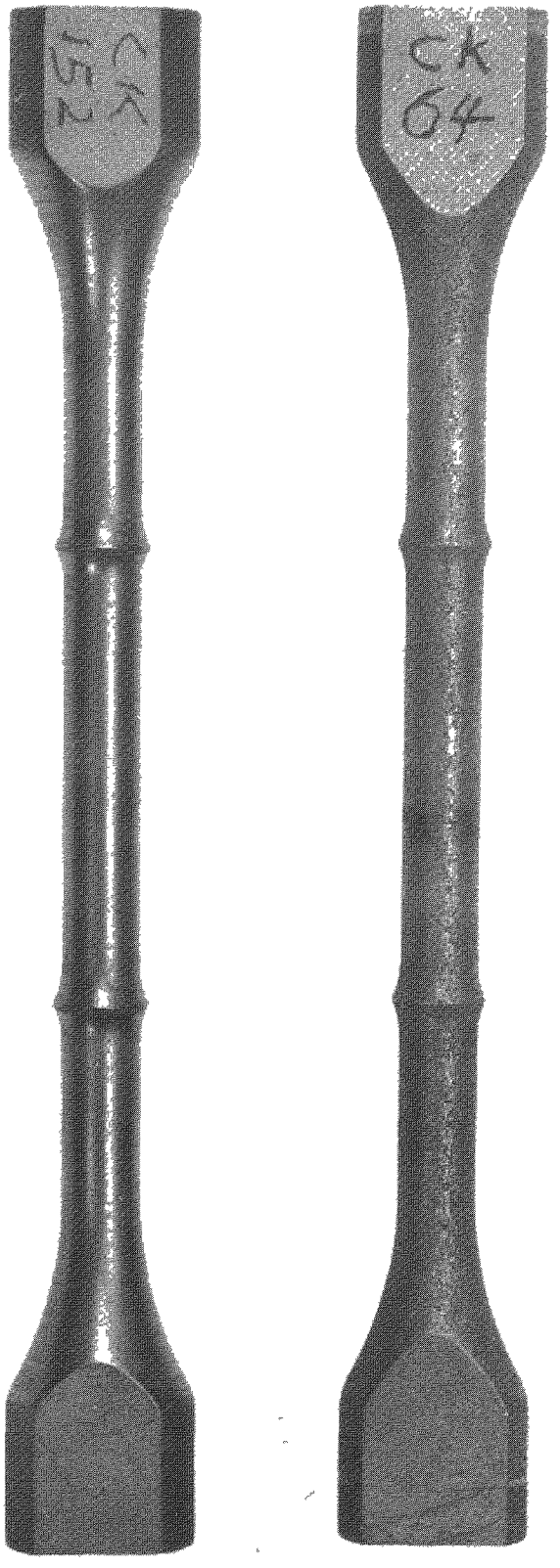

858-735

View of Tensile Specimens for Two Different Batches of CK Stock

Figure 70

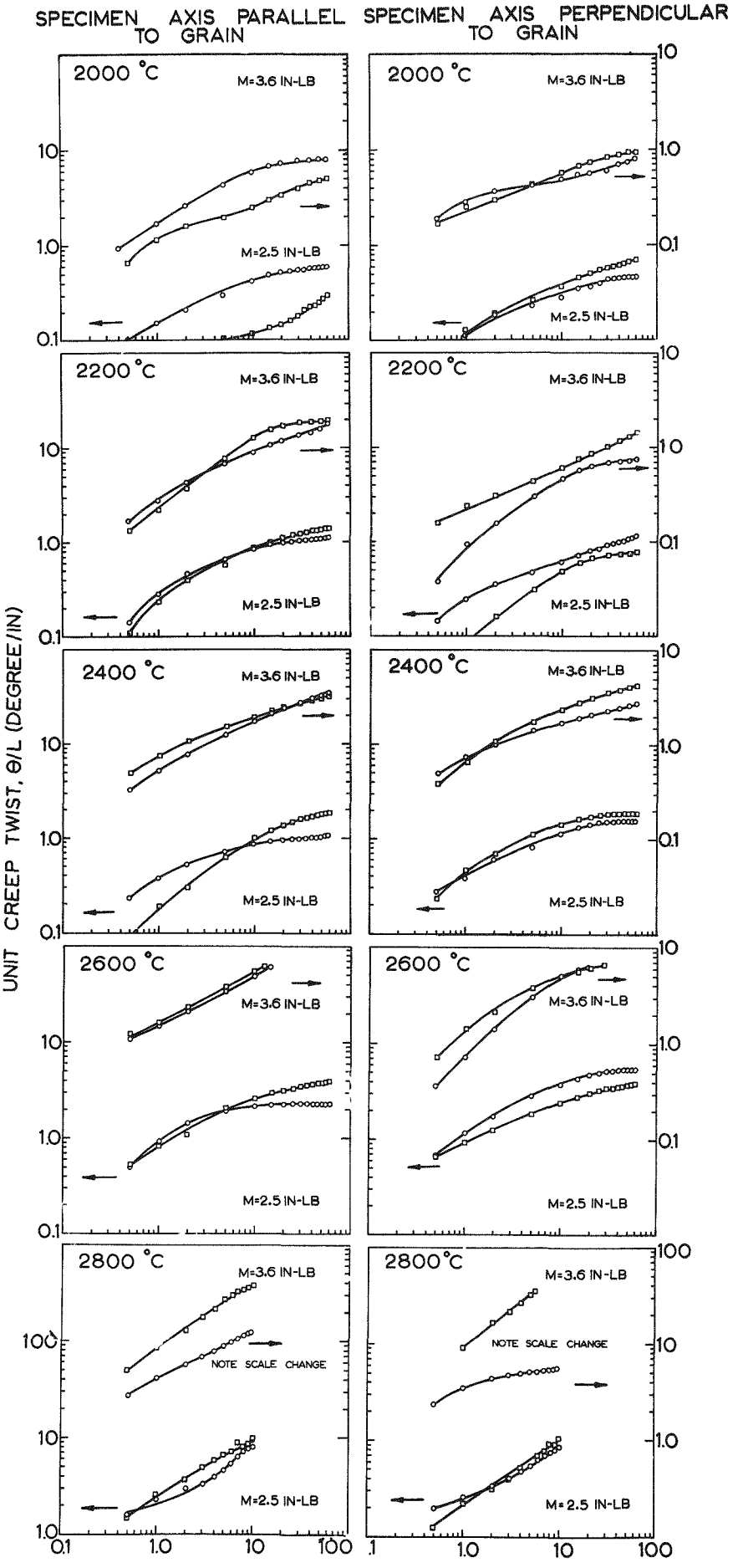

1158-926

Figure 71

Torsional Creep of Re-Impregnated H4LM Stock

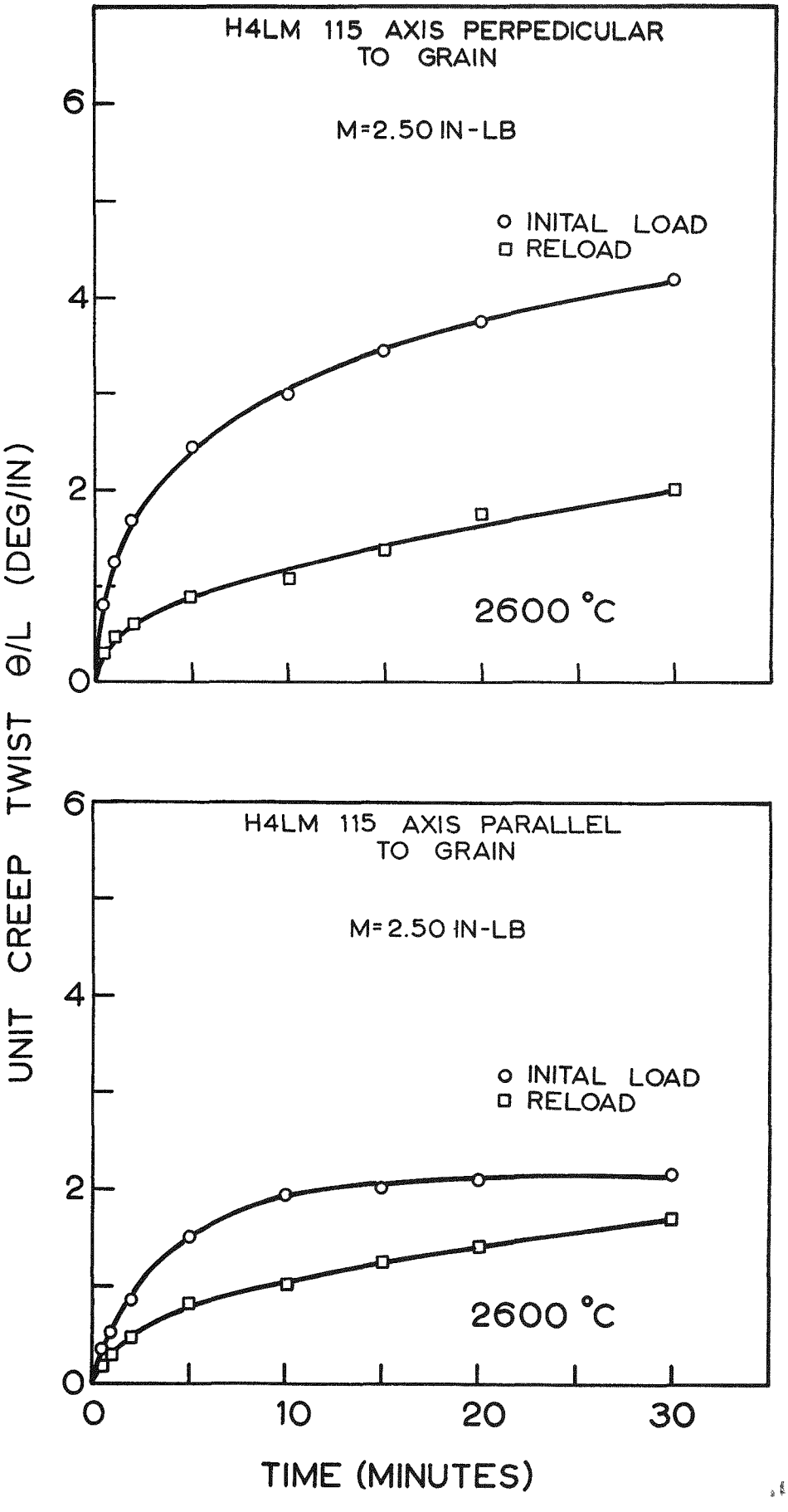

1158-934 Effect of Strain History on Transient Torsional Creep of Re-Impregnated H4LM Stock at 2400°C Figure 72

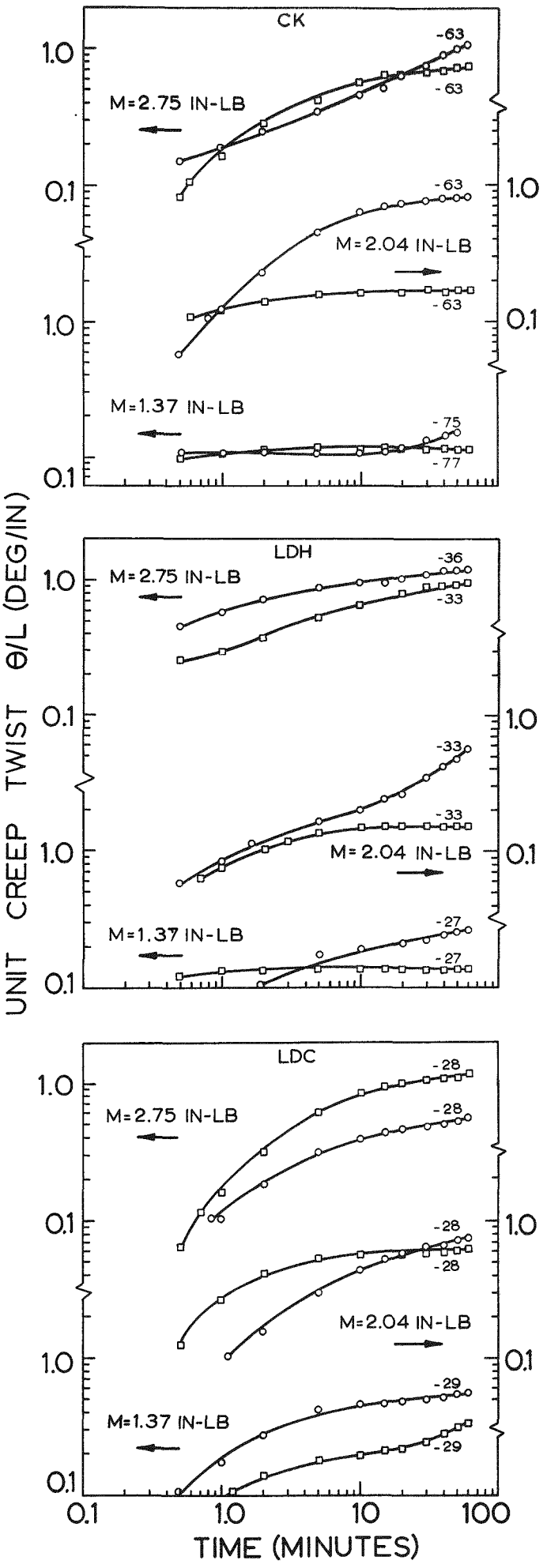

1158-921

Figure 73

Torsional Creep of Grades CK, LDH, and LDC Stock at 2000°C

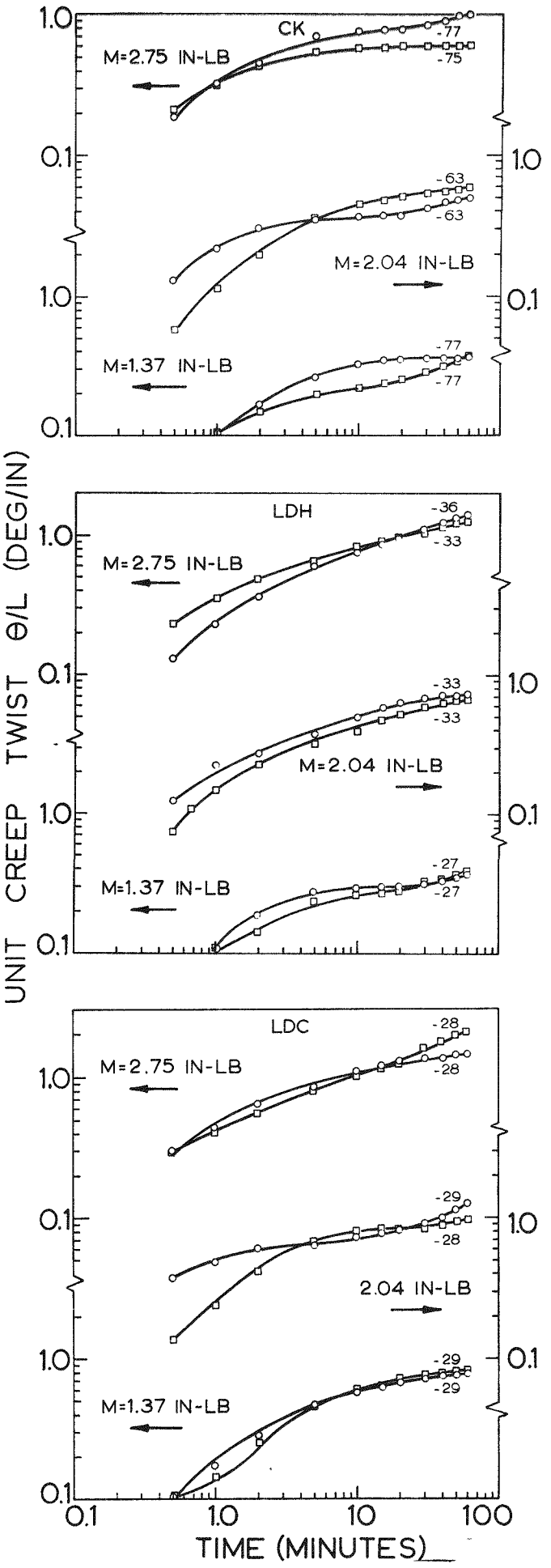

1158-922

Figure 74

Torsional Creep of Grades CK, LDH, and LDC Stock at 2200°C

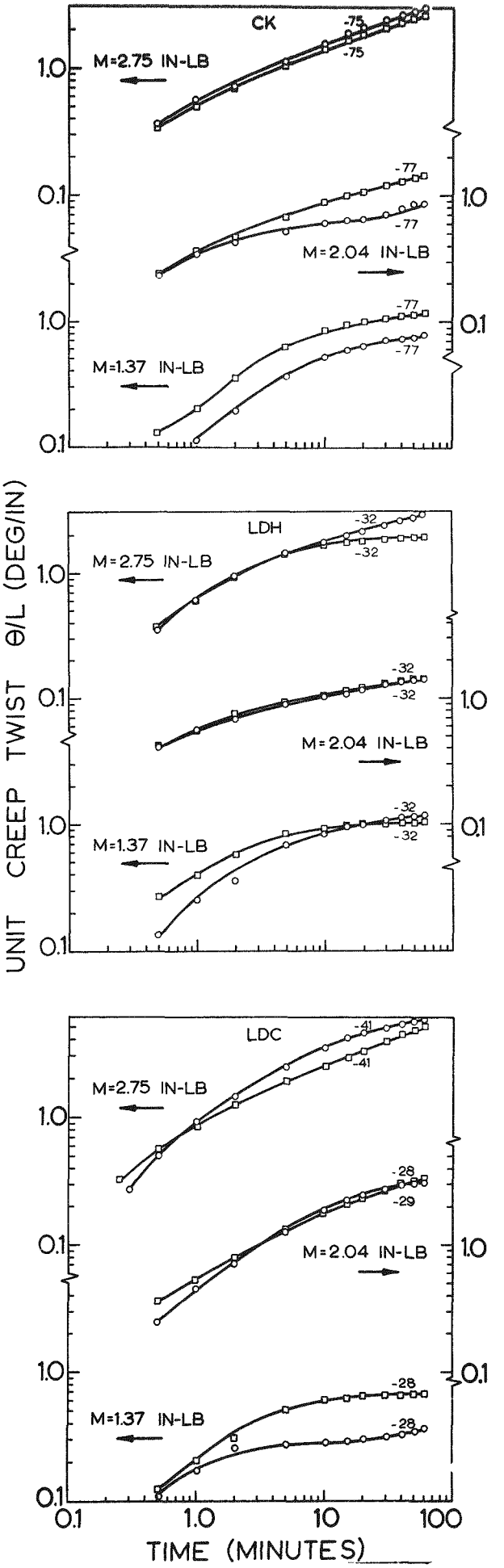

1158-923

Figure 75

Torsional Creep of Grades CK, LDH, and LDC Stock at 2400°C

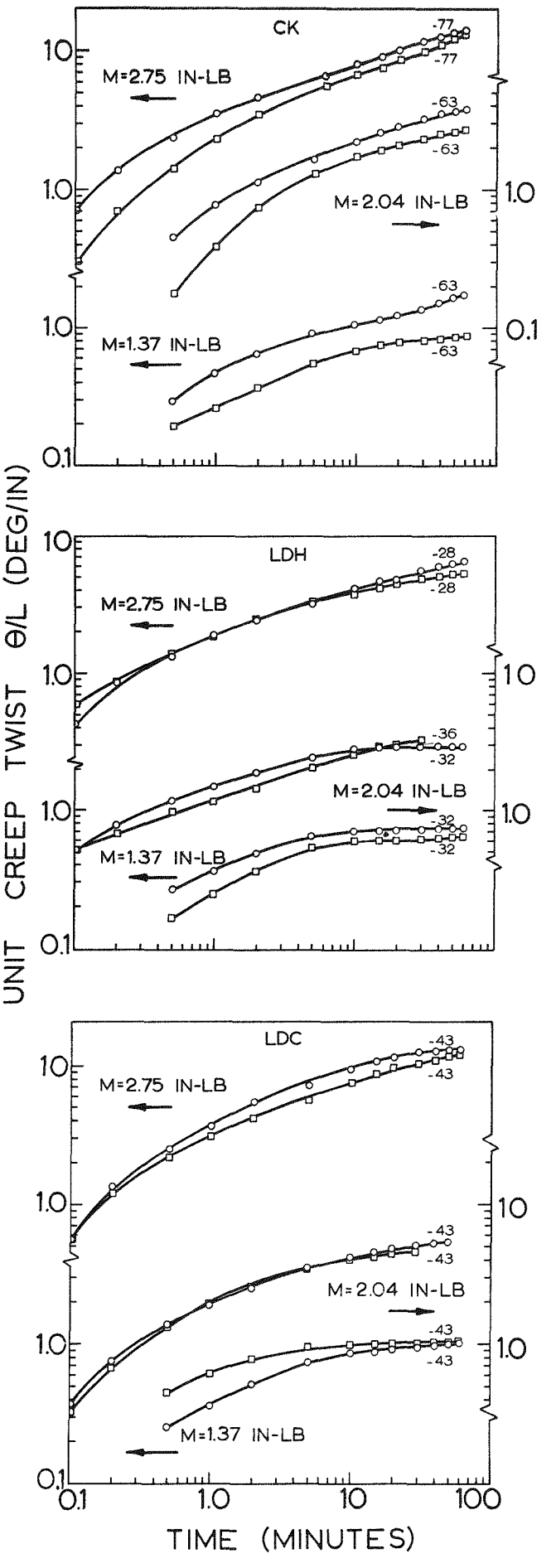

1158-924

Figure 76

Torsional Creep of Grades CK, LDH, and LDC Stock at 2600°C

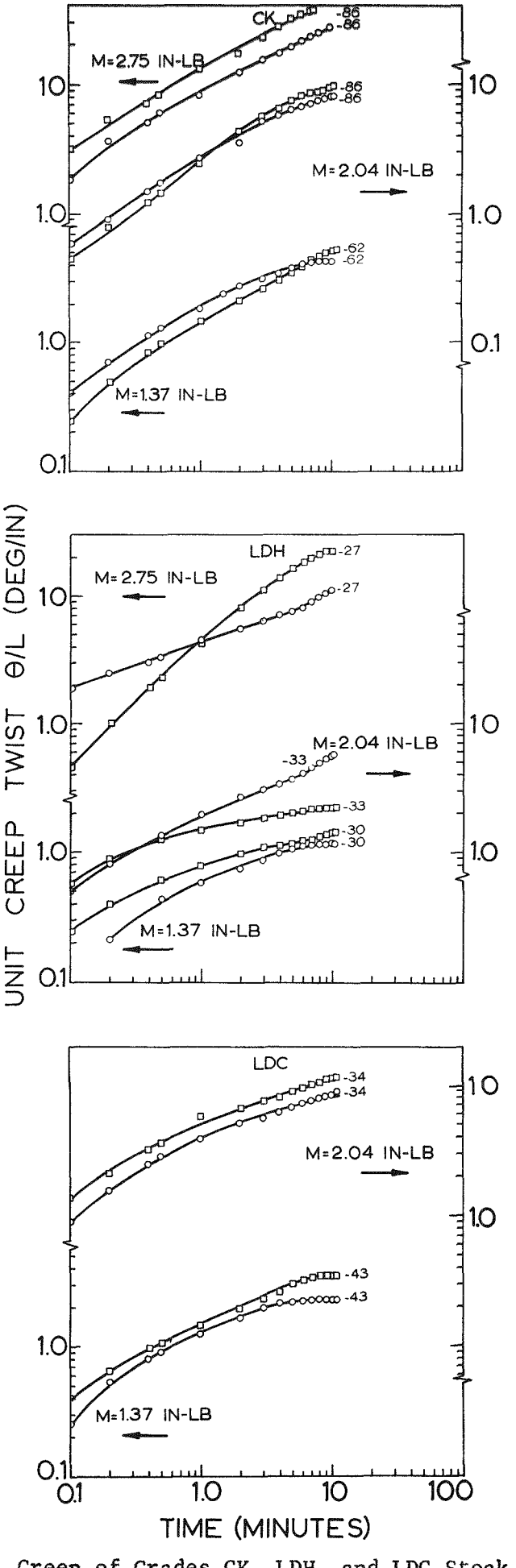

1158-911

Figure 77

Torsional Creep of Grades CK, LDH, and LDC Stock at 2800°C

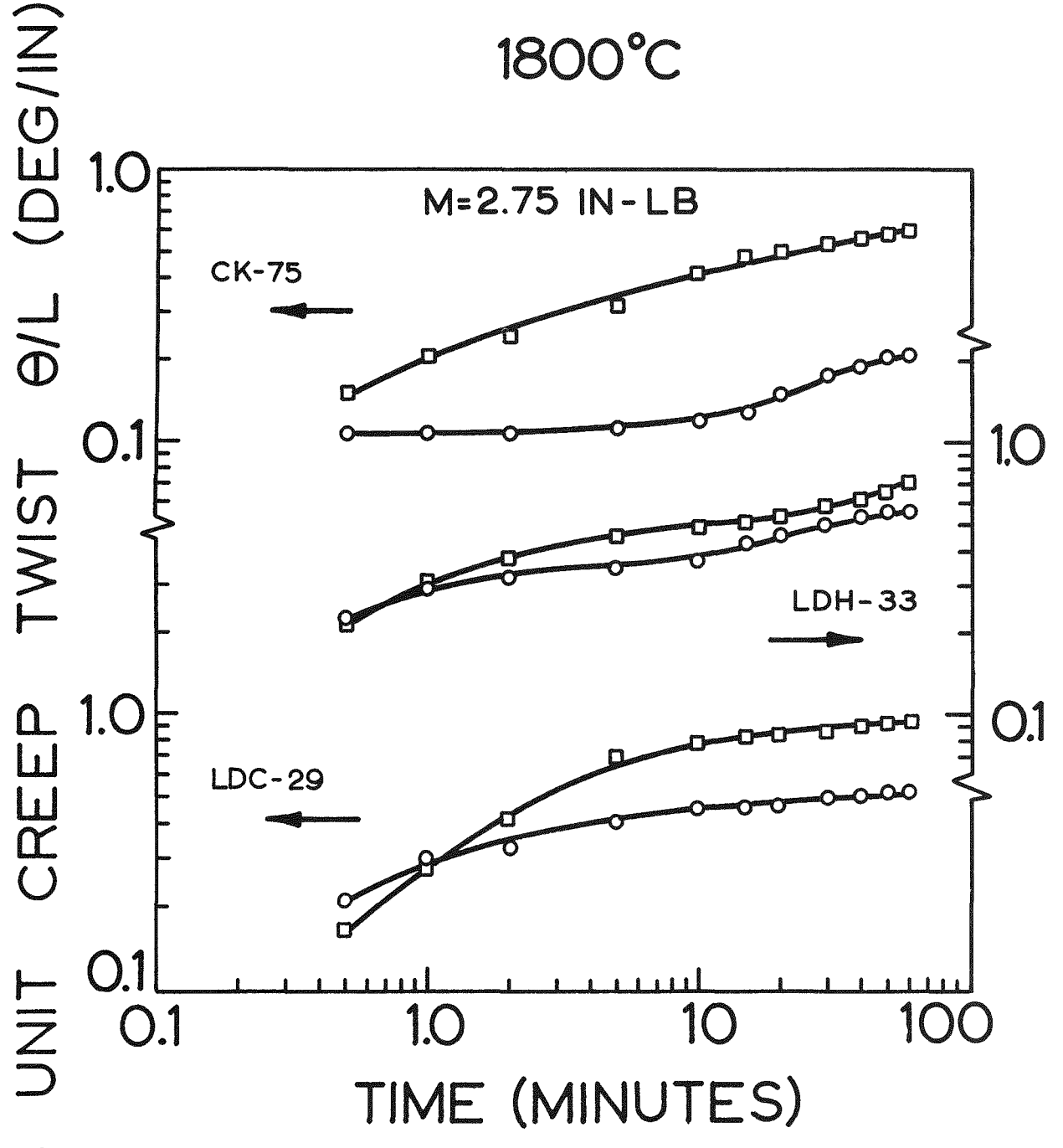

Torsional Creep of Grades CK, LDH, and LDC Stock at 1800°C

Figure 78

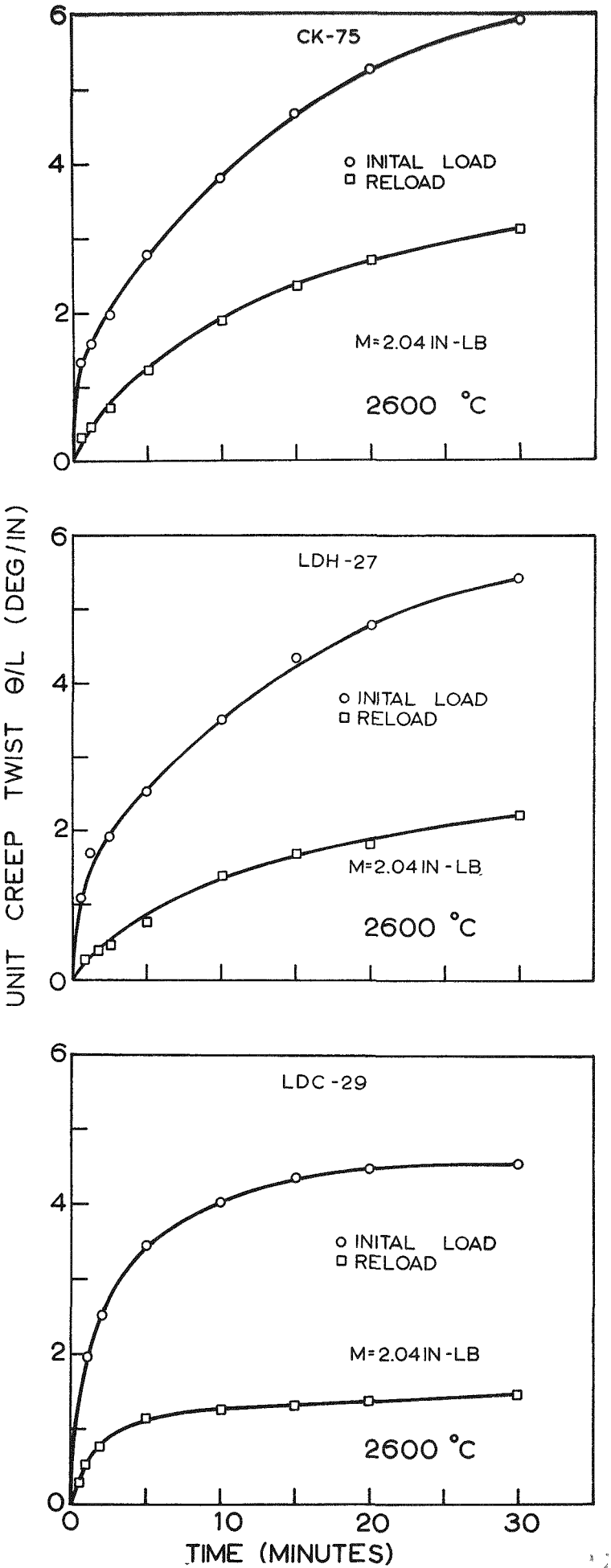

1158-929 Effect of Strain History on Transient Torsional Creep of Grades CK, LDH, and LDC at 2600°C Figure 79

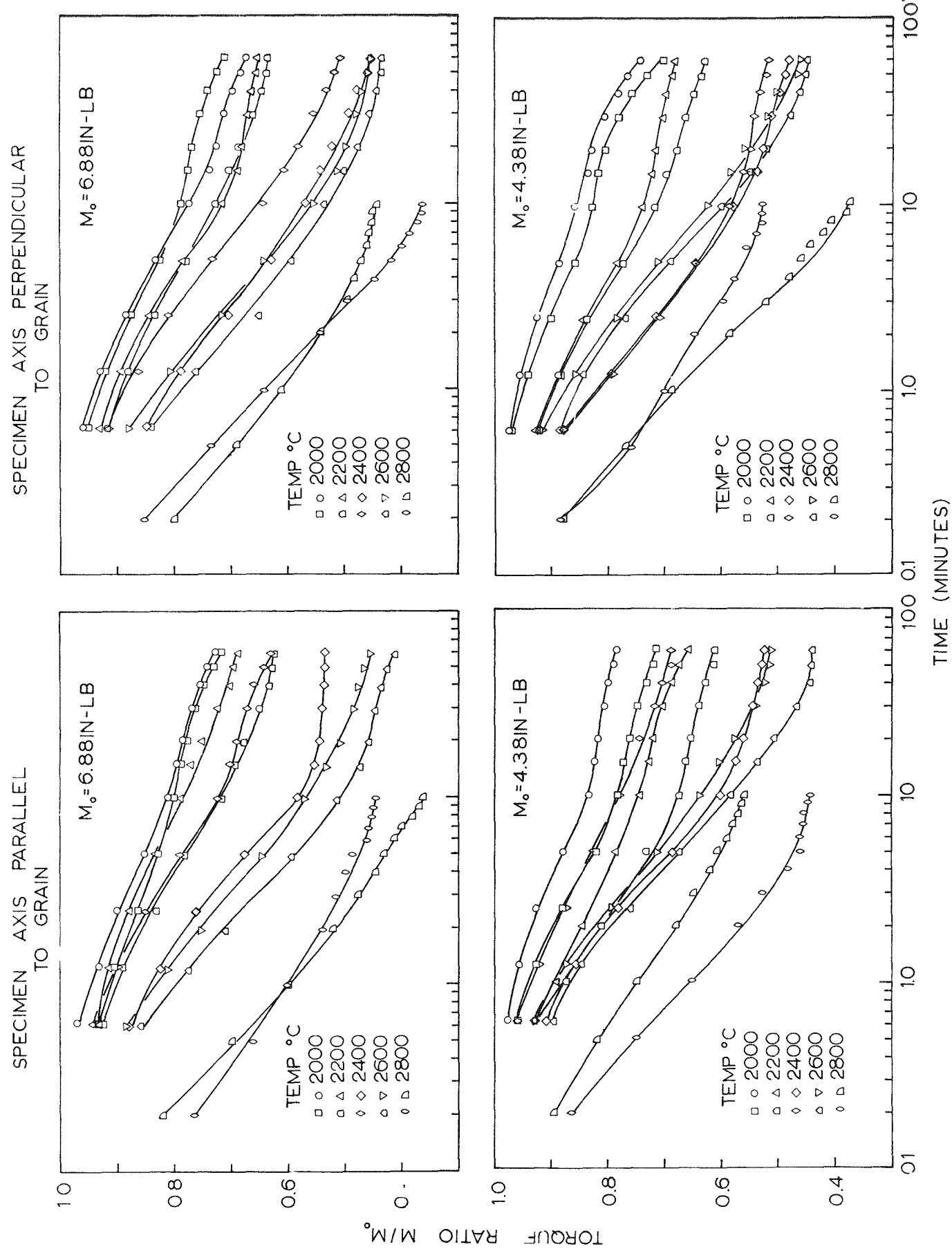

1158-890 Torsional-Stress Relaxation of Re-Impregnated H4LM Stock

Figure 80

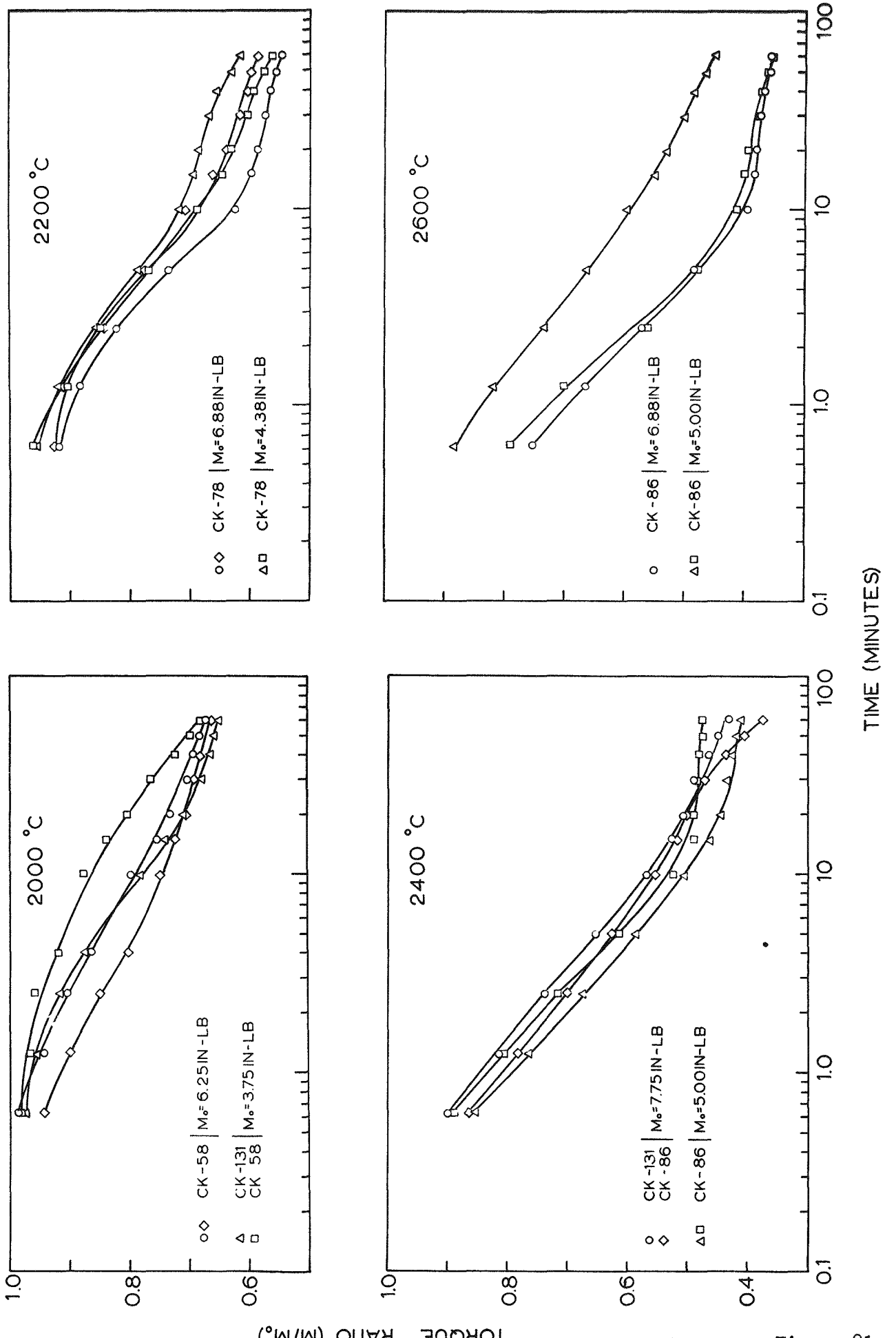

1158-917

Figure 81

Torsional-Stress Relaxation of Re-Impregnated CK Stock

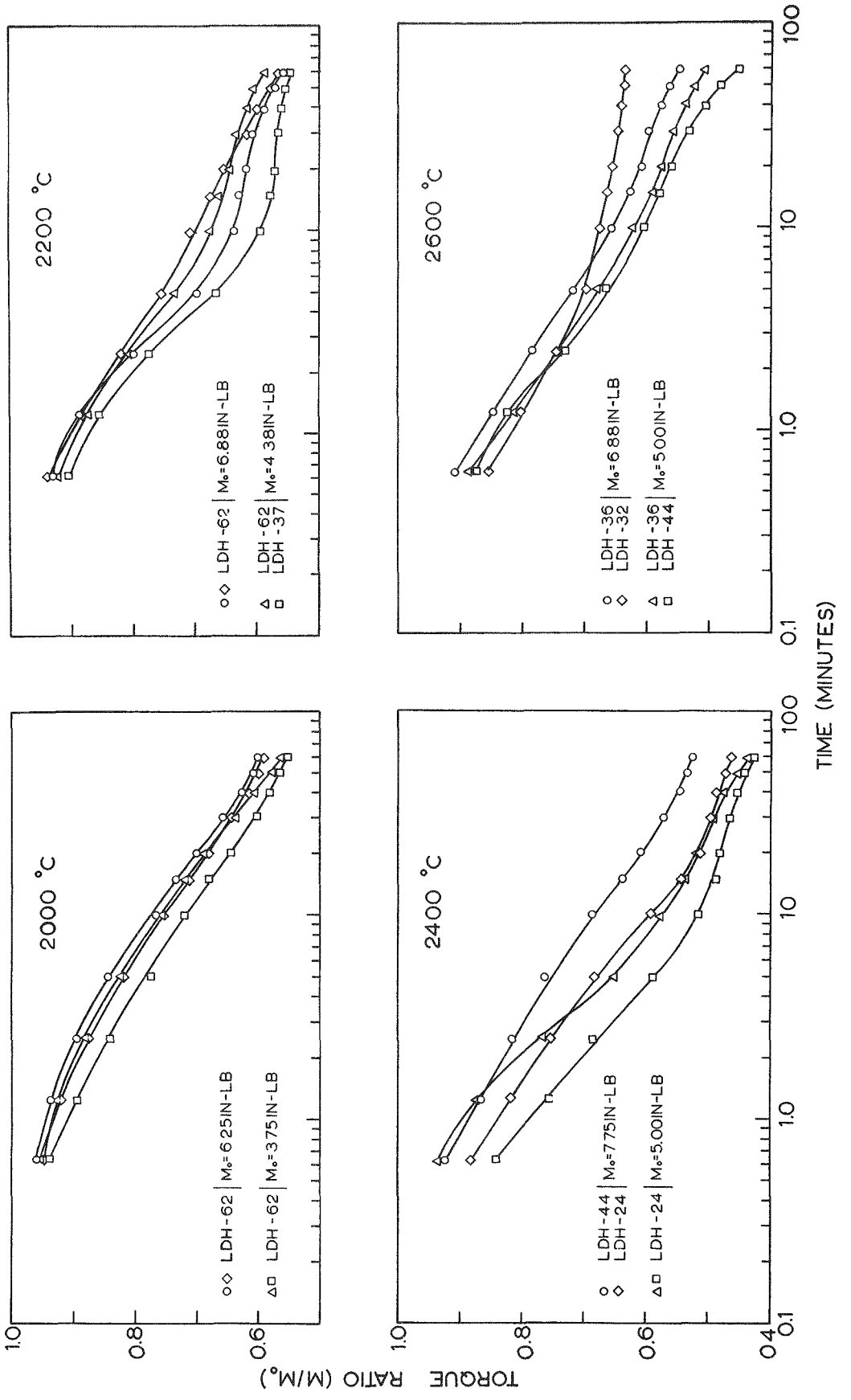

1158-909

Torsional-Stress Relaxation of Re-Impregnated LDH Stock

Figure 82

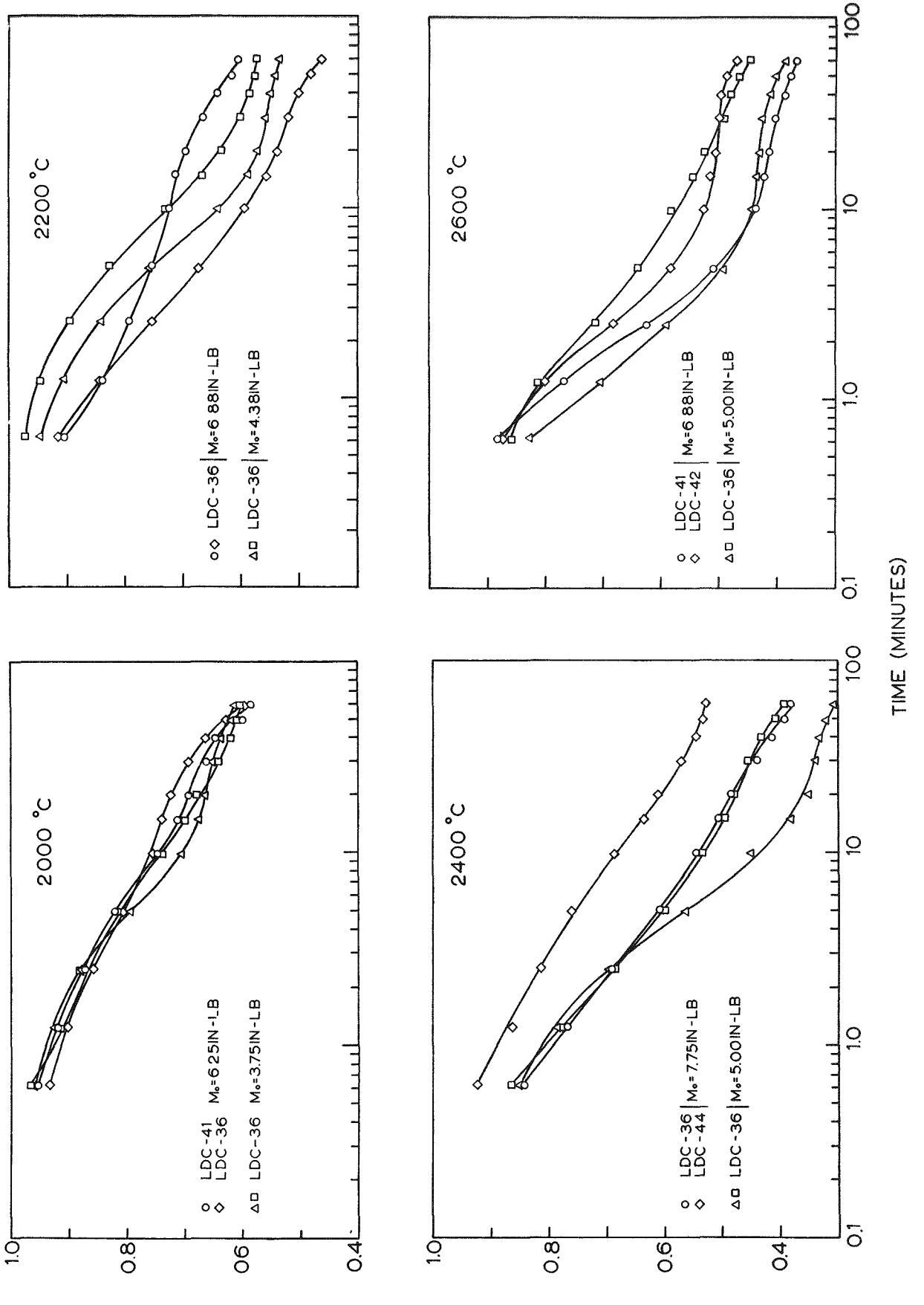

Torsional-Stress Relaxation of Re-Impregnated LDC Stock

1158-914

Figure 83

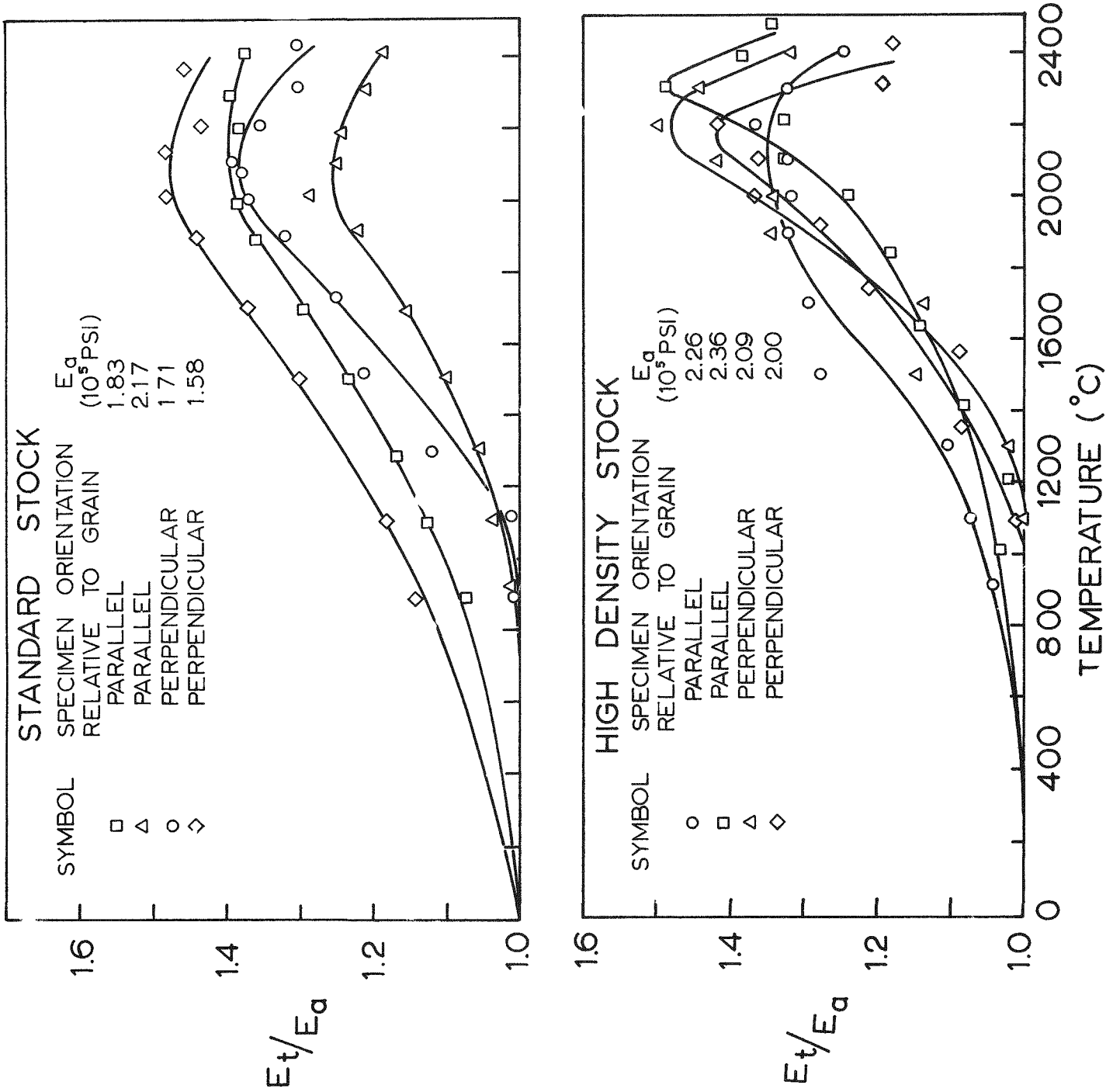

1158-892

Dynamic Young's Modulus for Standard and Re-Impregnated H4LM Stock

Figure 84

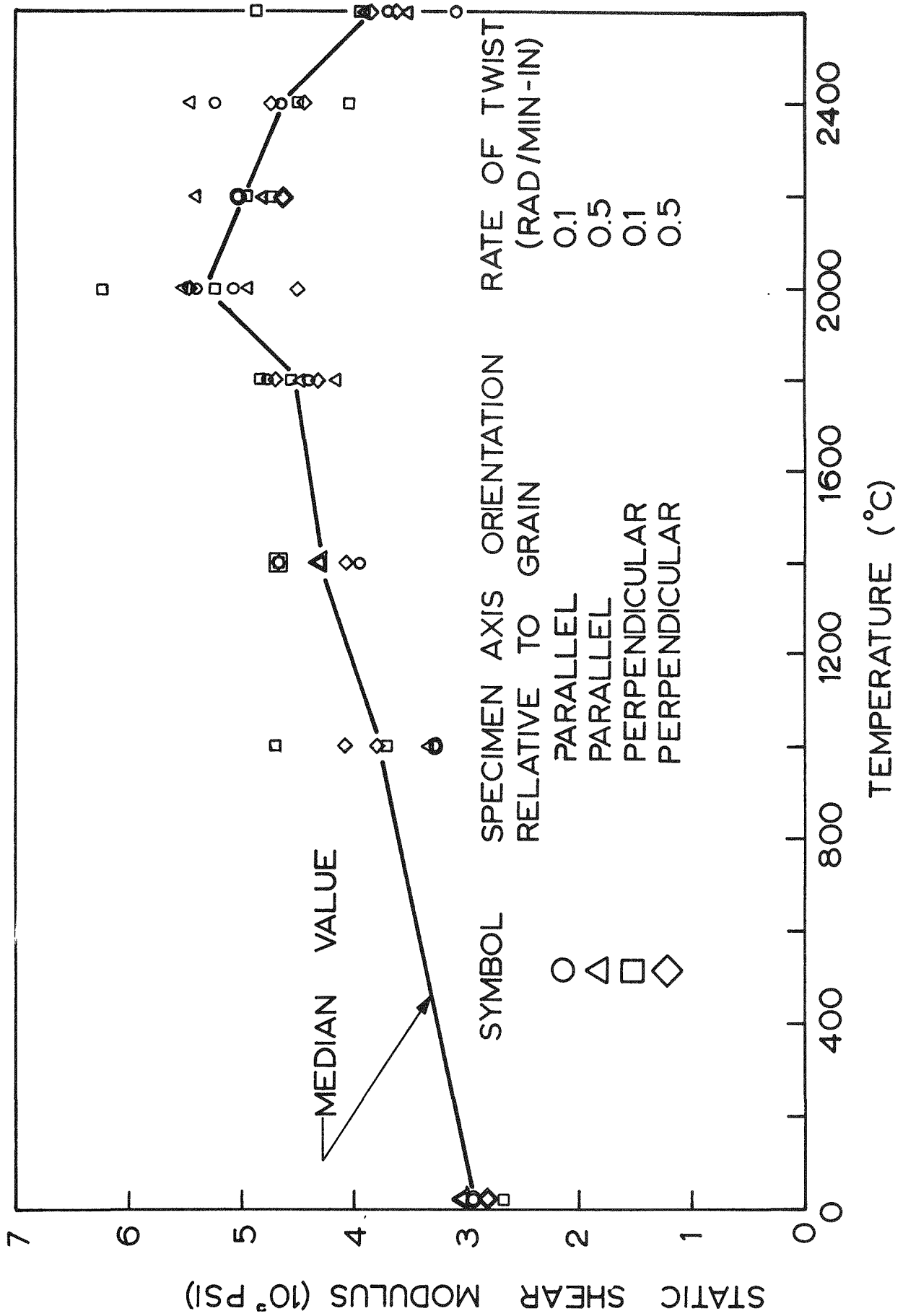

958-1040

Static Shear Modulus for Re-Impregnated H4LM Stock

Figure 85

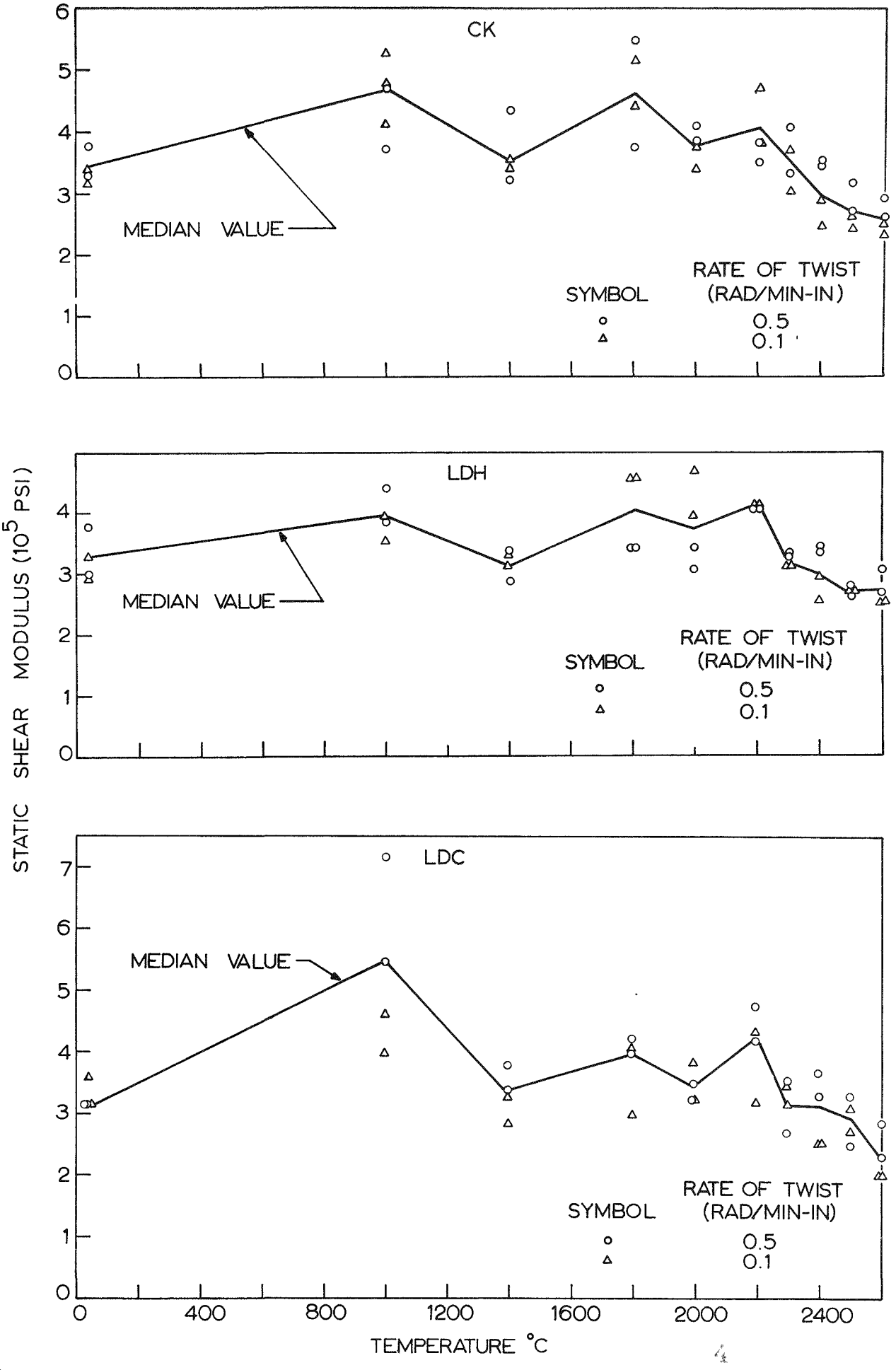

1158-898

Static Shear Modulus for Grades CK, LDH and LDC Stock

Figure 86

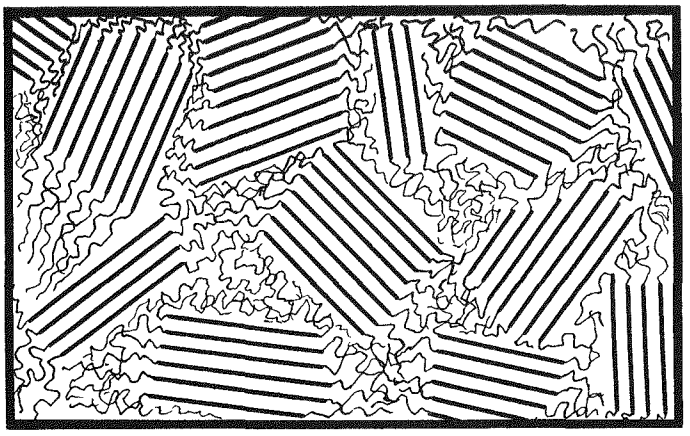

MORPHOLOGY OF A SEMICRYSTALLINE POLYMER. (AFTER FLORY)

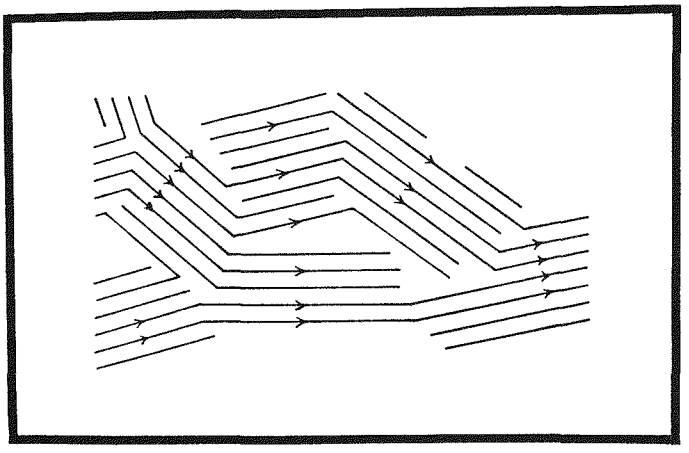

SCHEMATIC ARRANGEMENT OF CRYSTALLITES IN POLYCRYSTALLINE GRAPHITE. (AFTER CASTLE)

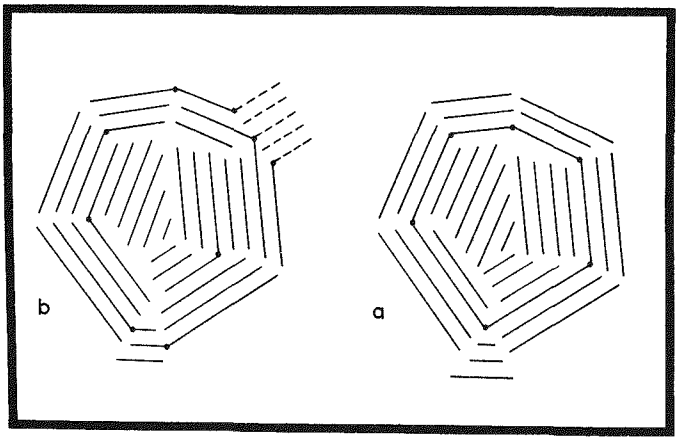

MICROCRYSTALS OF CARBON LINKED BY VALENCE BONDS. a) CLOSED RING ARRANGEMENT. b) RANDOM RING-LIKE LINKAGE. (AFTER MROZOWSKI)

Comparison of Schematic Concepts of the Structure of Graphite and of a Rubber-Like Polymer with Strain-Induced Crystallinity

Figure 87